Earth-Science Reviews 254 (2024) 104818

Contents lists available at ScienceDirect

Earth-Science Reviews

journal homepage: www.elsevier.com/locate/earscirev

Assessing the impact of crustal architecture and along-strike rifting propagation on salt deposition and tectonics: Insights from the Moroccan Atlantic margin

Rodolfo M. Uranga [a,*], Gianreto Manatschal [b], Mark G. Rowan [c], Josep A. Muñoz [a], Oriol Ferrer [a], Leonardo M. Pichel [d], Gonzalo Zamora [e]

[a] Departament de Dinàmica de la Terra i de l'Oceà, Facultat de Ciències de la Terra, Universitat de Barcelona, Martí i Franquès s/n, 08028 Barcelona, Spain
[b] University of Strasbourg, CNRS, ITES UMR 7063, F-67084 Strasbourg, France
[c] Rowan Consulting, Inc., 850 8th St., Boulder, CO 80302, USA
[d] Department of Earth Science, University of Bergen, Bergen, Norway
[e] Repsol, Méndez Álvaro, 44, 28045 Madrid, Spain

ARTICLE INFO

Keywords:
Rifting
Salt tectonics
Central Atlantic
Structural inheritance
Morocco

ABSTRACT

The salt-bearing conjugate rifted margins of Morocco and Nova Scotia contain one of the oldest stratigraphic records documenting the opening history of the Central Atlantic Ocean, starting in Late Triassic times. Although there is certain consensus on the Middle Jurassic to Present evolution of this ocean basin, the Early Jurassic rift to drift transition stage is still under discussion. Through the interpretation of unpublished, recently acquired deep seismic reflection data, integrated with legacy 2D surveys from offshore Morocco, this study presents new evidence supporting a revised 3D passive-margin evolutionary model with a focus on the rift-to-drift transition phase.

Eight regional seismic transects illustrate the along-strike variability of crustal structural styles, magmatic budget, and the interaction between rifting and evaporite deposition. Assuming evaporite deposition was near-isochronous along the margin, the interpretation of the autochthonous salt distribution elucidates the northward propagation of rifting and breakup. We interpret that salt was deposited during the exhumation stage in the Tarfaya and southern Agadir basins (southern segment) and during late *syn*-stretching to early syn-thinning in the Safi Basin and the Mazagan Plateau (northern segment). Furthermore, structural inheritance from Paleozoic tectonic boundaries, such as the South Atlas Fault Zone, were reactivated as transfer zones during rifting, separating segments with different crustal deformation styles and extension rates. Moreover, one of these inherited structures, the Sidi Ifni Transfer Zone, is located at the boundary between rheologically distinct pre-rift units and marks the transition between a magma-rich (south) and a magma-poor (north) segment of the margin, suggesting a direct link between compositional/structural inheritance and magmatic supply during rifting and breakup.

1. Introduction

Over the past two decades research on rifted margins has witnessed unprecedented progress. High-quality deep seismic imaging, analog/numerical modeling, and deep-sea drilling paired with the study of field analogues, set the foundation of a new conceptual framework describing the structure, rheological, and tectono-stratigraphic evolution of rifting leading to lithospheric breakup. This framework encompasses a series of deformation stages that ultimately result in the gradual thinning of the continental lithosphere and a transition from distributed to localized deformation (Brun and Beslier, 1996; Whitmarsh et al., 2001; Pérez-Gussinyé et al., 2001; Manatschal et al., 2007; Huismans and Beaumont, 2002, 2003, 2011; Chenin et al., 2022; amongst others). However, this new conceptual framework still needs to be tested in regions such as the Moroccan Atlantic margin.

The Central Atlantic rifted margins were the subject of intense geophysical surveying and ocean drilling campaigns in the 1980s (Weigel et al., 1982; Hinz et al., 1982a; Klitgord and Schouten, 1986).

* Corresponding author.
E-mail address: ruranga@ub.edu (R.M. Uranga).

https://doi.org/10.1016/j.earscirev.2024.104818
Received 22 February 2024; Received in revised form 3 May 2024; Accepted 14 May 2024
Available online 18 May 2024

However, the scarce deep well control and the uncertainty in the interpretation of the geophysical data promoted ambiguous interpretations regarding the crustal architecture of the distal domains (Roeser et al., 2002; Sahabi et al., 2004; Schettino and Turco, 2009; Sibuet et al., 2012). Furthermore, the segmentation of the rifted Moroccan margin is likely controlled by inherited structural and compositional features (Hinz et al., 1982a; Laville and Piqué, 1991; Le Roy and Piqué, 2001; Nemčok et al., 2005), adding challenges when applying simplistic concepts to explain its along-strike architecture and evolution.

A crucial element to consider when interpreting the evolution of rifted margins is that rifting and breakup may propagate along strike and therefore are not necessarily isochronous at the passive margin scale (Vink, 1982; Courtillot, 1982; Withjack et al., 1998; Le Pourhiet et al., 2018; Tetreault and Buiter, 2018). Moreover, there is a broad consensus that rifting is a polyphase process in which strain localization migrates along dip, from proximal to distal settings (Fig. 1), imposing an additional challenge on the regional correlation of stratigraphic markers (Lavier and Manatschal, 2006; Péron-Pinvidic and Manatschal, 2009; amongst others). In this scenario, salt can be considered as an excellent seismic marker thanks to its high seismic reflectiveness and frequent widespread deposition. Furthermore, if we consider that salt can be deposited mostly simultaneously along the length of the rifted margin, then it may be regarded as an isochronous stratigraphic "tape recorder". This is a reasonable assumption given the typically short time frame of evaporite accumulation in response to climate control and large-scale

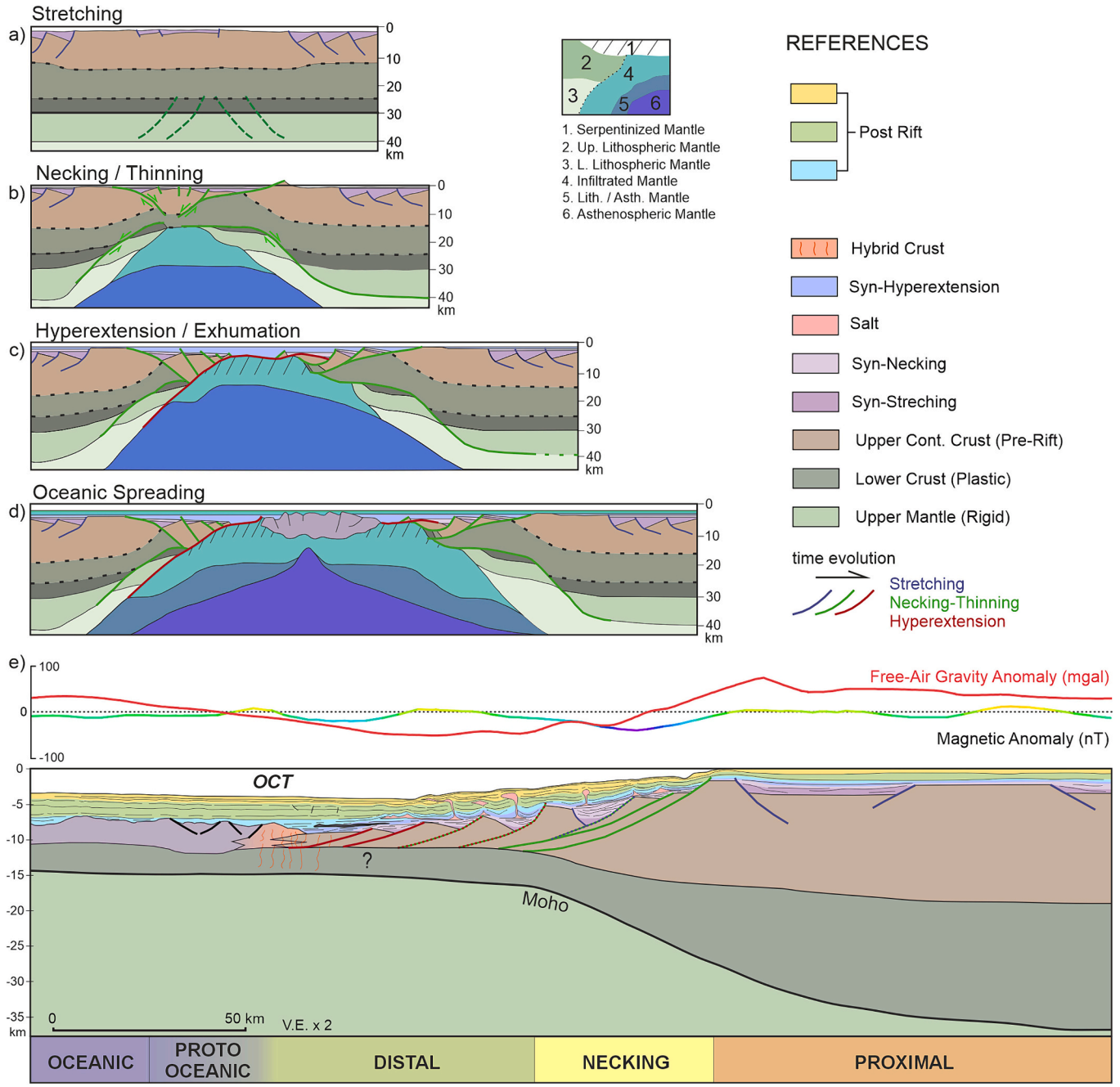

Fig. 1. a) to d) Stages during rifting evolution in magma-poor margins (modified from Péron-Pinvidic and Manatschal, 2009); e) Definition of magma-poor margin tectonic domains based on integrated seismic, gravimetric and magnetic data (modified from Contrucci et al., 2004 and Klingelhoefer et al., 2016, with the addition of the Proto-Oceanic domains as defined by Zhang et al., 2021); OCT: Ocean-Continent Transition. The dashed-line faults represent multistage reactivation.

basin isolation (Warren, 2006; Jackson and Hudec, 2017).

The aim of this study is twofold: firstly, to map the crustal tectonic domains of the Moroccan margin and their along-strike variations through the integration of geophysical legacy surveys and newly acquired unpublished seismic data; and secondly, to describe the lateral variations in the depositional setting of salt and consequent salt-related structural styles in the Moroccan salt basin. By comparing the observations made on the Moroccan margin with previous interpretations of the conjugate Nova Scotia margin, this study proposes a revised evolutionary model of the rift to drift transition in this segment of the Central Atlantic, highlighting the importance of rift propagation and structural inheritance.

1.1. Salt-bearing rifted margins

In this study, rifting is subdivided into different stages and the term "breakup" is considered to encompass the transition from crustal separation (i.e., crustal breakup) to the onset of steady-state seafloor spreading, referred to as lithospheric breakup (Chao et al., 2023). There are several models describing the different stages of rifting (McKenzie, 1978; Wernicke, 1985; Huismans and Beaumont, 2002, 2011; Pérez-Gussinyé et al., 2003). One of the most widely used, especially in magma-poor rifted margins, is the one proposed by Péron-Pinvidic and Manatschal (2009). This model is divided into four stages, which are the stretching, necking/thinning, hyperextension/exhumation, and oceanic spreading stages, through which deformation migrates progressively from proximal to distal (Figs. 1a-d). During the stretching stage (Fig. 1a), pure shear extension is dominant (McKenzie, 1978; Lavier and Manatschal, 2006). Brittle upper crustal deformation is decoupled in ductile mid-lower crustal levels promoting the development of isolated grabens and half-grabens. During the necking/thinning stage (Fig. 1b), the crust thins from about 30 to 10 km as a consequence of attenuating ductile layers in the middle and lower crust (Pérez-Gussinyé et al., 2001). The extensional deformation is focused on crustal-scale, basinward-dipping normal faults at the necking domain (Fig. 1e) (Péron-Pinvidic and Manatschal, 2009; Mohn et al., 2012; Tugend et al., 2015). During the hyperextension/exhumation stage (Fig. 1c), large offset detachment faults (Hölker et al., 2003) connect from the upper crust down into the mantle, resulting in the development of sag basins at the distal domain (Fig. 1e) (Nirrengarten et al., 2016). These major detachments are often associated with serpentinization of the mantle and can ultimately lead to mantle exhumation (Fig. 1c). Finally, the formation of a new spreading center and the accretion of oceanic crust marks the final lithospheric breakup (Fig. 1d).

The definition of tectonic domains is key for describing the tectono-stratigraphic architecture of rifted margins. In the absence of well data, tectonic domains are usually identified through the interpretation of seismic refraction, reflection, and potential field data (Tugend et al., 2015). In this study, the classification that fits best with the seismic interpretation is the one proposed by Péron-Pinvidic et al. (2013), which defines the proximal, necking, distal, proto-oceanic and oceanic domains (Péron-Pinvidic et al., 2013) (Fig. 1e). The proximal domain (Fig. 1e) is characterized by a thick ($\approx 30 \pm 5$ km) crust where high-angle normal faults bound grabens and half-grabens. Basinward, the necking domain (Fig. 1e) is identified by a wedge-shaped crustal geometry (crustal thinning from ≈ 30 km to ≈ 10 km) with an ascending Moho and crustal-scale detachment faults (in green in Fig. 1e) (Pérez-Gussinyé et al., 2003; Osmundsen and Redfield, 2011). The distal domain (Fig. 1e) is characterized by crustal thinning to <10 km (Péron-Pinvidic et al., 2013), with faults (in red in Fig. 1e) cross-cutting from the surface into the upper mantle (Pérez-Gussinyé et al., 2003; Péron-Pinvidic et al., 2013).

The OCT represents a gradual transition between the distal and the proto-oceanic domains and is usually characterized by a seaward step-up in top basement topography commonly associated with positive magnetic and free air gravity anomalies (Stanton et al., 2016) (Fig. 1e). In margins with late *syn*-rift salt, this so-called outer high often constitutes the distal breakup limit of the primary salt basin (Rowan, 2014; Nemčok and Rybár, 2016; Epin et al., 2021; Uranga et al., 2022; Araujo et al., 2023). Recent studies propose that lithospheric breakup at magma-poor rifted margins is a long-lasting stage that marks the transition between a tectonic-driven (faulting) to a magmatic-driven (oceanic accretion) process (Gillard et al., 2017; Sapin et al., 2021; Nemčok and Frost, 2023). In this context, the term hybrid crust (Fig. 1e) refers to the varied nature of the basement at the OCT, reflecting an interaction of different processes such as crustal thinning, mantle exhumation, and the intrusion/extrusion of *syn*-tectonic igneous material (Gillard et al., 2017; Zhang et al., 2021). In practice, when interpreting geophysical data, unequivocal continental crust displays a large-scale basinward-wedging geometry. More distally, the transition to the proto-oceanic domain is identified by a fault-dominated crust with an abnormal thickness and a highly reflective rough top basement topography (Fig. 1e) (Nemčok et al., 2018; Chao et al., 2023). Finally, the oceanic domain displays a crustal thickness ranging between 1.5 and 1.75 s TWT on average (≈ 6 km according to Epin et al., 2021) (Fig. 1e). The top basement is sub-horizontal and parallel to the seismic Moho with overlying flat-lying reflections.

Conversely to magma-poor margins, magma-rich margins are characterized by a high degree of mantle melting and a syn-magmatic, pure shear dominated breakup mechanism, associated with continentward dipping shear-zones (Ebinger and Casey, 2001; Geoffroy, 2005; Geoffroy et al., 2015; Nemčok and Rybár, 2016). The rifting stages that characterize magma-rich margins involve an initial dilation stage (Fig. 2a), where volcanic traps (large igneous provinces) cover large areas and crustal expansion occurs through dyking in the upper crust and magma underplating at the Moho. Following, the necking stage (Fig. 2b) is characterized by extreme crustal stretching and thinning which is accommodated by large continentward-dipping detachment faults connected to a flowing lower crust, while the subsiding blocks are filled in with a first unit of volcanic material identified as seaward-dipping reflectors (inner SDRs). The footwall of the two opposite continentward-dipping faults forms a central rigid continental block (C-Block in Fig. 2b and c). Finally, during the continental spreading stage (Fig. 2c), continued pure shear extension causes the fragmentation of the C-block with the synchronous formation of large SDRs (outer SDRs in Fig. 2c). As deformation migrates seaward, these evolutionary stages can be identified in different tectonic domains (Geoffroy, 2005; Nemčok et al., 2023). The proximal domain (Fig. 2d) is characterized by a continental crust intruded by dykes and sills and with normal thickness; the necking/distal domain is characterized by a typically narrow zone of crustal thinning with presence of SDRs delimited by continentward-dipping detachment faults and the presence of underplated high-velocity igneous bodies, and the proto-oceanic domain is characterized by a thicker-than-normal oceanic crust.

Salt can be deposited at any stage during rifting (Rowan, 2014). As a result, it displays distinctive structural styles depending on the timing of deposition relative to rifting stages and the width of the margin (Pichel et al., 2022). In addition, evaporites can be deposited very rapidly compared to siliciclastic sediments if climatic and basin isolation conditions are met (Warren, 2006). Given these combined characteristics, the autochthonous salt layer can be regarded as a near-isochronous stratigraphic tape recorder and its related structures will be influenced by the original depositional setting. Rowan (2014) proposed a classification of salt-bearing rifted margins with distinctive structural styles based on the four-stage evolutionary model defined by Péron-Pinvidic and Manatschal (2009), such that the salt can be classified as pre-rift, *syn*-stretching, syn-thinning and syn-exhumation (Fig. 3). In pre-rift salt basins, (e.g., Ferrer et al., 2008, 2012; Jammes et al., 2010; Roca et al., 2011), salt mobilization is triggered by thick-skinned extension developing a considerable base-salt structural relief (Fig. 3a). In syn-stretching salt basins (Fig. 3b) (e.g., Rasmussen et al., 1998; Alves et al., 2002, 2006), salt is deposited during crustal extension, mainly

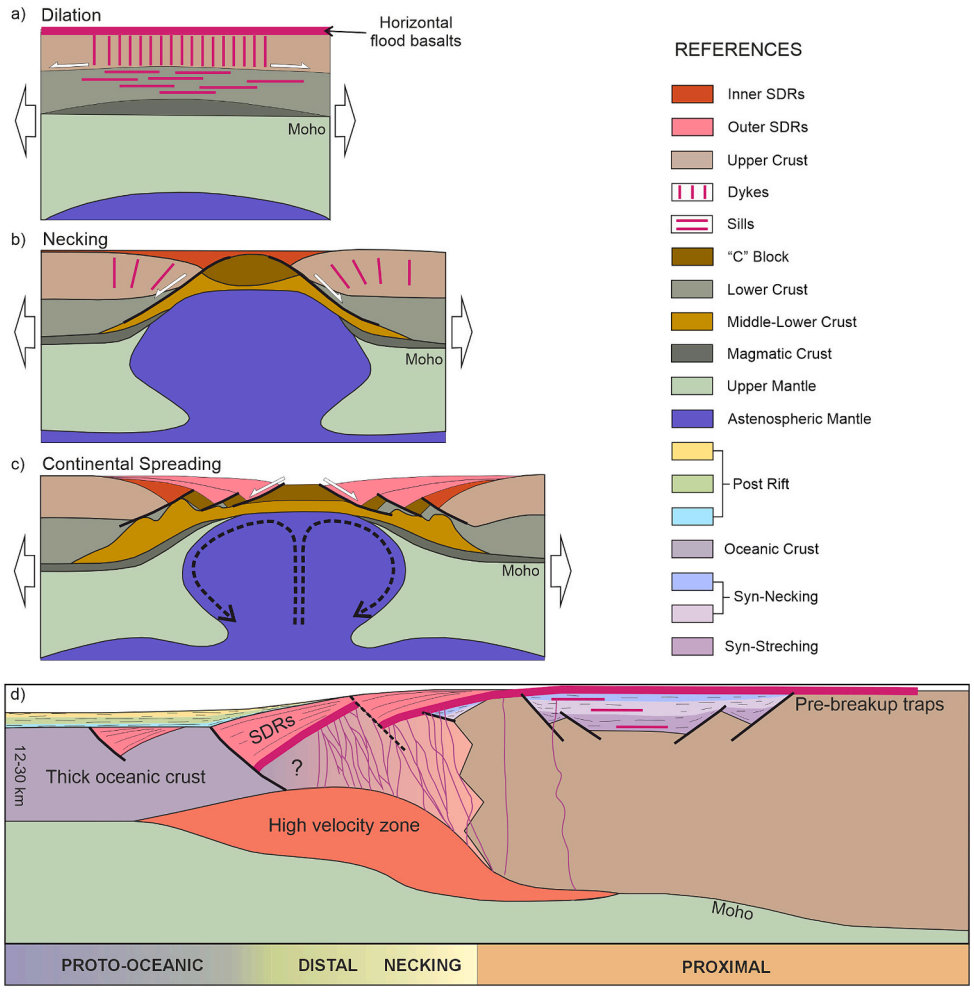

Fig. 2. a) to c) Stages during rifting evolution in magma-rich margins (redrawn from Geoffroy et al., 2015); d) Definition of tectonic domains in magma-rich margins based on Geoffroy (2005) and Nemčok et al. (2023).

concentrated in the proximal domain (Fig. 1e). In these basins, the base-salt relief is controlled by a stepped, faulted basement geometry. Syn-thinning salt (Fig. 3c) is mainly deposited in the necking/distal domain (Figs. 1e and 2b) during the crustal thinning stage (Fig. 1b). The base salt displays significant relief due to extension on thinning faults (in green in Fig. 1e), and the salt layer is highly attenuated or completely offset on the largest faults. Salt deformation is triggered by both thick- and thin-skinned extension and by gravitational processes, and allochthonous nappes may form at the distal toe of the salt (e.g, Tari and Jabour, 2013; Pichel et al., 2019) (Fig. 3c). Syn-exhumation salt (e.g., Rowan et al., 2012; Hudec et al., 2013; Quirk et al., 2013; Epin et al., 2021; Pichel et al., 2022; Rowan, 2022) is deposited as part of the sag sequence, controlled by regional subsidence during the hyperextension/mantle exhumation stage, with coeval brittle extension concentrated in the outer trough (Rowan, 2020, 2022; Epin et al., 2021) (Fig. 3d). The salt stretches and thins synchronously with the widening of the OCT. The base salt is generally unfaulted in the proximal and necking domains but is offset by up to 4 km in the outer trough. Aside from some thick-skinned extension in the outer trough, deformation is driven by gravity gliding and spreading, with allochthonous salt flowing over newly formed oceanic crust.

1.2. Geological setting

The Central Atlantic Ocean is bounded by the Pico and Gloria fracture zones to the north and by the Guinean fracture zone to the south (Fig. 4). Rifting started in the Triassic and led to the separation of the African and the North America plates (Le Pichon, 1968; Klitgord and Schouten, 1986). Most of the history of the relative motion between these two plates is well documented by magnetic lineations and fracture zones (Vine and Matthews, 1963; Heezen and Tharp, 1965). However, the initial drifting of the Central Atlantic took place during the Jurassic Magnetic Quiet Zone, a period in which the recorded magnetic anomalies are weak and hard to correlate (Roeser, 1982). In the study area, the S1 magnetic anomaly, located on the Moroccan side of the northern Central Atlantic (Fig. 4), is considered to mark the oceanward boundary of the OCT (Roeser et al., 2002).

1.2.1. Pre-rift stage

The pre-rift basement of Northwest Africa comprises several Precambrian and Paleozoic tectonic provinces. The Reguibat Shield (Fig. 4) is part of the Archaean to Paleo-Proterozoic West Africa Craton (Villeneuve and Cornée, 1994; Ennih and Liégeois, 2008), composed mainly of granitic and metasedimentary rocks. The West Africa Craton was affected by three episodes of convergence – the Pan- African (750 Ma – 560 Ma), the Caledonian (460–420 Ma), and the Variscan (360–300 Ma) orogenies – that ultimately led to the assemblage of Pangea (Choubert, 1963; Michard, 1976; Bertrand and Jardim de Sá, 1990; Black et al., 1994; Frizon de Lamotte et al., 2004; Simancas et al., 2005; amongst others). To the north, the Caledonian and Variscan belts, composed mainly of metasedimentary rocks, are widely exposed in the Anti Atlas and Meseta domains (Fig. 4) (Choubert, 1952; Piqué and Michard, 1989;

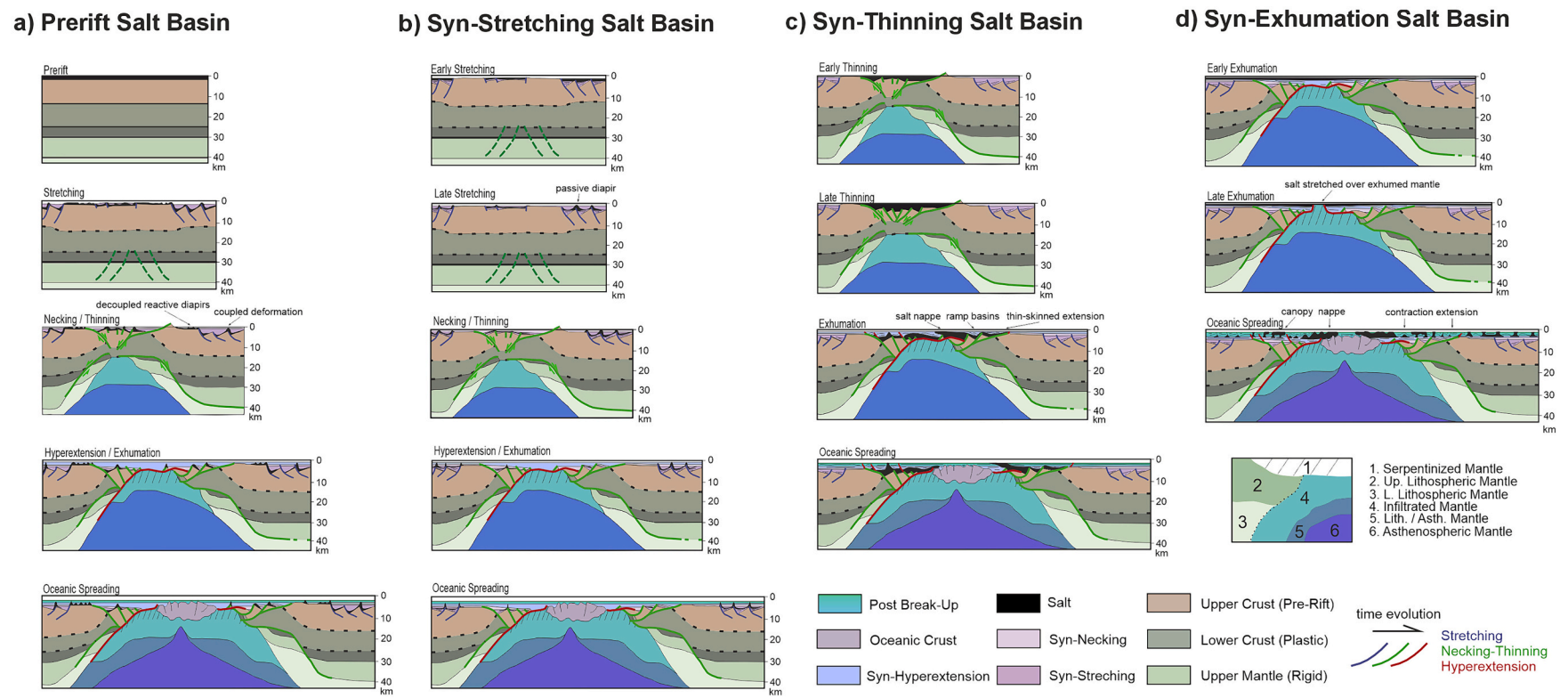

Fig. 3. Salt bearing passive margins classification (modified from Rowan, 2014). Note that the syn-exhumation geometry has been revised to include an outer trough in more recent depictions (Rowan, 2020).

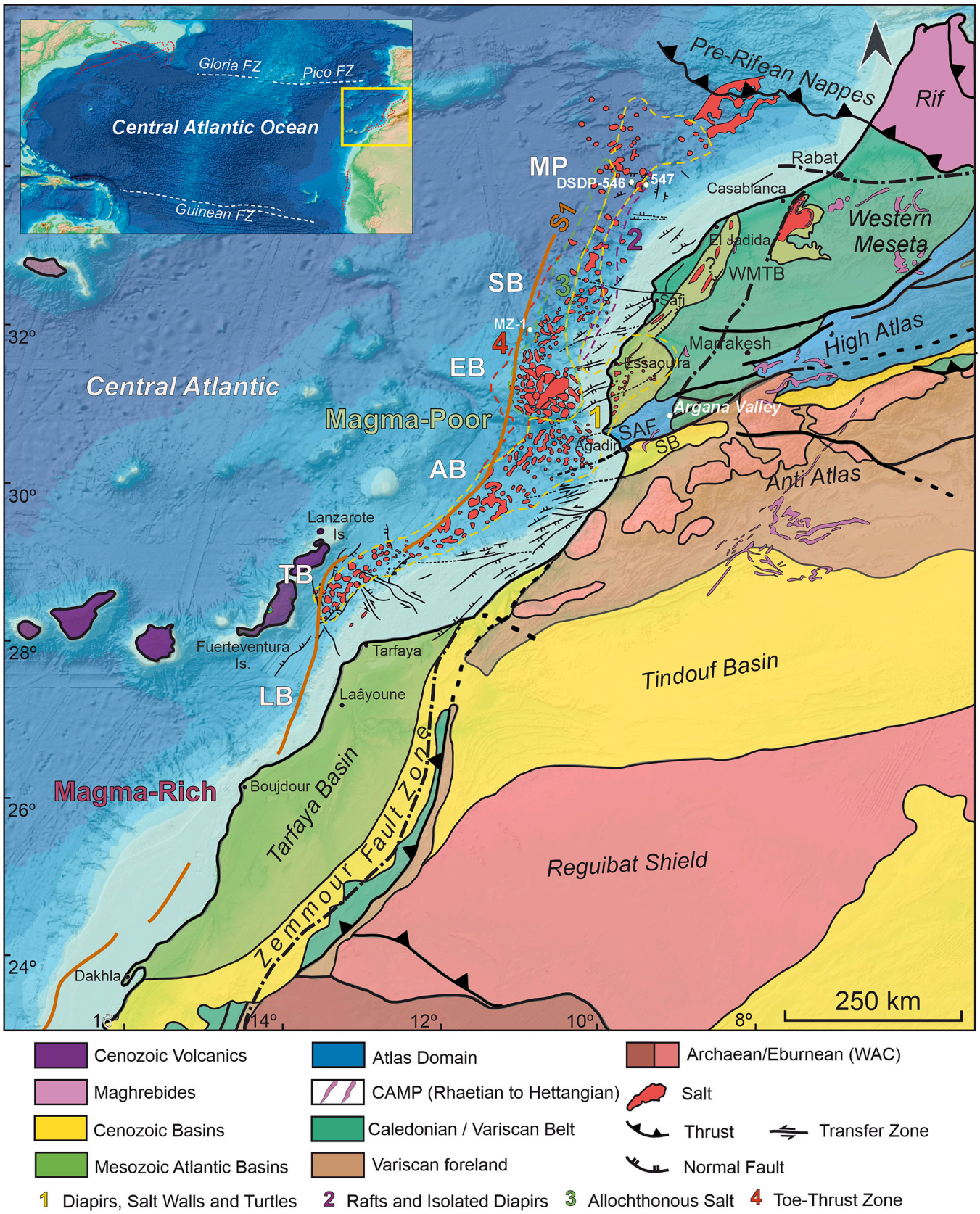

Fig. 4. Geological map of NW Africa and Moroccan salt basin (compiled from Le Roy and Piqué, 2001; Roeser et al., 2002; Lyazidi et al., 2003; Haddou and Tari, 2007; Michard et al., 2008a; Gouiza, 2011; Tari and Jabour, 2013; Louden et al., 2013; Marzoli et al., 2018 and Uranga et al., 2022). LB: Laâyounne Basin; TB: Tarfaya Basin; AB: Agadir Basin; EB: Essaouira Basin; SB: Safi Basin; MP: Mazagan Plateau; WMTB: Western Meseta Triassic basins; SAF: South Atlas Fault.

Michard et al., 2008). These tectonic provinces are characterized by the presence of major faults, striking both parallel and obliquely to the margin, like the Zemmour and the South Atlas faults, respectively (Fig. 4). These inherited structures were extensionally reactivated during the early opening of the Central Atlantic (Le Roy and Piqué, 2001).

1.2.2. *Syn-rift stage*

Rifting started with the development of predominantly NE-oriented half-grabens offset by E-W striking transtensional faults inherited from the Variscan orogeny (Heyman, 1989; Laville and Piqué, 1991; Medina, 1995; Piqué and Laville, 1996; Le Roy and Piqué, 2001; Leleu et al., 2016). The extensional deformation of the margin evolved diachronously, getting younger from east to west and from south to north (Medina, 1995; Le Roy and Piqué, 2001; Gouiza et al., 2010; Gouiza, 2011) (Figs. 5 and 6). During the Late Permian? To Early Triassic, early *syn*-rift sediments probably associated with the Atlas rifting are recorded in outcrops in the Western High Atlas (Argana Valley, see Fig. 4) (Tixeront, 1973; Brown, 1980; Medina, 1995), with an overlying Late Triassic succession possibly related to the Atlantic rifting (for a discussion on this matter please see Baudon et al., 2012). Westward, in the eastern Essaouira and Souss basins, the first syn-rift stage has a younger, Carnian to Norian age (Le Roy et al., 1997). Subsequently, a second stage of extensional deformation took place during Norian-Rhaetian times in all the coastal basins, accompanied by pelitic and evaporitic sedimentation (Fig. 5). The westward migration of extensional deformation ultimately affected the offshore basins, which record a thick Rhaetian-Hettangian succession of evaporites (Hafid et al., 2008; Tari and Jabour, 2013; Tari et al., 2017). Synchronously with rifting, basaltic magmas related to the Central Atlantic Magmatic Province (CAMP in future references; for a full review see Marzoli et al., 2018) were emplaced. The peak of magmatic activity is recorded at 201 Ma (earliest Hettangian), but in the High Atlas, the topmost lava flows yield a younger mean age of 196.6 ± 0.6 Ma (early Sinemurian) (Verati et al., 2007).

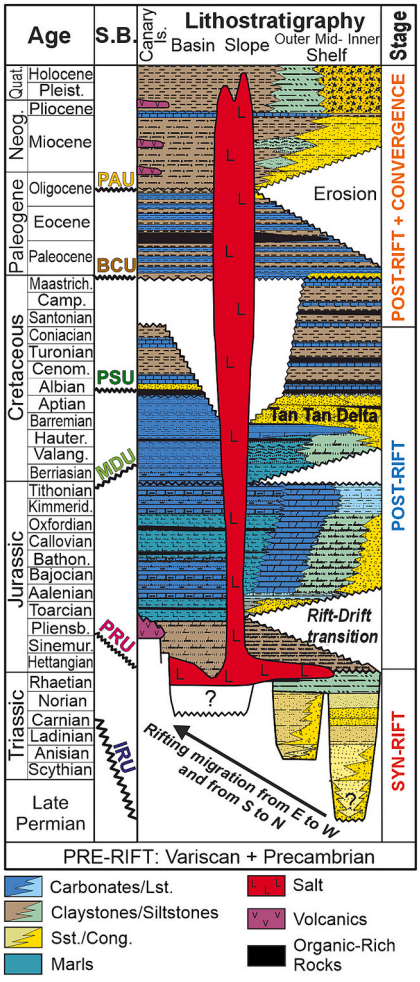

Fig. 5. Chronostratigraphic chart from the Tarfaya Basin, modified from Wenke (2014). The major chronostratigraphic subdivisions and tectonic events apply to the entire Moroccan Atlantic margin. IRU: Initial Rift Unconf., PRU: Post-Rift Unconf., MDU: Mature Drift Unconf., BCU: Base Cenozoic Unconf., PAU: Peak Atlasian Unconformity.

The eastern Central Atlantic salt province trends N-S to NE-SW along >1000 km offshore Morocco as well as 400 km in a NE-SW direction across the onshore Essaouira and the Western Meseta Triassic basins (WMTB in future references), including the Doukhala, Mohammedia, Benslimane, El Gara and Berrechid basins. Evaporite deposition took place during the Late Triassic – Early Jurassic (Klitgord and Schouten, 1986; Piqué and Laville, 1996; Hafid, 2000; Tari et al., 2000; Tari and Jabour, 2013). In the onshore Essaouira Basin, the syn-rift sediments assigned by Hafid (2000) to the sequence Tr1a (Carnian) (Fig. 7), record the oldest evidence of salt in the coastal basins. They correlate in age with the Osprey evaporites of the conjugate North American margin (Holser et al., 1988). This sequence was drilled by several onshore wells (MAC-1, NDK-2, JRP-1, IH-1, see lower left insert in Fig. 7 for location), where it is interfingered with the CAMP basalt β1 and offset by normal faults bounding half-grabens (Hafid, 2000). During the late syn-rift, evaporite deposition continued in "sag basins" where syn-rift faults were already inactive. This evolution is recorded by sequences Tr1b and Tr2 (Late Triassic – Hettangian?) (Fig. 7), which consist of a succession of evaporites, red mudstones and sandstones interfingered with the β2 basalt and capped by the β3 basalt (Fig. 7). A similar interdigitation is also observed northward, in the Western Meseta Triassic basins (see Fig. 4 for location) (see Fig. 6 in Afenzar and Essamoud, 2017).

In the offshore Moroccan salt basin, the base of the salt has rarely been drilled and is thus poorly sampled (Hafid et al., 2008). Moreover, dating of the top of the salt in this area relies mainly on one study based on the sampling of palynomorphs from clay inclusions (mostly *Corollina meyerian* and *Perinopollenites elatoide*) interfingered in the salt cored at DSDP-546 well (Fenton, 1984) (see location in Fig. 4). The results yielded a Rhaetian to Hettangian age, which is the most widely accepted age interval for salt deposition of the Moroccan offshore basins (Hafid et al., 2000; Tari et al., 2000; Tari and Jabour, 2013; Hafid et al., 2008, amongst others), and agrees with data from the conjugate Nova Scotia margin (Barss et al., 1979; Jansa et al., 1980; Allen et al., 2020; Decalf and Heyn, 2023). Furthermore, the absence of older salt layers in the distal offshore setting supports the idea of a westward migration of rifting (see above). However, caution is necessary due to the limited chronostratigraphic data, particularly in the basal salt section, which hinders precise dating of the interval of evaporite deposition.

Although the timing of the initial breakup of the Central Atlantic is still debated, most authors agree it took place between 195 and 175 Ma (i.e., between Sinemurian and Toarcian times) (Klitgord and Schouten, 1986; Roeser et al., 2002; Sahabi et al., 2004; Davison, 2005; Schettino and Turco, 2009; Labails et al., 2010; Sibuet et al., 2012). Uncertainties rise mainly due to different interpretations and dating of the S1 magnetic anomaly (Fig. 4) and its conjugate East Coast Magnetic Anomaly (ECMA in future references) (Sahabi et al., 2004). According to a recent biostratigraphic reinterpretation of the deep MZ-1 well (Bishop, 2020), located offshore Morocco (Fig. 4), Sinemurian sediments are overlying proto-oceanic crust, adding a new constraint to date the early stages of drifting (Ady et al., 2022; Neumaier et al., 2019).

1.2.3. *Post-rift stage*

The Jurassic postrift sequence of the Moroccan Atlantic margin consists of a prograding siliciclastic system followed by a widespread passive margin carbonate platform including shallow-marine to deeper-water carbonates (Fig. 5) (Michard, 1976; Jansa, 1981; Hinz et al., 1984;

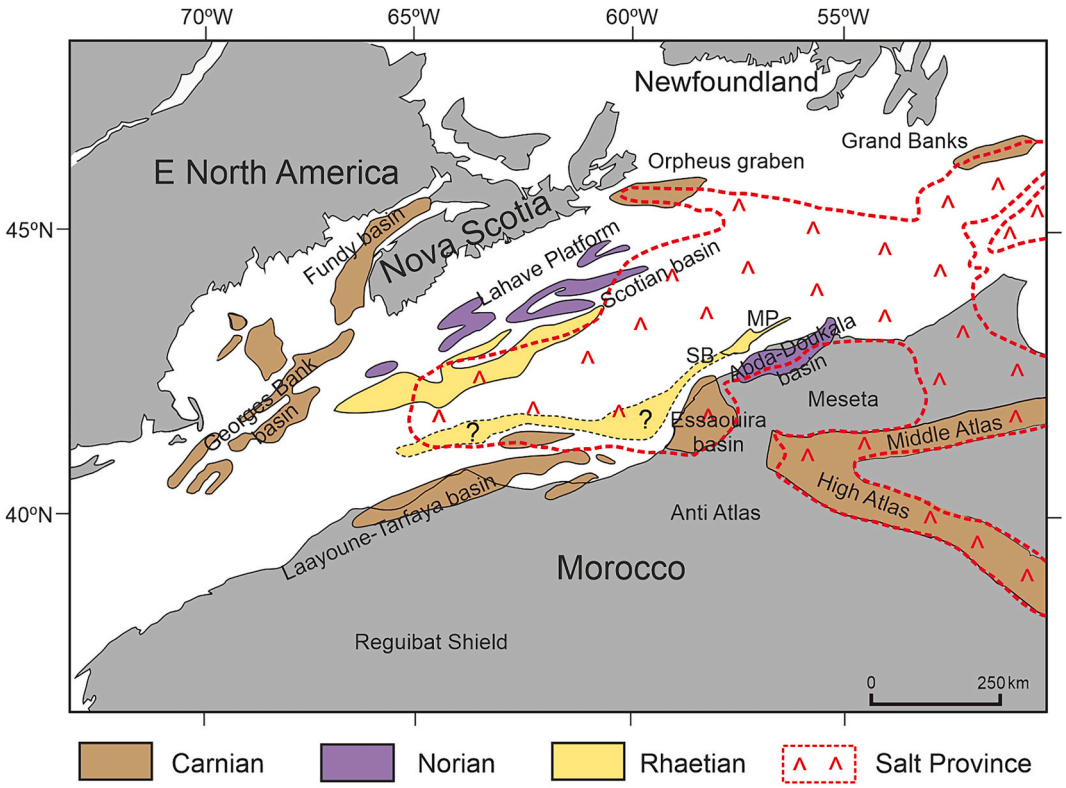

Fig. 7. N-S Triassic to Early Jurassic correlation panel from the onshore Essaouira Basin, including wells MAC-1, JRP-1 and IH-1 and the Argana Valley outcrops, modified from Hafid (2000). Basalt layers are labelled β1 to β3. Note that initial salt deposition is interpreted as Carnian in age.

Hafid et al., 2008; Bertotti and Gouiza, 2012) This depositional environment persisted until Berriasian times, when a basinwide regression exposed and eroded the Jurassic carbonate platform. In specific regions, such as the Tarfaya and Agadir basins, this resulted in the development of deltaic systems (e. g. Tan-Tan delta, see Fig. 5), which were active until the Albian (El Khatib, 1995; Zühlke et al., 2004; Bertotti and Gouiza, 2012; Wenke, 2014).

From Late Cretaceous times, the Moroccan margin was affected by the N-S oriented convergence between the Eurasian and African plates (Guiraud and Bosworth, 1997; Frizon de Lamotte et al., 2009; Neumaier et al., 2016; Gouiza, 2011). This resulted in localized tectonic inversion, erosion (Sehrt, 2014 Leprêtre et al., 2015; Gouiza, 2011) and the rejuvenation of salt structures (Tari et al., 2017; Pichel et al., 2019; Uranga et al., 2022). One of the most conspicuous features marking the early stages of convergence is the Base Cenozoic Unconformity (BCU in Fig. 5), which constitutes a regional seismic marker. In addition, since Late Cretaceous times, a sub-lithospheric thermal anomaly underlying the oceanic crust and regarded as the residue of an old mantle plume (Holik et al., 1991; Carracedo et al., 1998; Fullea et al., 2015) was responsible for the formation of the Canary Islands and the associated swell.

1.2.4. *Crustal architecture and OCT characterization*

Existing crustal interpretations of the Moroccan margin are based on 4 deep reflection and refraction seismic transects that define the first-order crustal architecture of the margin (Fig. 8) (Klingelhoefer et al., 2016; Biari et al., 2017; Biari et al., 2021) and offer a regional template for the definition of tectonic domains in this study. Of particular interest to this work is the characterization of the necking and distal domains and the OCT. The present study is located on the southern, central and northern segments as defined by Klingelhoefer et al. (2016). From south to north, the distal domain in the Dakhla profiles (Figs. 8a and b) is interpreted as igneous intrusions (Klingelhoefer et al., 2009). This profile approximately correlates with the LASE profile located on the conjugate Baltimore Canyon Trough where seaward dipping reflectors (SDRs) were described (Diebold and Stoffa, 1988), defining this segment as magma rich. Moreover, this segment includes the SMART 3 (Scotian MARgin Transect) profile located in the southernmost segment of Nova Scotia (Fig. 8) (Keen and Potter, 1995; Dehler et al., 2004; Funck et al., 2004; Louden et al., 2013), and conjugate to the southern Tarfaya Basin on the Moroccan margin. It is noteworthy that, in this magma-rich segment of the Central Atlantic, salt deposits are scarce or absent. (see Rowan, 2014).

Northward on the Moroccan margin, the distal domain in the Meteor refraction profile (Fig. 8) (Goldflam et al., 1980; Weigel et al., 1982) has been interpreted as serpentinized mantle (Klingelhoefer et al., 2016). Similarly, on the Central Nova Scotian margin, Keen et al. (1991) and Wu et al. (2006) interpreted the OCT imaged by the SMART 2 profile (Fig. 8) as partially serpentinized mantle. Further north, the SMART 1 and MIRROR profiles represent conjugate transects on the Scotian and Moroccan margins, respectively (Fig. 8) (Klingelhoefer et al., 2016). The distal domain in the SMART 1 profile has been interpreted as continental crust transitioning basinward to strongly serpentinized mantle (Funck et al., 2004). On the Moroccan margin, Biari et al. (2015) interpreted that the distal domain is characterized by continental crust transitioning basinward to a proto-oceanic domain (OC-1 in Biari et al., 2015; Klingelhoefer et al., 2016). Even farther northward, the OETR (Offshore Energy Technical Research) and SISMAR transects (Jaffal et al., 2009) can also be considered as conjugate profiles (Fig. 8). The distal domain and the OCT on the SISMAR profile is characterized by a smooth top basement topography, interpreted as thinned continental or transitional crust (Contrucci et al., 2004). The conjugate OETR profile shows a similar velocity layering (Fig. 8c) but, in this case, the authors interpret the presence of an underplated magmatic body in the distal domain (Makris et al., 2010). Overall, the available geophysical data supports a regional-scale subdivision of the Moroccan/Nova Scotia margins into a magma-rich segment in the south and a magma-poor segment in the north. However, there are still uncertainties in defining the along-strike

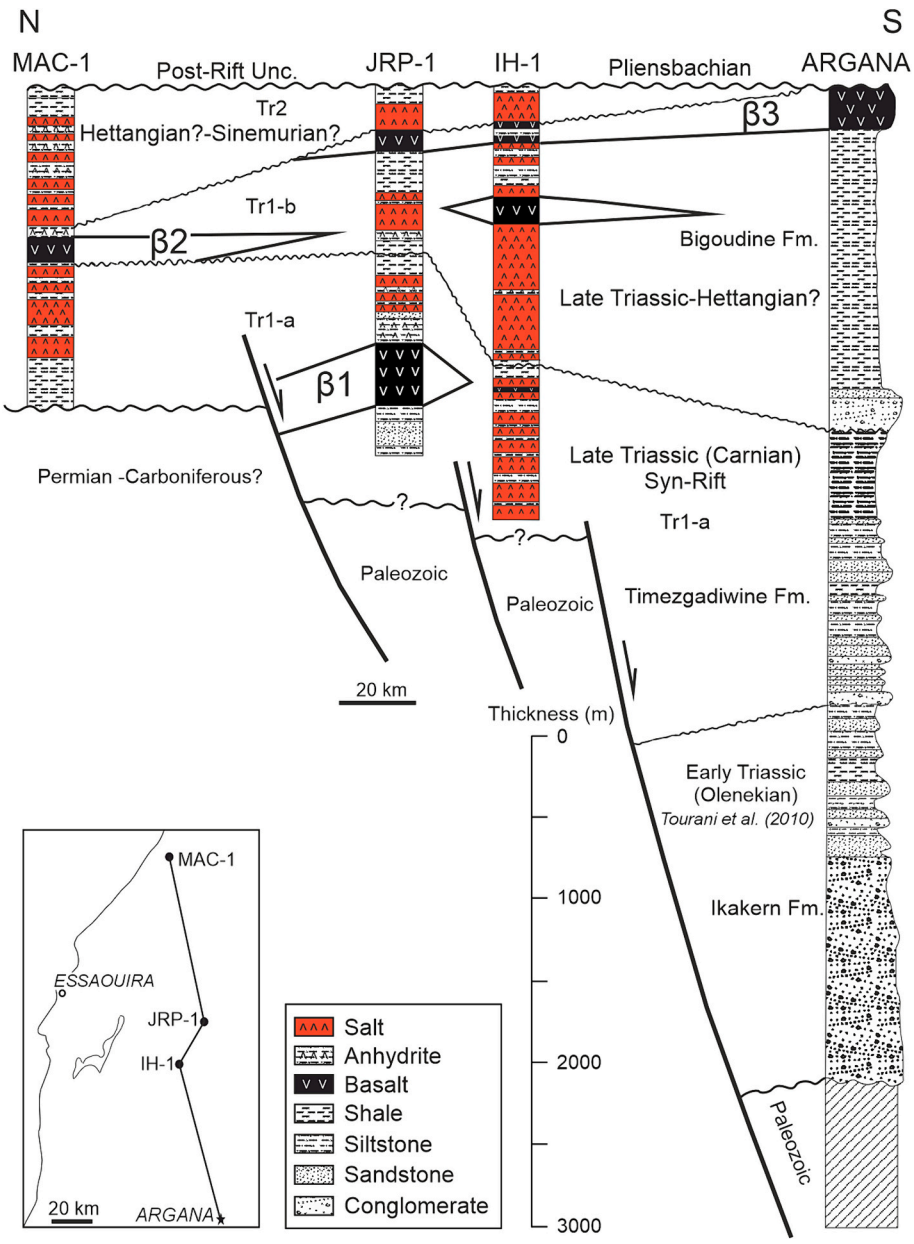

Fig. 6. Map showing the pre-breakup stage of the Central Atlantic between E North America and Morocco, showing the syn-rift depocenter migration (from Gouiza, 2011, modified after Labails, 2007; Le Roy et al., 1997; Sahabi et al., 2004; Tari and Jabour, 2013). The dashed line representing the Rhaetian depocenter on the Moroccan conjugate is speculative, since no well has drilled the Triassic succession in this area.

compositional variations of the OCT and what role inheritance may have played in setting up the transition between these two segments.

2. Dataset and methodology

The study area comprises 200,000 km2 on the Moroccan Atlantic margin (Fig. 9). The 2D seismic dataset comprises 7 surveys acquired between 1983 and 2018, with a total length of 11,700 km. The quality of the seismic imaging is variable, largely due to the influence of salt bodies that negatively affect the underlying seismic resolution. In this study we will present eight seismic transects that were selected based on their good imaging quality, representativeness and orientation. Most of the seismic sections have not been published to date, except for sections A-A' (Uranga et al., 2022), *E*-E' (Biari et al., 2015; Klingelhoefer et al., 2016) and F-F′ (Klingelhoefer et al., 2016). A total of 13 seismic horizons were interpreted, with a special focus on the Upper Triassic to Lower Jurassic interval. The stratigraphic well tops and time-depth relationships database constraining the seismic horizons interpretation presented in this study is based on a compilation of published data from several articles and PhD theses (Hinz et al., 1982b; El Khatib, 1995; Hafid et al., 2000, 2008; Gouiza, 2011; Wenke, 2014; Pichel et al., 2019; Bishop, 2020; Ady et al., 2022) (Fig. 9). The scarcity of deep wells reaching the Upper Triassic to Lower Jurassic succession in distal settings increases the uncertainty of the seismic interpretation at these levels. Therefore, seismic interpretation relies mainly on the extrapolation of stratigraphic data from wells located on the shelf. Two significant exceptions are the DSDP-544 and MZ-1 wells, located offshore El Jadida and Essaouira, respectively (Fig. 9), which reached the basement (Hinz et al., 1982b, 1984; Bishop, 2020; Ady et al., 2022).

The seismic data displayed in this study follow the American standard polarity criteria (SEG), i.e., an increase in acoustic impedance with depth is represented by a positive reflection event (colored in red). For

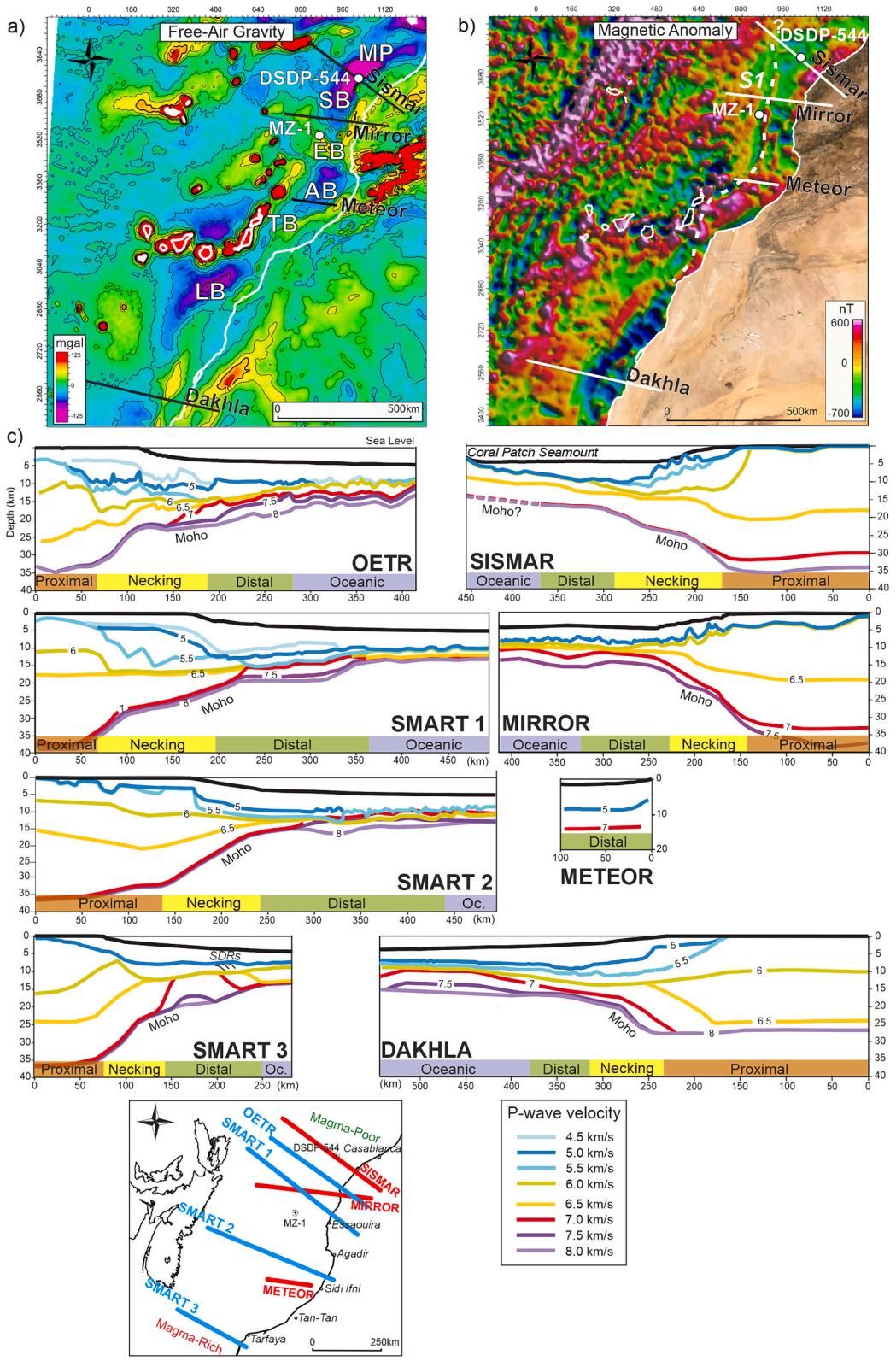

Fig. 8. a) Free Air gravity anomaly map from the Earth Gravitational Model 2008 (Pavlis et al., 2012); b) Magnetic anomaly map (Dyment et al., 2015); c) Deep seismic reflection profiles from the Nova Scotia (left side) – Morocco (right side) conjugate margins, modified from Contrucci et al. (2004), Funck et al. (2004), Dehler et al. (2004), Wu et al. (2006), Labails et al. (2009), Makris et al. (2010), Biari et al. (2015), Klingelhoefer et al. (2016), Lau et al. (2018). Tectonic domains and terminology were adopted from the criteria proposed by Péron-Pinvidic et al. (2013). For the purpose of this figure, the proto-oceanic domain is considered to be included in the oceanic domain. Location map showing the paleo-geographic reconstruction at the minimum closure of the conjugate margin after Louden et al. (2013) with Nova Scotia seismic profiles in blue and Moroccan profiles in red. (For interpretation of the references to colour in this figure legend, the reader is referred to the web version of this article.)

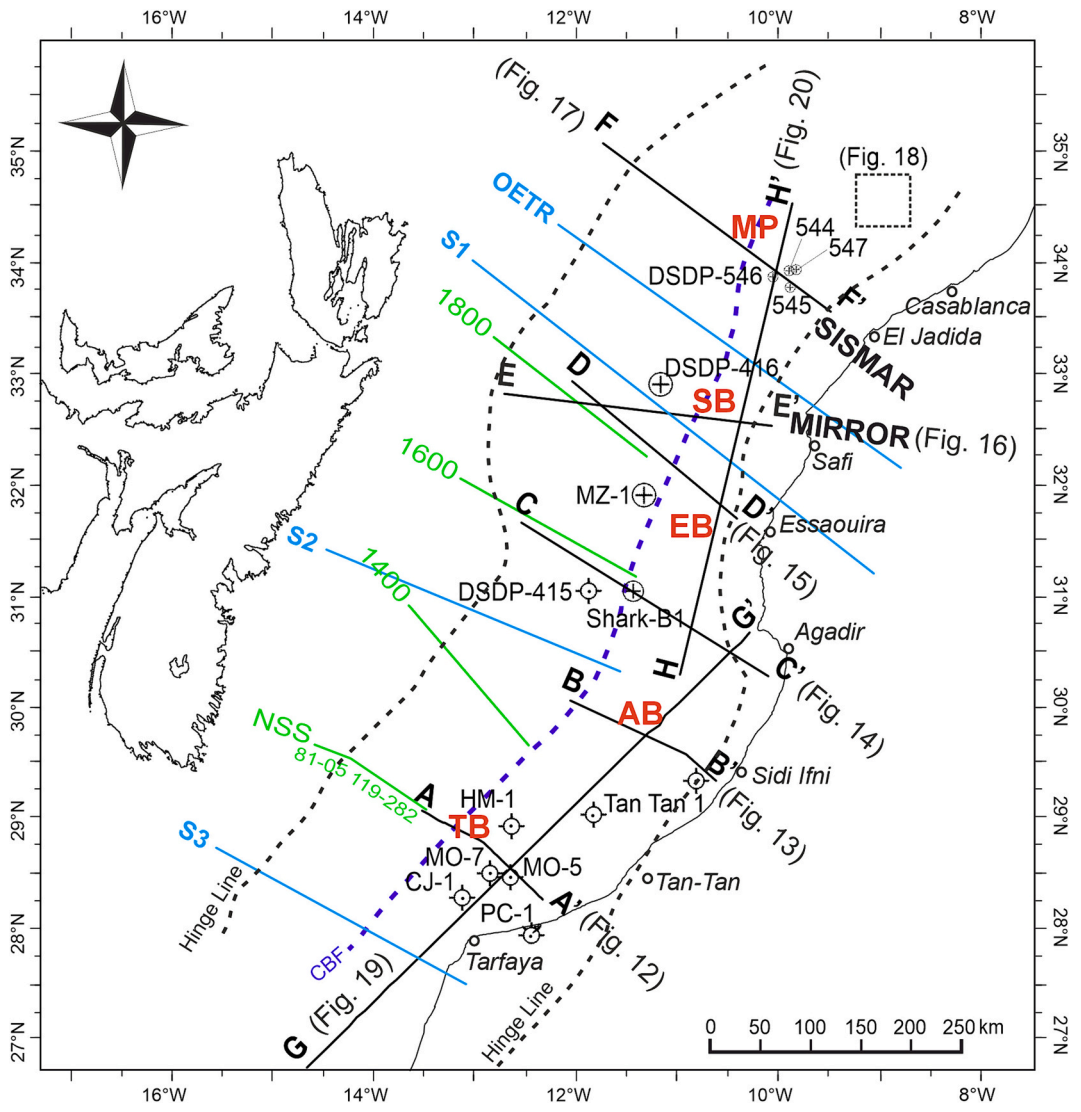

Fig. 9. Paleoreconstruction based on Sahabi et al. (2004) reconstruction poles and modified from the version presented by Louden et al. (2013). The location of the African continent is maintained as a fixed reference and Nova Scotia is rotated to its relative position with respect to Africa at 195 Ma. Black lines correspond to the seismic transects from the Moroccan margin, green lines correspond to key seismic transects on the Scotian Basin and light-blue lines represent the seismic refraction / deep reflection profiles acquired on the Scotian margin. Mirror and Sismar seismic transects match the path of the profiles presented in Fig. 8c; CBF: Continental Breakup Front; TB: Tarfaya Basin; AB: Agadir Basin; EB: Essaouira Basin; SB: Safi Basin; MP: Mazagan Plateau. (For interpretation of the references to colour in this figure legend, the reader is referred to the web version of this article.)

the sake of coherency, all the seismic sections will be presented in two-way travel time (TWT), except for transect G-G' (Fig. 19), which will be presented in depth (TVDSS). Amplitude balancing between the different surveys was performed prior to the interpretation to minimize differences in the response of the correlated seismic events. Furthermore, free-air gravity (Pavlis et al., 2012) (Fig. 8a) and magnetic anomaly maps (Dyment et al., 2015) (Fig. 8b) were integrated to aid in the interpretation and the definition of the tectonic domains. The potential field dataset, together with the available deep seismic profiles (MIRROR, SISMAR and METEOR, see Fig. 8) allowed for a confident identification of the OCT.

2.1. *Seismic interpretation criteria*

Setting up a well-defined seismic interpretation criterion is crucial for establishing the distribution and the tectonic setting of the primary salt basin (Fig. 10), especially in the pre-salt units which are usually subject to alternative interpretations and rely on potential field data and wide-angle/refraction velocity models. Furthermore, the autochthonous salt interpretation is sometimes challenging due to several factors such as an unsuitable seismic acquisition geometry, variable subsalt lithologies, and the generally complex overlying diapirs and sheets that hinder illumination of deep seismic events (Jones and Davison, 2014; see Chapter 13 in Jackson and Hudec, 2017). Due to these inherent difficulties, this study aims to integrate all available seismic transects from various directions to construct a robust 3D model. This comprehensive approach significantly reduces the uncertainty in our interpretations. The main criteria for interpreting the autochthonous salt considers its high reflectivity and its triangular geometry, reflecting the lateral divergence of the top and base salt from primary welding surfaces. In our study, we categorize the seismic facies into four main types based on their geophysical signatures and tectonic contexts (Fig. 10). The *syn*-tectonic facies, usually described at the proximal and necking domains, includes *Facies A*, characterized by deep, discontinuous, and fault-bounded reflections with low reflectivity and signal-to-noise ratio, and *Facies B*, which exhibits semi-continuous, laterally truncated reflections with a wedge-shaped geometry and medium reflectivity. The autochthonous salt facies, commonly observed at the proximal, necking

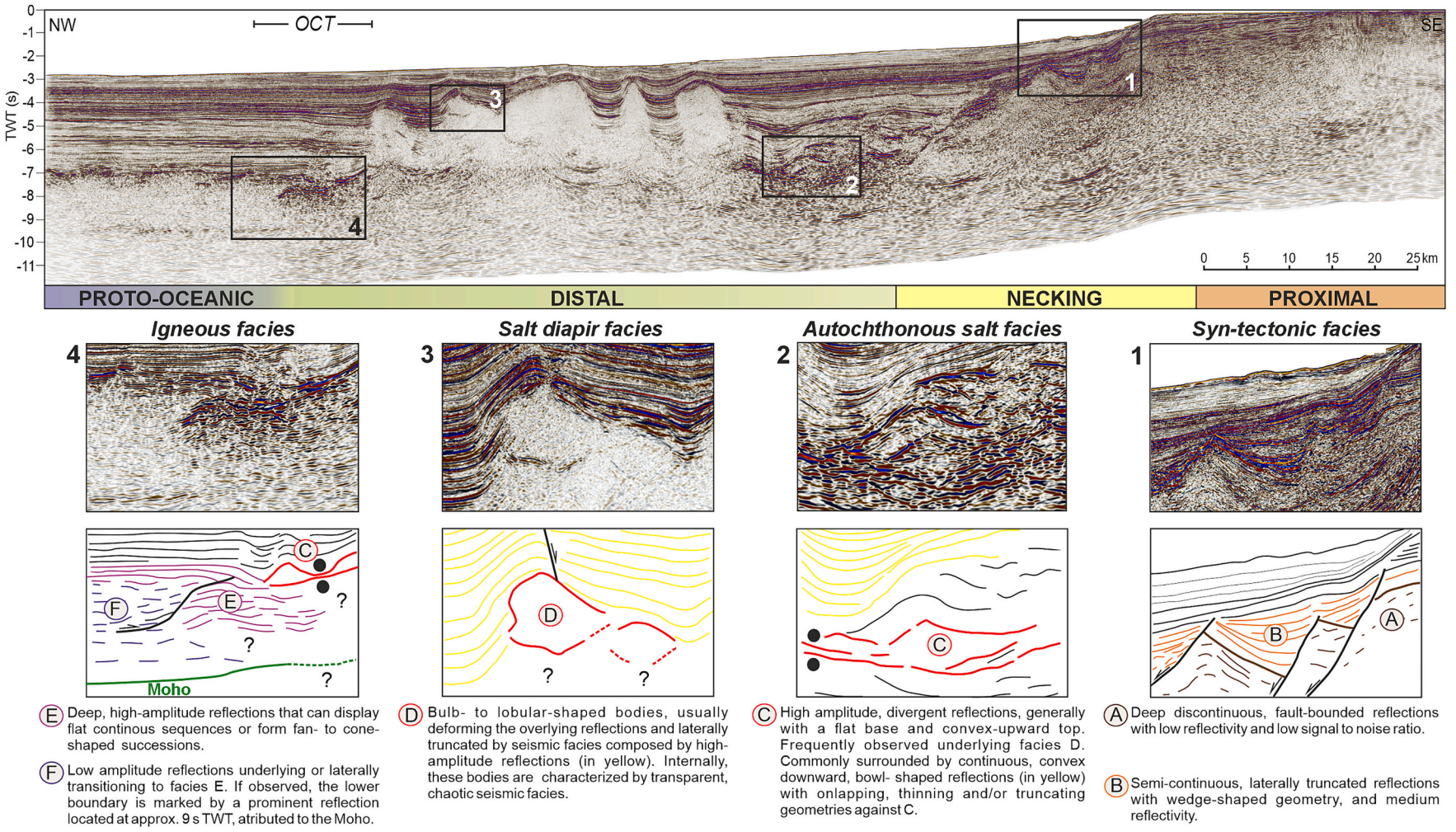

Fig. 10. Seismic transect B-B′ (Fig. 14) is used to illustrate the criteria adopted for the definition of key seismic facies that are useful to define the depositional setting of salt. In the figure, the different seismic facies associations are located at the tectonic domains where they are most frequently (but not exclusively) observed.

and distal domains, *Facies C*, is distinguished by high-amplitude, divergent reflections with a flat base and a convex-upward top, often underlying or associated with bowl-shaped reflections that display onlapping, thinning, or truncating against it. The salt diapir facies, most commonly observed at the distal domain and less frequently at the proximal and necking domains, *Facies D*, comprises bulb- to lobular-shaped bodies that deform overlying layers and are internally characterized by a transparent, chaotic seismic signal. Lastly, the igneous facies commonly described at the distal and proto-oceanic domains, is divided into *Facies E*, featuring deep, high-amplitude reflections that form flat continuous sequences or fan- to cone-shaped successions, and *Facies F*, noted for its low-amplitude reflectors that transition laterally to *Facies E* or underlie it, sometimes with a prominent underlying reflection at approximately 9 to 10 s TWT, attributed to the Moho.

This study employs terminology specific to salt tectonics. To clarify the key terms used throughout, we provide a succinct summary based on the comprehensive glossary by Jackson and Hudec (2017), and referenced cited therein (Fig. 11). A *salt diapir* is a mass of salt that has moved in a ductile manner, creating discordant contacts with the surrounding overburden. Salt diapirism can be broadly classified into three main types based on their formation and behaviour: *reactive diapirism* occurs when an elongated, sharp-crested diapir is pushed into spaces created by regional extensional thinning during processes such as rifting or gravity spreading; *passive diapirism* is characterized by the syndepositional growth of a diapir. As sediments accumulate around the diapir, its exposed or shallowly buried crest rises episodically. The base of the diapir, along with the encasing strata, subsides by salt withdrawal as sediments continues to fill the basin; *active diapirism* involves the diapir rising by arching, uplifting, or shouldering aside a thick (> 300 m) roof. In our study area active diapirism occurs when a buried and inactive diapir with a depleted source layer that gets rejuvenated during shortening (Rowan and Giles, 2021). Moreover, in our study area it is important to differentiate between *autochthonous or primary salt*, which is a salt layer that rests on its original, stratigraphically older subsalt strata or basement. Conversely, an *allochthonous* salt body is a subhorizontal or moderately dipping, sheetlike salt diapir emplaced at stratigraphic younger levels above the autochthonous source layer. In addition, some descriptive terms that will be used through this article include: *salt roller* which is an asymmetric salt structure that develops a normal-faulted contact with the overburden and constitutes a sign of regional thin-skinned extension; *salt anticlines*, defined as elongated mounds of salt having concordant overburden; a *salt sheet* is an allochthonous salt sourced from a single feeder whose breadth is several times greater than its maximum thickness; a *salt weld* is a surface or zone joining strata originally separated by autochthonous (primary weld) or allochthonous salt (secondary or tertiary weld); the *stem or feeder* of a diapir is a comparatively slender part of a salt diapir below the bulb and a minibasin is a small intrasalt basin largely surrounded by and subsiding into relatively thick allochthonous or autochthonous salt.

In this study, eight seismic transects covering the Moroccan Atlantic margin will be presented: six representative dip-oriented transects, from south to north; and two margin-parallel transects to illustrate the along-strike variations in structural style. The interpreted seismic units are: the Paleozoic pre-rift basement, the Upper Triassic pre-salt deposits, the Rhaetian-Hettangian salt, the Lower Jurassic interval (Hettangian to Pliensbachian), the Pliensbachian to Toarcian interval, the Middle to Upper Jurassic (Aalenian to Tithonian) succession, the Cretaceous strata, and the Cenozoic sediments. The delineation of tectonic domains (proximal, necking, distal, proto-oceanic, and oceanic) was based primarily on seismic interpretation, applying the criteria established in section 1.1. In cases where the seismic transects are not deep enough, the definition of tectonic domains is more uncertain and relies in part on potential methods and the extrapolation of wide-angle seismic reflection and refraction data from the MIRROR and SISMAR profiles (Fig. 8).

3. Interpretation

In the following sections, we present the observations and corresponding interpretations of the seismic profiles. For each dip-oriented profile, and starting in the south, we describe first the crustal features, then the autochthonous salt, and finally the shallow diapir and sheet geometries. We then describe the two strike lines from south to north.

3.1. Tarfaya Basin

Seismic transect A-A' (Fig. 12) is a composite seismic section located in the offshore Tarfaya Basin (Figs. 4 and 9), on the southernmost segment of the study area. The crustal architecture in this transect is characterized by a proximal domain with high free-air gravity and magnetic anomaly values. Despite the poor quality of the 2D seismic data covering this domain, an association of seismic facies A and B (Fig. 10) allowed us to define horsts and grabens with a top of the acoustic basement located at a minimum depth of 4 s TWT (Fig. 12). Basinward, the boundary between the proximal and necking domains is uncertain due to the limited vertical extension of the 2D seismic data (dashed line in Fig. 12). It is confined by the delimitation of domains on seismic transect G-G' (Fig. 19) and by a progressive decrease in the free-air gravity value to the NW. In the necking domain, the deepening of the basement is interpreted to be caused by normal faults delimiting half-grabens where wedge-shaped reflections are interpreted as the *syn*-tectonic deposits (facies A and B in Fig. 10). Basinward, the distal domain is 45 km wide and is characterized by low free-air gravity anomaly values. The top basement at the distal domain is located at and average of 7 s TWT (Uranga et al., 2022). The seaward limit of the distal domain is marked by an outer high (OH in Fig. 12) located at 6.2 s TWT, which displays discontinuous high amplitude reflections (seismic facies E in

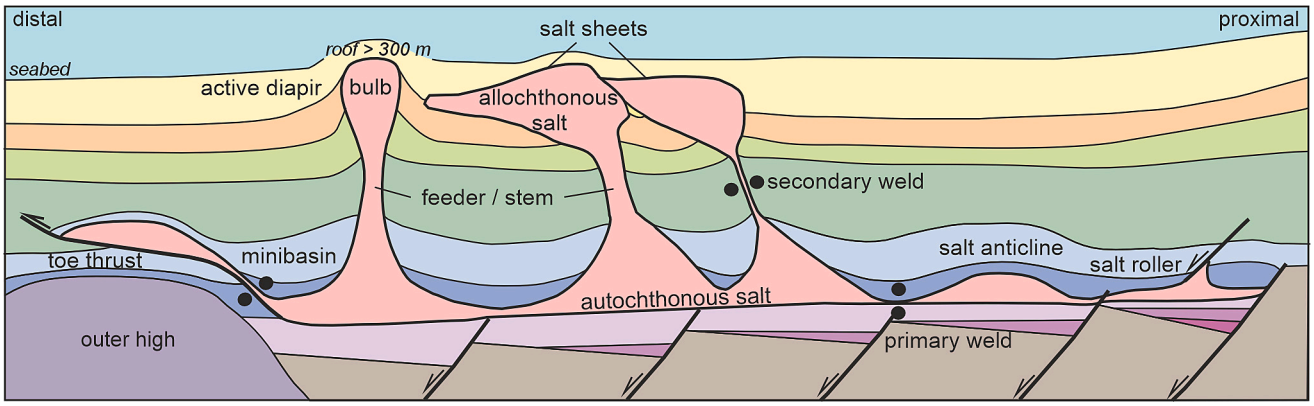

Fig. 11. Cartoon illustrating the most common salt-tectonic terminology used in this study.

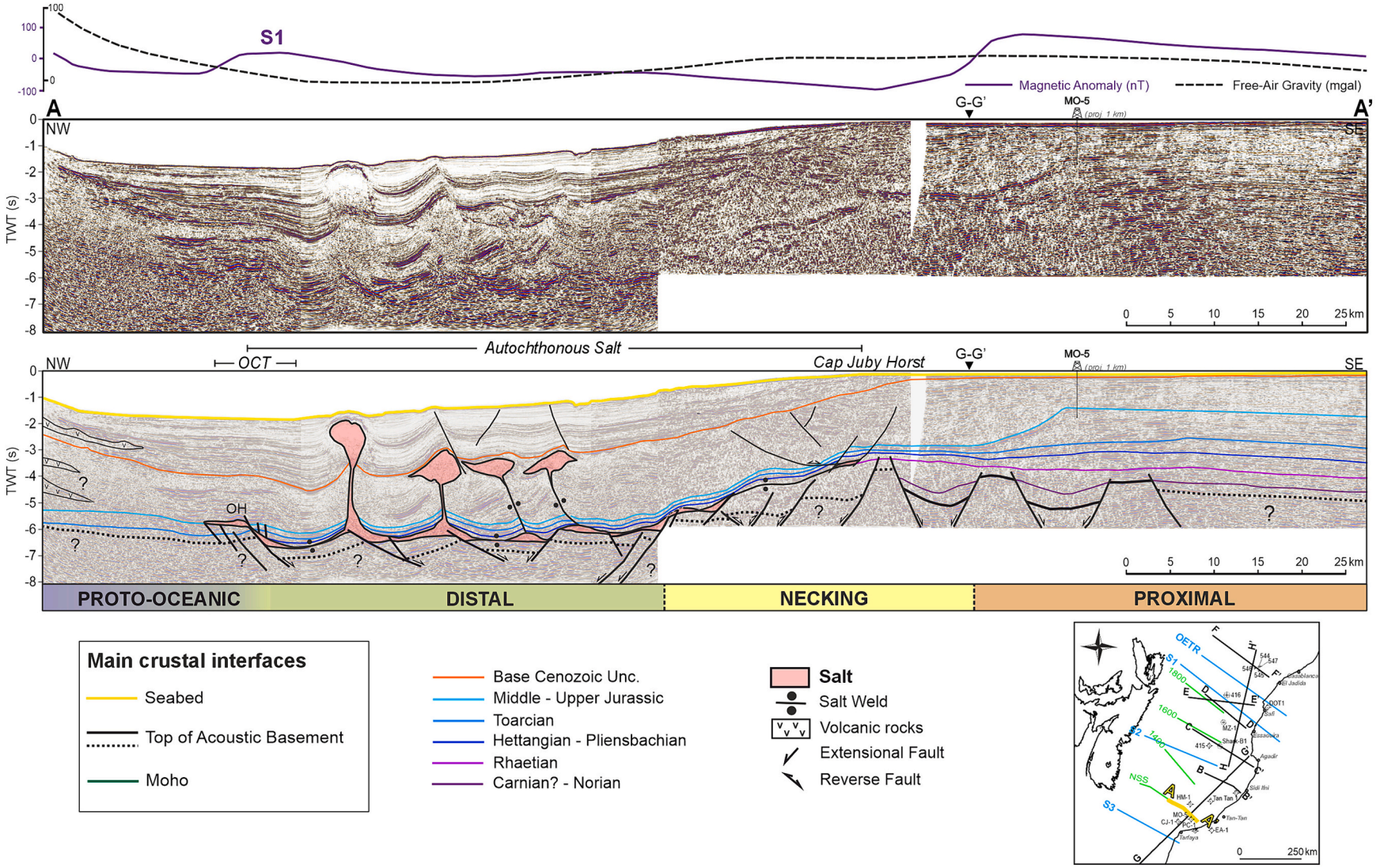

Fig. 12. Uninterpreted and interpreted versions of seismic transect A-A' located in the offshore Tarfaya Basin, on the southernmost segment of the study area. On top, magnetic and free-air gravity anomalies. For a more detailed interpretation of the Mesozoic succession, please see Uranga et al. (2022). OH: Outer High. Seismic data courtesy of Repsol. For a high-resolution version of this transect, the reader is referred to the supplementary material available online.

Fig. 10) and coincides with the S1 magnetic anomaly, representing the limit of the OCT.

The autochthonous salt is interpreted above the syn-tectonic succession across the necking and distal domains (Fig. 12). In the necking domain, the autochthonous salt is characterized by a triangular geometry (seismic facies C in Fig. 10) overlain by gently folded strata, interpreted as a salt roller that marks the landward limit of the salt basin. Both the base and top of the salt are offset by major normal faults at the transition between the necking and distal domains. Basinward, the main salt depocenter is located in the distal domain where the autochthonous salt is thicker and feeding diapiric structures (seismic facies D in Fig. 10). Here, the base salt is interpreted to be offset by low-angle normal faults, which are best observed at the distalmost salt pedestal (Fig. 12). The distal boundary of the autochthonous salt is represented by high-amplitude, wedging reflections stepping up and onlapping onto the outer high. On top of this high, a small allochthonous salt sheet is interpreted.

The distal domain is characterized by two main sets of diapirs: a proximal set displaying welded, counter regional (seaward-leaning) feeders associated with salt sheets; and a distal set of squeezed, nearly vertical stocks deforming the modern-day seabed (Fig. 12). According to Uranga et al. (2022), both sets were rejuvenated by shortening during the Atlasian contraction, causing the secondary welding of the proximal structures and ongoing diapirism of the distal ones. In summary, the autochthonous salt in the Tarfaya Basin is found mostly in the distal domain, where normal faults offset the base salt.

3.2. Agadir Basin

Seismic transect B-B′ (Fig. 13) is located in the southern segment of the Agadir Basin (Figs. 4 and 9). The crustal architecture along this transect is characterized by a proximal domain with basement horsts and grabens infilled by *syn*-tectonic deposits (seismic facies A and B in Fig. 10). The top basement is interpreted at approximately 2.5 s TWT, coinciding with high gravity-anomaly values. Basinward, the transition to the necking domain is characterized by an abrupt deepening of the top of the basement, from 2.5 s to 7 s TWT (Fig. 13), caused by a set of crustal-scale, basinward-dipping normal faults delimiting rotated basement blocks, but the Moho cannot be interpreted with confidence. To the northwest, the distal domain (Fig. 13) has a width of 68 km (23 km wider than in the Tarfaya Basin) and is characterized by the deepening of the top basement (from 7 to 8 s TWT) in association with low free-air gravity-anomaly values. In the central and distal segments of this domain, the interpretation of the top of the basement is hindered by the presence of the overlying salt and, therefore, speculative. However, at the salt-free OCT, it is possible to identify a set of high-amplitude reflections (seismic facies E in Fig. 10) forming an outer high (OH in Fig. 13), which coincides with the S1 magnetic anomaly and an increase in free-air gravity values. Basinward, the transition to the proto-oceanic domain is represented by a set of layered, high-amplitude reflections, located at 7 s TWT (seismic facies E) and interpreted as volcanic rocks, overlying transparent seismic facies (seismic facies F) interpreted as igneous intrusions. At deeper levels (9.5 s TWT), a sharp, sub-horizontal and continuous reflection is interpreted as the oceanic Moho discontinuity.

The autochthonous salt in transect B-B′ is confined to the distal domain (Fig. 13). On its landward limit, the base of the salt is interpreted to be truncated by the extensional faults marking the boundary between the necking and the distal domains. The interpretation of the proximal salt structures in the distal domain is based on the identification of seismic facies C and D (Fig. 10) related to salt antiforms and sheets. In this segment of the transect, it is possible to observe that the base of the salt is subtly offset by normal faults developing a seaward-stepped geometry. Basinward, the presence of salt structures at shallower levels reduces the quality of the underlying seismic data and increases the uncertainty in the interpretation of the autochthonous salt (Fig. 13), making it impossible to assess whether the base salt is offset by normal faults or not. However, the distal pinch-out of the autochthonous salt is well-imaged and represented by an onlapping surface against the outer high at the OCT (Fig. 13).

The distal domain is characterized by isolated, flaring diapirs and salt sheets (seismic facies D in Fig. 10) (Fig. 13) that were rejuvenated by shortening during the Late Cretaceous to Cenozoic until the feeders became welded. Conversely to what is observed in the Tarfaya Basin, it is not possible to differentiate between a proximal set of buried structures and a distal set of actively growing structures (compare Figs. 12 and 13). Moreover, it is noteworthy that in neither area is there evidence for the existence of a linked salt-detached gravitational system.

Seismic transect C-C′ (Fig. 14) is located in the northern segment of the Agadir Basin (Figs. 4 and 9). The landward crustal architecture of this transect is characterized by a progressive deepening of the top basement (from 4 s to 7 s TWT) from SE to NW. This matches a correlative decrease in free-air gravity-anomaly values and is accommodated by a set of faulted and tilted crustal blocks (seismic facies A and B) defining the necking domain. Basinward, the top of the acoustic basement in the distal domain is poorly imaged due to the effect of the overlying salt. However, low free-air gravity-anomaly values and the interpretation of the autochthonous salt can be used as a proxy for delimiting this domain, which is 18 km wider than in the southern segment of the basin. The presence of an allochthonous salt nappe at the OCT does not allow us to confidently interpret the limit of the distal domain, which is mainly delineated by the S1 magnetic anomaly (Fig. 14). Seaward, the top of the acoustic basement is well defined (between 6 and 6.5 s TWT) and characterized by seismic facies E and F (Figs. 10 and 14). Deeper in the section, a discontinuous reflection observed at 9 s TWT (Fig. 14) is interpreted as the Moho marking the base of a thick (average thickness of 2.2 s TWT) crust defined here as the proto-oceanic domain. The Moho discontinuity serves as a detachment for a set of normal faults, some of which have been reactivated in the Cenozoic. In addition, 1 s TWT above the Moho, an acoustic interface separates an upper strongly reflective layered package from a lower, more transparent, and chaotic seismic facies, which is interpreted as a detachment surface for some of the normal faults. This detachment could correspond to a preserved brittle/ductile boundary. Finally, the transition to the oceanic domain is marked by a decrease in crustal thickness (from 3 s TWT to 1.5 s TWT) (Fig. 14).

One important difference between transect C-C′ (Fig. 14) and transects A-A' (Fig. 12) and B-B′ (Fig. 13) is that autochthonous salt in the former is well developed in the necking domain. In the proximal area of the transect, divergent seismic facies C (see Fig. 10 for definition) and growth wedges above transparent triangular bodies are used to interpret salt pedestals and isolated anticlines with thick and arched isopachous roofs. The base of the autochthonous salt in these structures is interpreted to be offset by normal faults (Fig. 14). Interpretation of the more landward salt structures in the distal domain is based on the identification of seismic facies C and D (Fig. 10), related to salt pedestals and diapirs respectively. However, the poor quality of the seismic data of the pre-salt succession precludes confident interpretation of basement structures. In addition, the presence of thick allochthonous bodies in basinward areas hinders the identification of the autochthonous salt, increasing the uncertainty in the delineation of its distal limit.

The salt structures developed in the necking and distal domains are identified by seismic facies C and D, interpreted as isolated squeezed diapirs and salt sheets. Common folding of thick pre-kinematic roofs and even the modern seabed is interpreted to be caused by the contractional rejuvenation of the salt structures, dated as Cenozoic (cf. Pichel et al., 2019; Uranga et al., 2022) by *syn*-kinematic strata (see thinning successions in Fig. 14). Basinward, we interpret an allochthonous salt nappe emplaced out over proto-oceanic crust in the Meso-Cenozoic succession (label 1 in Fig. 14), the base of which is represented by a high-amplitude, semi-continuous, sub-horizontal reflection. The nappe is locally thick and associated with Cretaceous minibasins. It is unclear whether or how

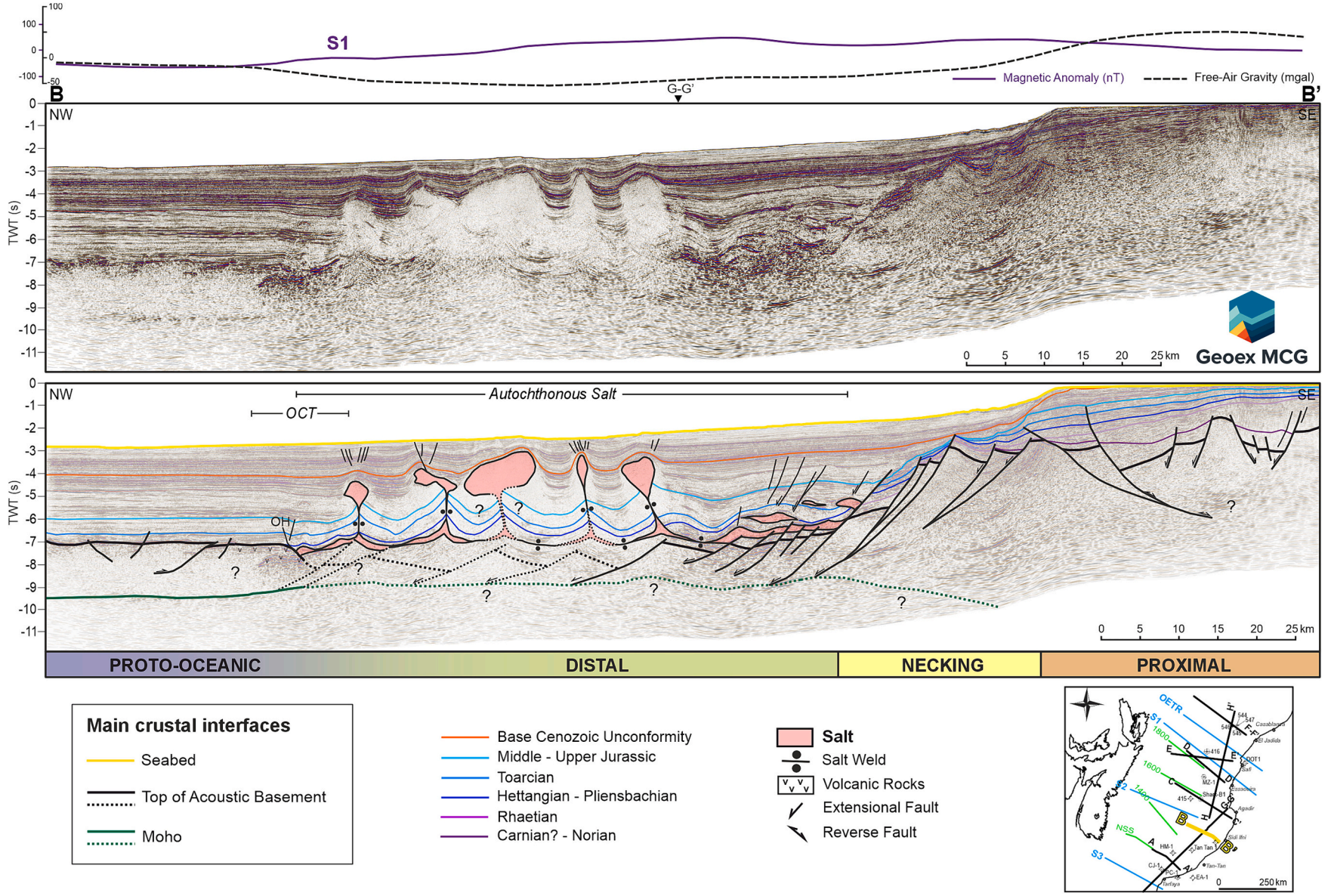

Fig. 13. Uninterpreted and interpreted versions of seismic transect B-B′, located in the southern segment of the Agadir Basin. On top, magnetic and free-air gravity anomalies. Seismic data courtesy of Geoex MCG Ltd. For a high-resolution version of this transect, the reader is referred to the supplementary material available online.

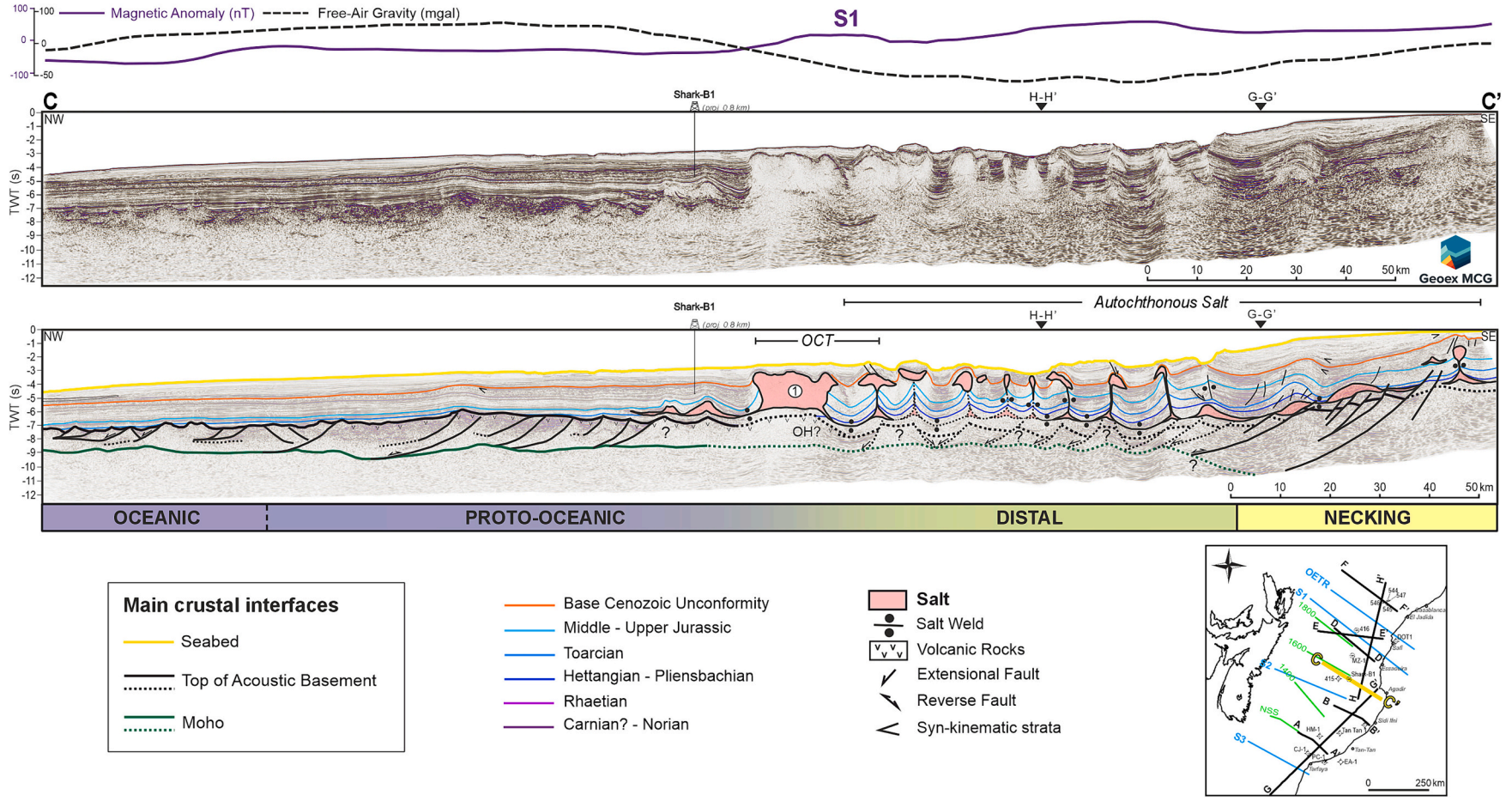

Fig. 14. Uninterpreted and interpreted versions of seismic transect C-C′, located in the northern segment of the Agadir Basin. On top, magnetic and free-air gravity anomalies. Seismic data courtesy of Geoex MCG Ltd. For a high-resolution version of this transect, the reader is referred to the supplementary material available online.

much the nappe served as a toe-thrust (see Tari et al., 2000, Tari and Jabour, 2013; Pichel et al., 2019), but the folded BCU and the onlapping lower Cenozoic reflections at the toe suggest at least some contractional reactivation in the Early Cenozoic.

3.3. Essaouira Basin

Northward, seismic transect D-D′ (Fig. 15) cuts obliquely through the proximal and necking domains of the offshore Essaouira Basin and the distal, proto-oceanic, and oceanic domains of the southern Safi Basin (Figs. 4 and 9). The top basement in the proximal domain is interpreted to lie between 1 s and 3 s TWT, coinciding with high free-air gravity-anomaly values (Fig. 15). The basement is seismically characterized by fault bounded, chaotic, discontinuous facies and overlying continuous, wedge-shaped reflections (seismic facies A and B in Fig. 10) interpreted as syn-tectonic sediments. Basinward, a narrow necking domain is characterized by deepening of the top basement from 2 s to 6 s TWT, matching progressively decreasing free-air gravity-anomaly values (Fig. 15), interpreted to be caused by a series of crustal-scale, seaward-dipping normal faults. Basinward, the distal domain in transect D-D′ has a width of 28 km (about one quarter of the width in seismic transect C-C′, see Fig. 14 for comparison), although this comparison must consider the obliquity of the transect. The interpretation of the top basement is highly uncertain due to a lower signal-to-noise ratio caused by the overlying salt and to the addition of igneous material indicated by high-relief paleo-volcanoes (with abruptly onlapping strata) and associated intrusions (seismic facies E and F in Fig. 10) and supported by analysis of the free-air gravity- and magnetic-anomaly values (Fig. 15). The proto-oceanic domain is characterized by a deepening of the Moho discontinuity (i.e., thicker oceanic crust) and the shallowing of the top basement (average depth of 7.5 s TWT). According to Ady et al. (2022), proto-oceanic crust was drilled by the MZ-1 well located 40 km to the SW of transect D- D′ (for location see Fig. 9). Seismic facies E and F (as defined in Fig. 10) are interpreted as volcanic wedges dipping both landward and basinward and infilling half-grabens. Some of the faults bounding these half-grabens are inverted and propagate through the Mesozoic cover, folding the BCU (Figs. 14 and 15). Onlapping reflections against the folded BCU indicate a Paleogene age for this tectonic inversion. The limit between the proto-oceanic and the oceanic domain is characterized by a shallowing of the Moho discontinuity from 10 s to 8.5 s TWT and the top basement from 7.5 to 7 s TWT on average (i.e., a thinner oceanic crust).

The autochthonous salt in the Essaouira Basin covers the proximal, necking, and distal domains (Fig. 15), indicating an abrupt landward shifting of the proximal edge of the primary salt basin compared to the Tarfaya and Agadir basins. In the proximal domain, small autochthonous salt bodies are confined within a shallow graben, with second-order normal faults offsetting the base salt. Similarly, the transition between the necking and the distal domains also contains bodies with seismic facies C (Fig. 10), interpreted as small salt anticlines and the pedestal of a large diapir. Here too, the autochthonous salt is bounded by faults delimiting basement blocks with a basinward-stepped geometry (Fig. 15). On the northwestern flank of the triangular paleo-volcano, divergent high-amplitude reflections indicative of salt (seismic facies C) are interpreted to be interfingered with high-amplitude reflections attributed to volcanic materials, suggesting that salt deposition was synchronous with volcanism, as it is the case in the onshore Essaouira Basin (Hafid, 2000) (Fig. 7).

A striking difference between seismic transects C-C′ (Fig. 14) and D-D′ (Fig. 15) is the number of salt structures identified (nine diapirs/salt sheets are interpreted in the distal domain of transect C-C′ but only one in transect D-D′, as well as only very small diapirs in the proximal domain). However, this is not representative of the structural style of the Essaouira Basin which, on the contrary, is a salt-rich segment of the Moroccan margin as shown by Hafid et al. (2000), Tari and Jabour (2013), Tari et al. (2017) and Pichel et al. (2019). The large salt diapir observed in the distal domain of transect D-D′ (Fig. 15) is asymmetric and has a steep upturned flap on its proximal flank, involving Lower Jurassic reflections interpreted as the pre-kinematic roof of this structure. The stratal cutoffs on the northwestern flank of the diapir suggest that flaring of the salt started in the Late Cretaceous.

3.4. Safi Basin

Seismic transect E-E' (Fig. 16) is located in the Safi Basin and corresponds to the MIRROR profile (Fig. 8c). The delineation of tectonic domains in this transect is in part based on the work of Biari et al. (2015). As can be seen, the top of the basement in the proximal domain ranges between 0.75 s TWT and 3 s TWT, matching high free-air gravity-anomaly values. This domain is characterized by an association of seismic facies A and B (Fig. 10), interpreted as half-grabens infilled by Rhaetian to lower Jurassic sediments. Basinward, the necking domain is defined by a deepening of the top of the acoustic basement, from 3 s TWT to 7.5 s TWT. This domain is characterized by tilted basement blocks delimited seaward by seaward-dipping crustal-scale faults, detached on the upper mantle, and marking the transition to the distal domain (Fig. 16). The top basement in the distal domain is poorly imaged by seismic data and its depth relies mainly on the interpretation of the base of the autochthonous salt layer and the velocity modeling carried out by Biari et al., 2015 (Fig. 8c). At its seaward boundary, a step up in the top basement topography matches the S1 magnetic anomaly and is interpreted as the limit of the OCT (Fig. 16). In contrast to what is observed on seismic transect D-D′ (Fig. 15), no paleo-volcanoes are identified at the OCT.

The autochthonous salt in the Safi Basin covers the proximal, necking, and distal domains. Due to the fair seismic quality, it is possible to identify high amplitude divergent reflections (seismic facies C in Fig. 10) suggesting the occurrence of salt pedestals and anticlines. Overall, the primary salt is distributed separately within distinct half-grabens and is absent on the intervening basement highs. One of the main differences between transect D-D′ (Fig. 15) and E-E' (Fig. 16) is that, in transect E-E', it is possible to interpret that both base and top of the autochthonous salt is offset by the main faults. Although the interpretation of the basement can be challenging, particularly in the distal domain where seismic quality is hindered by the overlying diapirs, the stepped and abrupt basinward deepening of the autochthonous layer suggests it has a syn-tectonic origin. The distal limit of the autochthonous salt basin is marked by a basement high matching the S1 magnetic anomaly, with an overlying allochthonous salt nappe associated with a series of salt anticlines.

The salt structures in transect E-E' (Fig. 16) can be recognized by an association of seismic facies C and D (Fig. 10). They consist of isolated, squeezed, rejuvenated diapirs, salt sheets, and salt anticlines. The Upper Cretaceous and the Cenozoic successions overlying these structures are frequently folded, and syn-kinematic strata suggest that this stage of contractional rejuvenation took place during the Cenozoic (Fig. 16).

3.5. Mazagan Plateau

Seismic transect F-F′ (Fig. 17) is located on the Mazagan Plateau and matches the location of the SISMAR profile (Fig. 8c). The delineation of tectonic domains in this transect is based on the works of Biari et al. (2015) and Klingelhoefer et al. (2016). The top basement in the proximal domain lies approximately at 3.5 s TWT and is characterized by landward-dipping extensional faults and related half-grabens (seismic facies A and B in Fig. 10), coinciding with an area of high free-air gravity-anomaly values (Fig. 17). Basinward, the transition to the necking domain is marked by the deepening of the basement from 3.5 s to 8 s TWT with a correlative decrease in free-air gravity-anomaly values. This deepening of the basement is caused by large basinward-dipping normal faults, one of which controls the location of the modern Mazagan Escarpment (Hinz et al., 1984) (Fig. 17). The DSDP-544

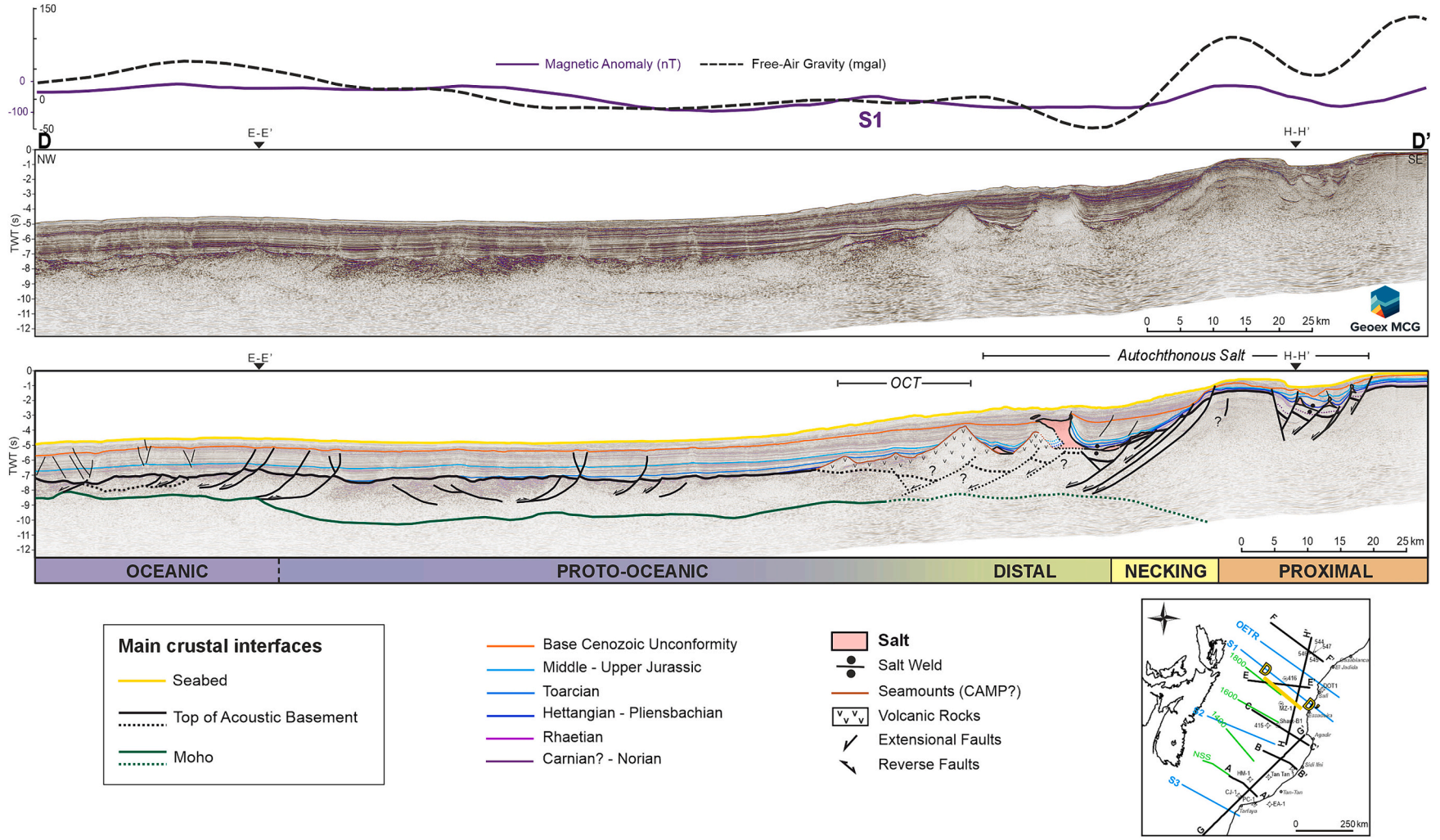

Fig. 15. Uninterpreted and interpreted versions of seismic transect D-D′, located in the offshore Essaouira Basin. On top, magnetic and free-air gravity anomalies. Seismic data courtesy of Geoex MCG Ltd. For a high-resolution version of this transect, the reader is referred to the supplementary material available online.

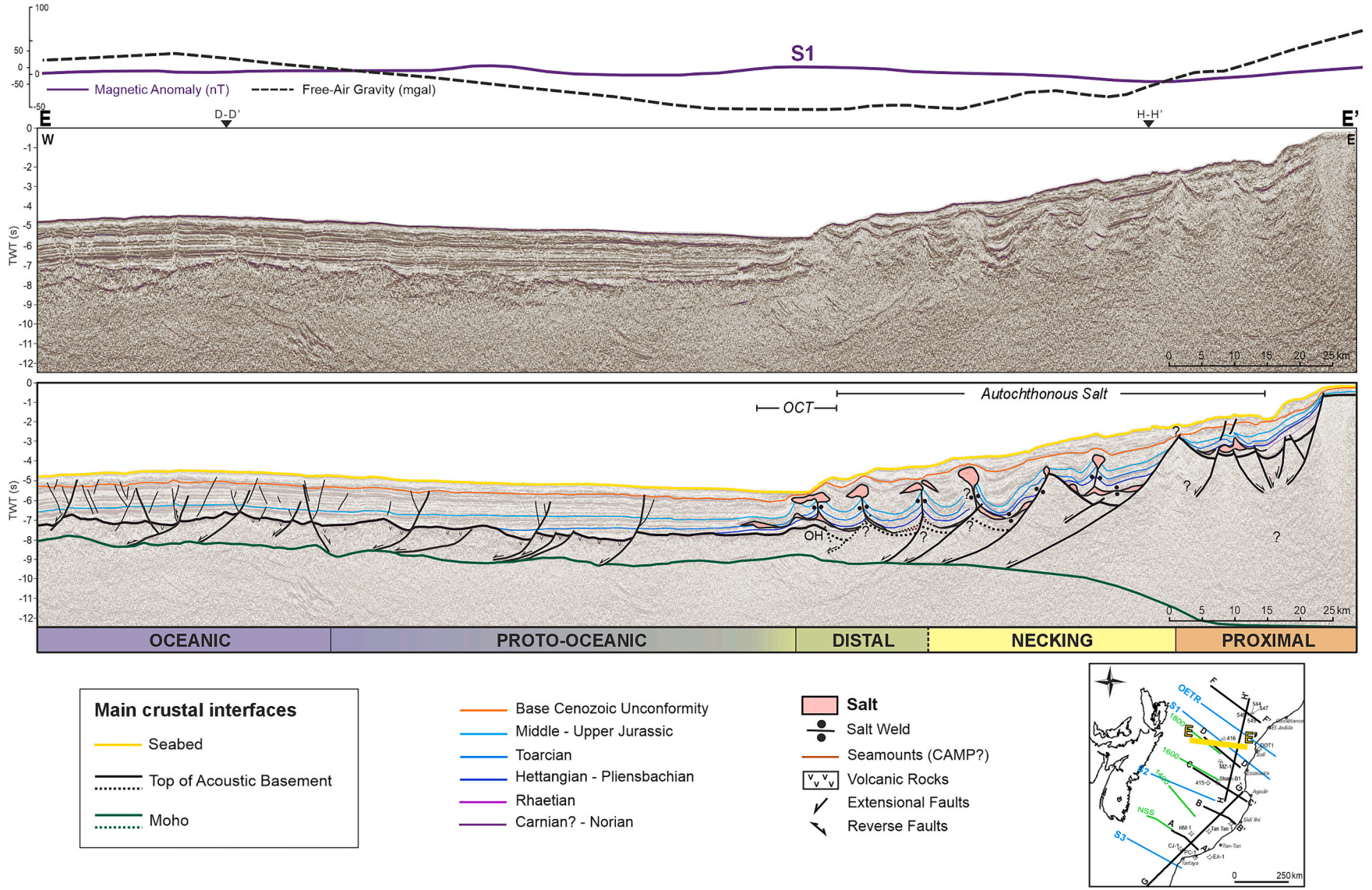

Fig. 16. Uninterpreted and interpreted versions of seismic transect E-E', located in the Safi Basin. On top, magnetic and free-air gravity anomalies. Seismic data courtesy of IFREMER (Biari et al., 2015). For a high-resolution version of this transect, the reader is referred to the supplementary material available online.

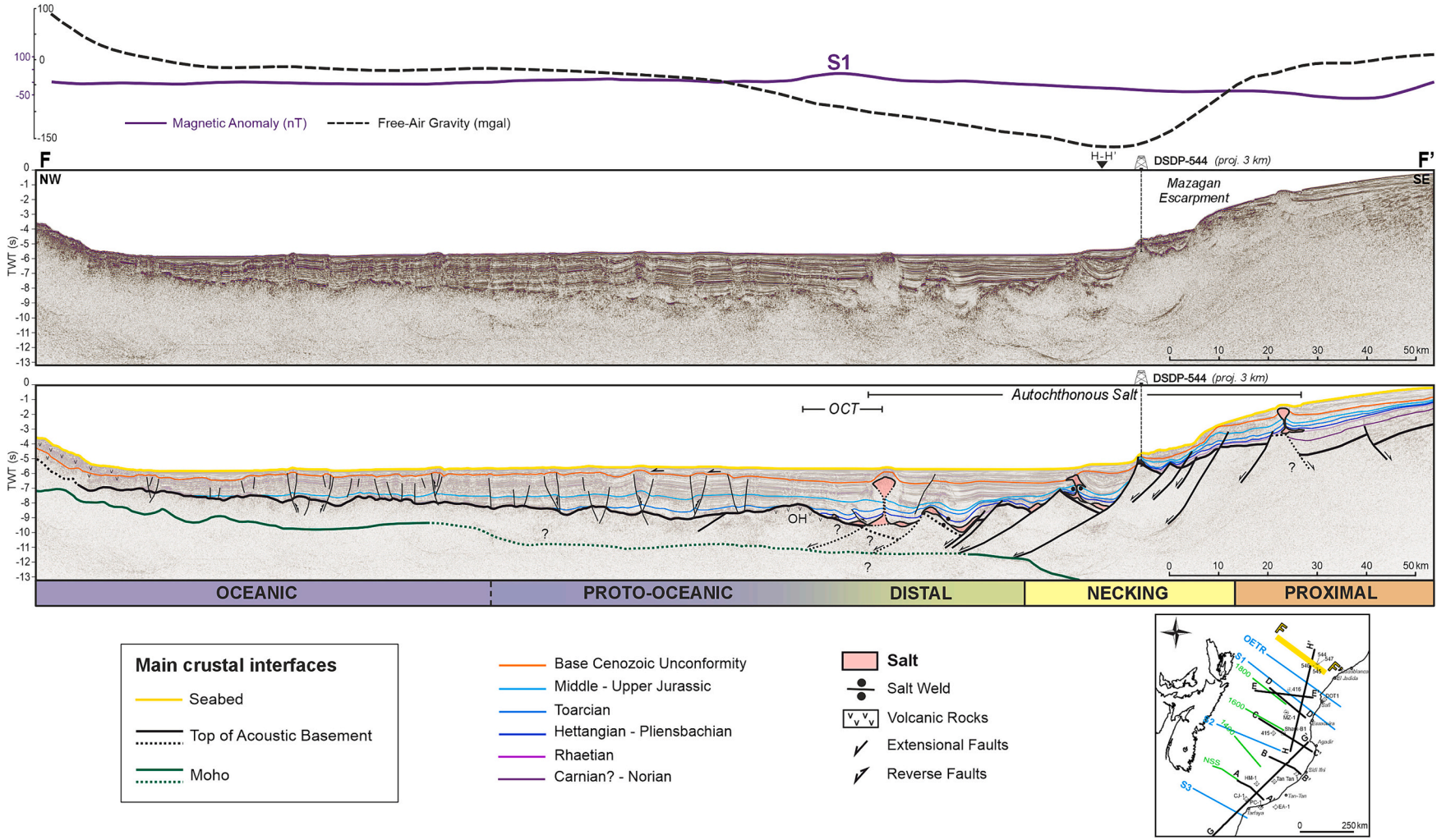

Fig. 17. Uninterpreted and interpreted versions of seismic transect F-F′, located in the Mazagan Plateau, offshore El Jadida. On top, magnetic and free-air gravity anomalies. Seismic data courtesy of IFREMER. For a high-resolution version of this transect, the reader is referred to the supplementary material available online.

well was drilled into its footwall and reached the top basement, which is composed of Paleozoic (556 ± 10 Ma) and Proterozoic (1950 to 1640 Ma) granodiorites (Kuiper et al., 2021). Basinward, the distal domain is characterized by a relatively narrow trough with a top basement interpreted between 9 s and 10 s TWT and the Moho inferred at 11 s TWT. Its distal limit is identified by an outer high, matching the location of the S1 magnetic anomaly, with a top basement at 8 s TWT and characterized by seismic facies E and F (Fig. 10) that are interpreted as volcaniclastic rocks. The transition to the proto-oceanic and oceanic domains is characterized by an ascending Moho from 11 s TWT to an average of 9.5 s TWT) and a relative increase in the relative proportion of seismic facies F. Moreover, it is possible to distinguish reverse faults, frequently decoupled from the basement, which are responsible for the folding of the Cenozoic succession. Finally, at the distalmost end of seismic transect F-F′ (Fig. 17), a bathymetric rise associated with the growth of a Cenozoic submarine volcano is observed.

The autochthonous salt in the Mazagan Plateau transect is distributed across the proximal, necking, and distal domains (Fig. 17). In all domains, most basement faults offset both the base and the top of the salt layer, such that the base salt steps progressively deeper from proximal to distal (from 3 s to 9.5 s TWT). Moreover, salt is usually observed in the core of faulted drape folds in the hanging walls of the half grabens. In the distal domain, Cenozoic reflections show wedge-shaped geometries and proximal offlaps against the flanks of a thick (700 ms TWT) roof related to the bulging of the modern seabed, in agreement with the folding of the Cenozoic succession observed in the proto-oceanic and oceanic domains. Basinward, the distal limit of the autochthonous salt basin is marked by the outer high identified at the OCT (Fig. 17).

Fig. 18 shows a NNW-SSE-oriented 2D seismic section from offshore Casablanca. According to its relative position with respect to the coastline and a comparison with seismic transect F-F′ (Fig. 17), this section is located in the necking domain. The improved seismic quality of Fig. 18 allows for a more detailed characterization of salt structural styles along this transect, with salt anticlines and salt-cored fault drape folds interpreted to be completely offset by normal faults. The salt diapirs and anticlines are contractionally rejuvenated.

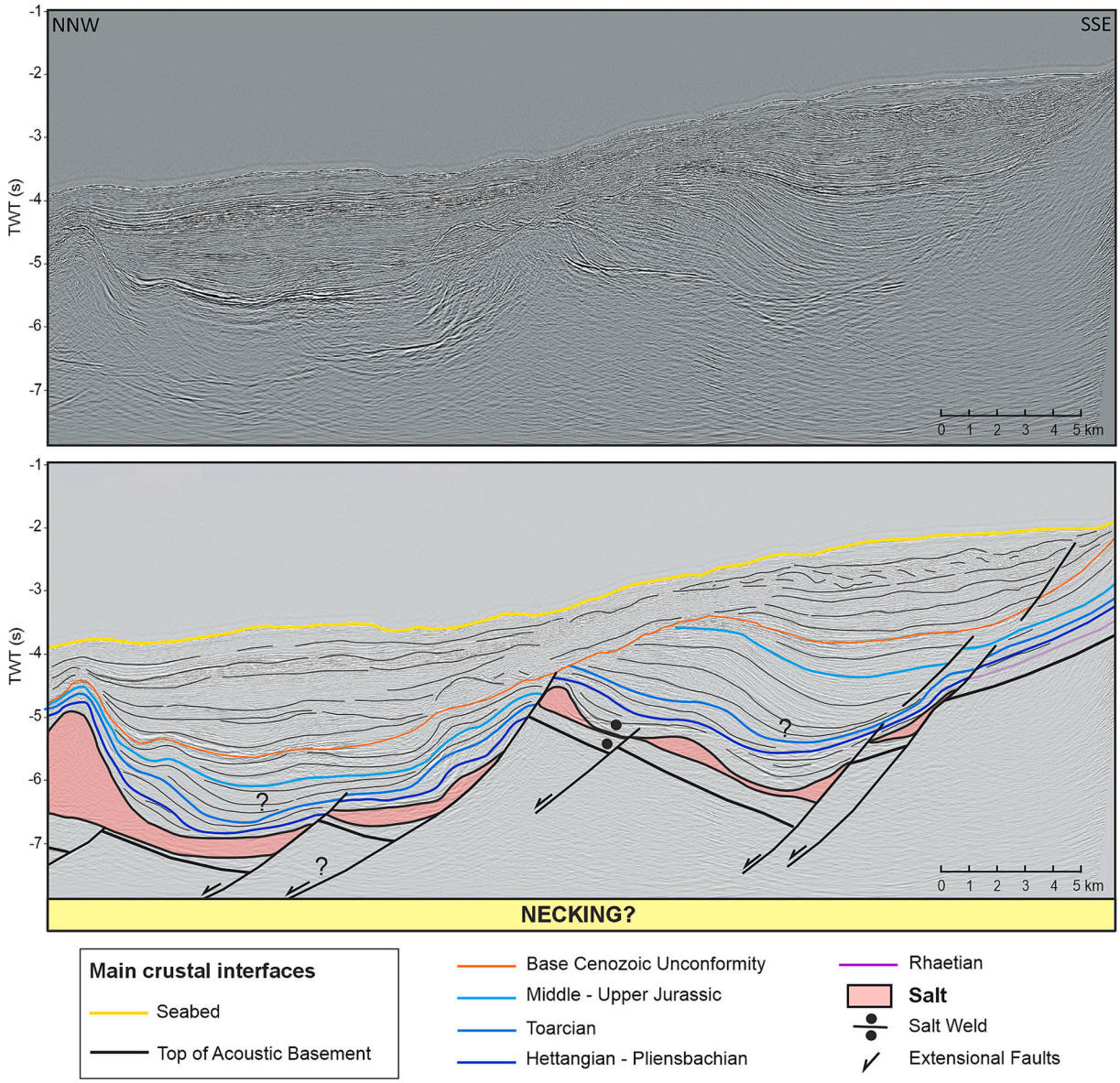

Fig. 18. Seismic section courtesy of ONHYM from a confidential, unspecified location offshore Casablanca (for an approximate location reference see Fig. 9). The interpreted stratigraphy in this section is based on analogies with the observations made on seismic transects E-E' (Fig. 16) and F-F′ (Fig. 17) since no well-seismic tie is available for this particular line. See text for description.

3.6. Strike-oriented transects

In this section, we will present two margin-parallel transects covering the entire study area. First, seismic transect G-G' (Fig. 19) covers the Tarfaya and Agadir basins. In the Tarfaya Basin, the Cap Juby high (CJH in Fig. 19a) constitutes a paleo high that controlled the evolution of the offshore Tarfaya Basin since Triassic times (Uranga et al., 2022). It separates a southwestern magma-rich segment of the Tarfaya Basin, where no salt was deposited, from a northeastern magma-poor segment where salt was accumulated (Louden et al., 2013) (Fig. 19b). From the Cap Juby High to the southwest, the top of the acoustic basement is interpreted to deepen progressively from 7 km to 14 km TVDSS at the transition from the proximal to the necking domain, coinciding with a gradual decrease in the free-air gravity-anomaly values. A series of high-amplitude, oblique-dipping reflections, observed between 10 and 13 kms TVDSS could correspond to SDRs. From the Cap Juby High to the northeast, the deepening of the top of the basement is more abrupt and accommodated by a set of transfer faults (Le Roy and Piqué, 2001). This set of faults is referred to here as the Sidi Ifni Transfer Zone (SITZ in further references) and marks the boundary between the Tarfaya and Agadir basins (Fig. 19b).

Transect G-G' (Fig. 19a) shows that the autochthonous salt basin is largely confined to the distal domain. However, the low seismic resolution at deep levels makes the detailed interpretation of the autochthonous salt highly uncertain. In some cases, it is possible to identify salt pedestals (seismic facies C in Fig. 10), with no apparent significant offsets in base-salt relief. This is due to the orientation of transect G-G' and contrasts with the base-salt topography interpreted on the dip-oriented transects B-B′ (Fig. 13) and C-C′ (Fig. 14).

Northward, seismic transect H-H′ (Fig. 20) images part of the distal domain in the Agadir Basin, the proximal and necking domains in the Essaouira and Safi basins, and the necking domain in the Mazagan Plateau. In the Agadir Basin, the low signal to noise ratio of the seismic data does not allow a confident interpretation of the subsalt reflections. However, the structural position of the autochthonous salt suggests that its base is offset by normal faults, as was observed on seismic transect C-C′ (Fig. 14). The limit between the Agadir and the Essaouira basins is characterized by a set of transpressional faults striking obliquely to the margin, which constitute the offshore extension of the South Atlas Fault zone (SAF in Figs. 4 and 20) (Le Roy and Piqué, 2001). Northward, in the offshore Essaouira Basin, inverted Paleozoic basement blocks represent the offshore termination of the Western Atlas, a tectonic province known as the Cap Tafelney Folded Belt (sensu Hafid et al., 2000, Fig. 21) or Atlantic Atlas (sensu Benabdellouahed et al., 2017). Further north, the transition to the Safi Basin is characterized by the presence of an inverted basement block (Fig. 20). From this point northward, the Safi Basin and the Mazagan Plateau are characterized by a necking domain where salt structures are completely offset by normal faults and confined to half-grabens separated by tilted basement blocks, as was observed on seismic transects *E*-E' (Fig. 16) and F-F′ (Fig. 17, see also Fig. 18).

3.7. Spatial distribution of tectonic domains and autochthounous salt

Interpretation of the entire seismic dataset (Fig. 9) enabled us to map the distribution of the tectonic domains and the autochthonous salt within that framework. Significant along strike variations occur on each (Fig. 21), along with contrasting relationships between the salt and the rift-related faults, which we describe in turn below.

The top basement time structural map shown in Fig. 21 shows the boundaries of the proximal, necking, distal, and proto-oceanic domains. In the south, the necking and distal domains of the Tarfaya Basin (TB in Fig. 21) are narrow when compared to the neighboring Agadir Basin (AB in Fig. 21). The Sidi Ifni Transfer Zone (SITZ in Fig. 21) marks the transition to the Agadir Basin, where the distal and necking domains progressively widens to the north (see Figs. 13 and 14). Both the distal and necking domains reach their widest extent in the northern Agadir Basin. The transition from the Agadir to the Essaouira Basin is marked by an abrupt narrowing and westward displacement of the two domains and by basement uplift caused by thick-skin inversion (Figs. 19 and 21), matching the offshore extension of the South Atlas Fault zone (SAF in Fig. 21). Northward, the Safi Basin displays a narrower distal domain than in the Essaouira Basin. Moreover, the proximal domain is characterized by prominent Paleozoic basement highs.

Finally, the transition to the Mazagan Plateau is marked by a progressive seaward shifting of the tectonic domains relative to the coastline, caused by the presence of stable Paleozoic basement blocks in the near offshore and onshore area (Western Meseta in Fig. 4).

The distribution of the salt basin relative to the tectonic domains and rift-related faults changes significantly from south to north (Fig. 21). In the Tarfaya and southern Agadir basins, the autochthonous salt is almost exclusively confined to the distal domain, where only its base is offset by seaward-dipping normal faults (Figs. 12 and 13). In the northern segment of the Agadir Basin, the salt basin expands continentward into the necking domain, and normal faults offset both the base and top salt but little of the overburden (Figs. 14 and 21). In the Essaouira Basin, salt-detached thin-skinned and thick-skinned inversion are responsible for the NE-SW oriented anticlines forming the Cap Tafelney fold belt (Fig. 21). Interestingly, the landward limit of autochthonous salt moves well into the proximal domain in the onshore portion of the Essaouira Basin (Fig. 21), matching the NE-SW orientation of the major Permo-Triassic fault system subsequently inverted during the Atlasian orogeny. Moreover, at the transition between the offshore Essaouira Basin and the Safi Basin, volcanic rocks are interpreted to be interfingered with the base of the autochthonous salt in the distal domain (Figs. 15 and 21). From here to the north, through the Mazagan Plateau, the autochthonous salt occupies the distal, necking, and proximal domains. The salt is confined within isolated grabens and half-grabens bounded by large basement-involved faults that offset both its base and top, and the supra-salt Jurassic strata (Figs. 16–18).

4. Comparison with the Nova Scotia conjugate margin

The definition of tectonic domains on the conjugate Nova Scotia margin is based on the interpretation of the four wide-angle refraction profiles presented in Fig. 8c and complemented with publicly available reflection profiles (Fig. 23, for location see Fig. 22). To facilitate a meaningful comparison between the conjugate margins, we reinterpreted the seismic transects from the Scotian margin, building upon the Nova Scotia Offshore Petroleum Board (OETR, 2011) published version. We made minor modifications of the salt structures and added to the authors' original stratigraphic criteria the Rhaetian, Pliensbachian, and Toarcian horizons. These horizons were interpolated from the adjacent markers, assuming constant sediment-accumulation rates. The reinterpreted profiles are matched up with a selection of the Moroccan transects presented in this study in Fig. 23.

Along the Nova Scotia margin the pre-rift topography exerted a primary control on the configuration of the salt basin (Figs. 22 and 23). In the south, the Yarmouth Arch (Fig. 22) constitutes a paleo high composed of Paleozoic metamorphic and plutonic rocks (Savva et al., 2016), separating the salt-rich West Shelburne Subbasin (WSS in Fig. 22, as defined by Shimeld, 2004) from the salt-poor Georges Bank Basin. In the West Shelburne Subbasin, the top basement deepens abruptly at the slope, where a thick autochthonous salt layer is interpreted (see Fig. 6a in Deptuck and Kendell, 2017). The distal limit of the salt basin coincides with the occurrence of SDRs at the OCT (Dehler and Welford, 2012; Louden et al., 2013). Interestingly, on the conjugate Moroccan segment (see Tarfaya South Subbasin / Laâyoune Basin, TB and LB in Fig. 22), no salt has been identified on the seismic data (Uranga et al., 2022). Moreover, deep reflections described on seismic transect G-G' (Fig. 19) suggest the presence of SDRs on the Moroccan side as well. As can be noted on Fig. 22, the Scotian salt basin extends farther south than its Moroccan counterpart. This asymmetry between the salt-rich West

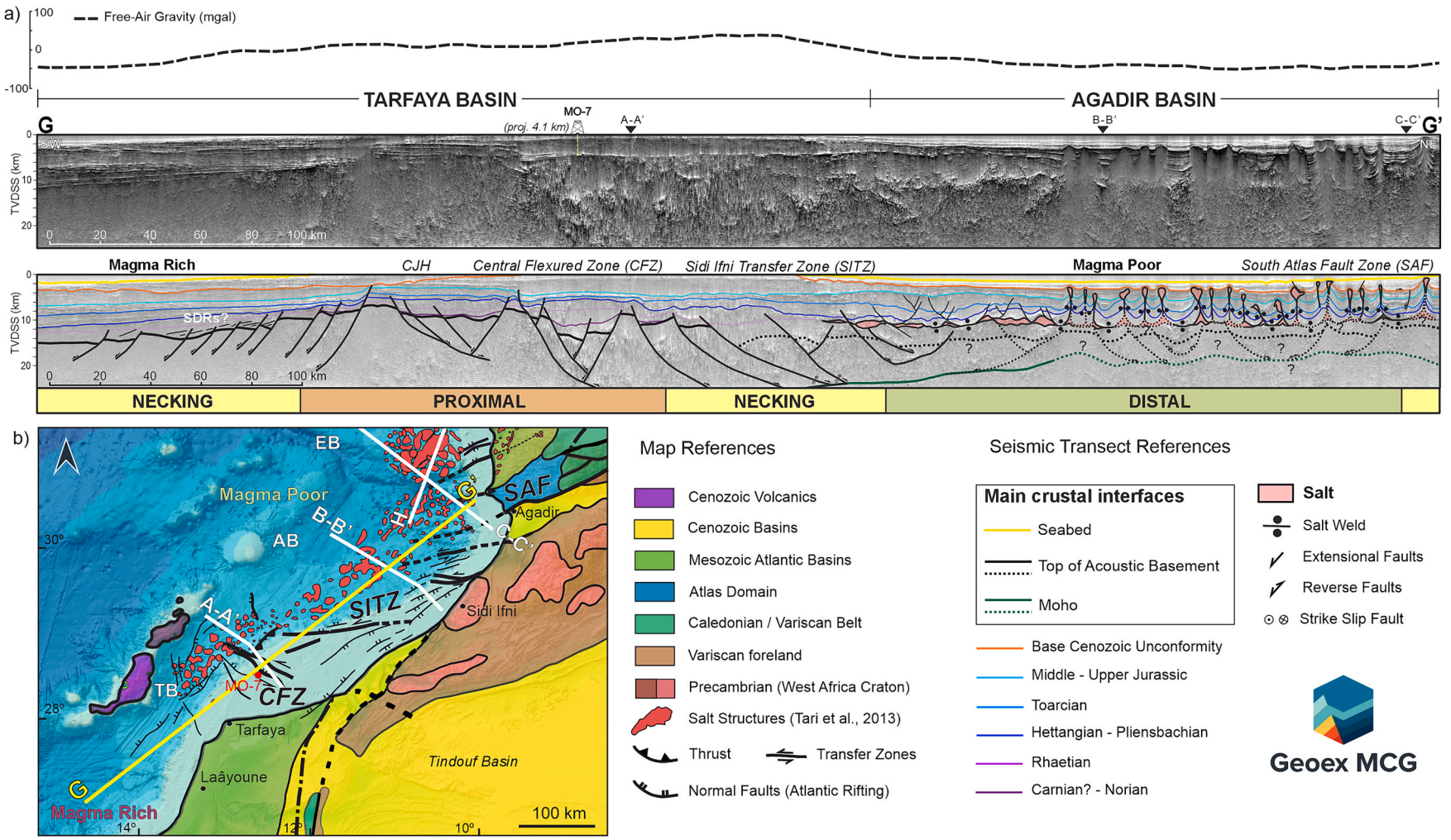

Fig. 19. a) Uninterpreted and interpreted versions of seismic transect G-G', through the Tarfaya and Agadir basins. Vertical scale is in TVDSS. On top, free-air gravity anomaly. CJH: Cap Juby high. Seismic data courtesy of Geoex MCG Ltd. For a high-resolution version of this transect, the reader is referred to the supplementary material available online; b). Enlarged view of Fig. 4 zoomed in at the Tarfaya and Agadir basins. Magma-rich and magma-poor margins as defined by Louden et al. (2013); CFZ: Central Flexured Zone (as defined by Le Roy and Piqué, 2001); SITZ: Sidi Ifni Transfer Zone (this work).

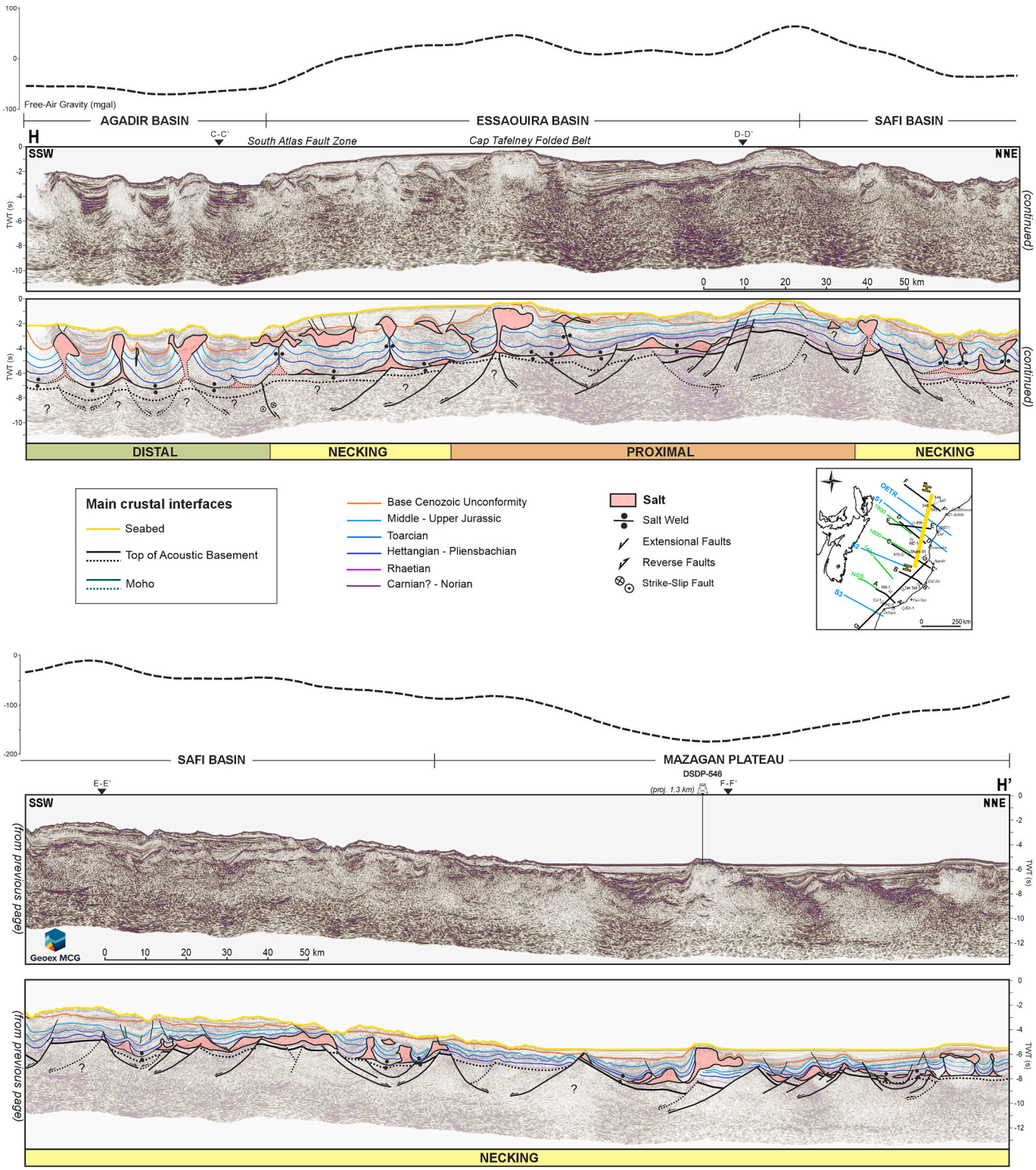

Fig. 20. Uninterpreted and interpreted versions of the strike-oriented seismic transect H-H′. On top, free-air gravity anomaly data. Seismic data courtesy of Geoex MCG Ltd. For a high-resolution version of this transect, the reader is referred to the supplementary material available online.

Shelburne Subbasin and the salt-poor Tarfaya South Subbasin is also observed in other conjugate margins such as the Santos and Namibe basins in the South Atlantic (Strozyk et al., 2017; Pichel et al., 2023; Moragas et al., 2023).

The transition from the West Shelburne Subbasin to the Shelburne Subbasin (ShS in Fig. 22) is marked by the Yarmouth Transform zone (Deptuck et al., 2015), a NW-SE (E-W in the paleo-restored map of Fig. 22) right-lateral strike-slip fault zone trending obliquely to the Scotian margin and marking the northern limit of the Yarmouth Arch. This is matched on the conjugate Moroccan margin by the similarly right-lateral Sidi Ifni Transfer Zone (SITZ) limiting the Cap Juby Horst (Fig. 12; CJH in Fig. 22). On both margins, the northward transition

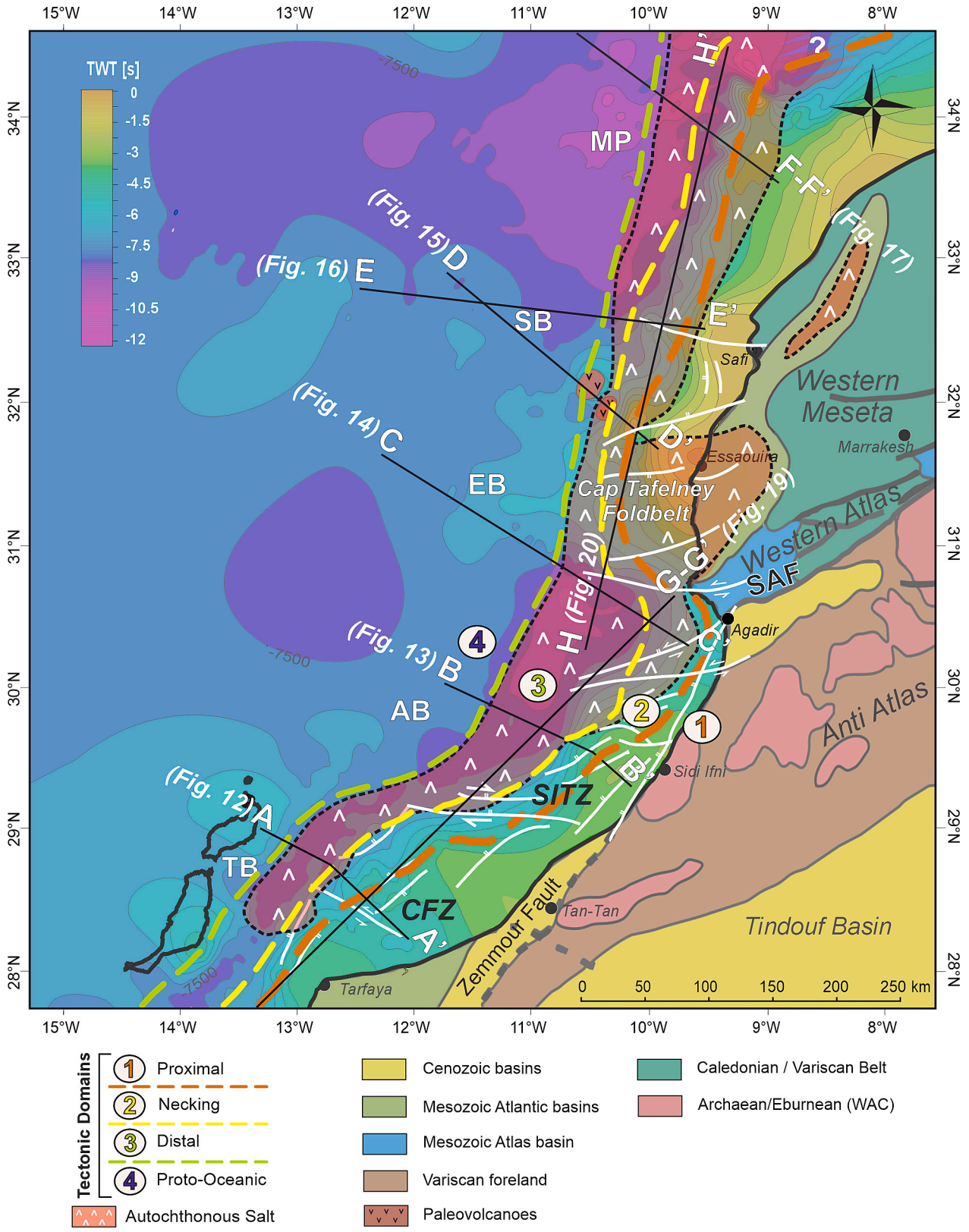

Fig. 21. Structural map of the top of the acoustic basement in TWT synthetizing the tectonic domains and autochthonous salt distribution of the Moroccan Atlantic margin as defined in this study. The salt distribution onshore of the onshore Essaouira Basin is based on the maps presented by Haddou and Tari (2007). Major offshore faults outlined in white after Le Roy and Piqué (2001). TB: Tarfaya Basin; AB: Agadir Basin; EB: Essaouira Basin; SB: Safi Basin; MP: Mazagan Plateau; CFZ: Central Flexured Zone SITZ: Sidi Ifni Transfer Zone; SAF: South Atlas Fault.

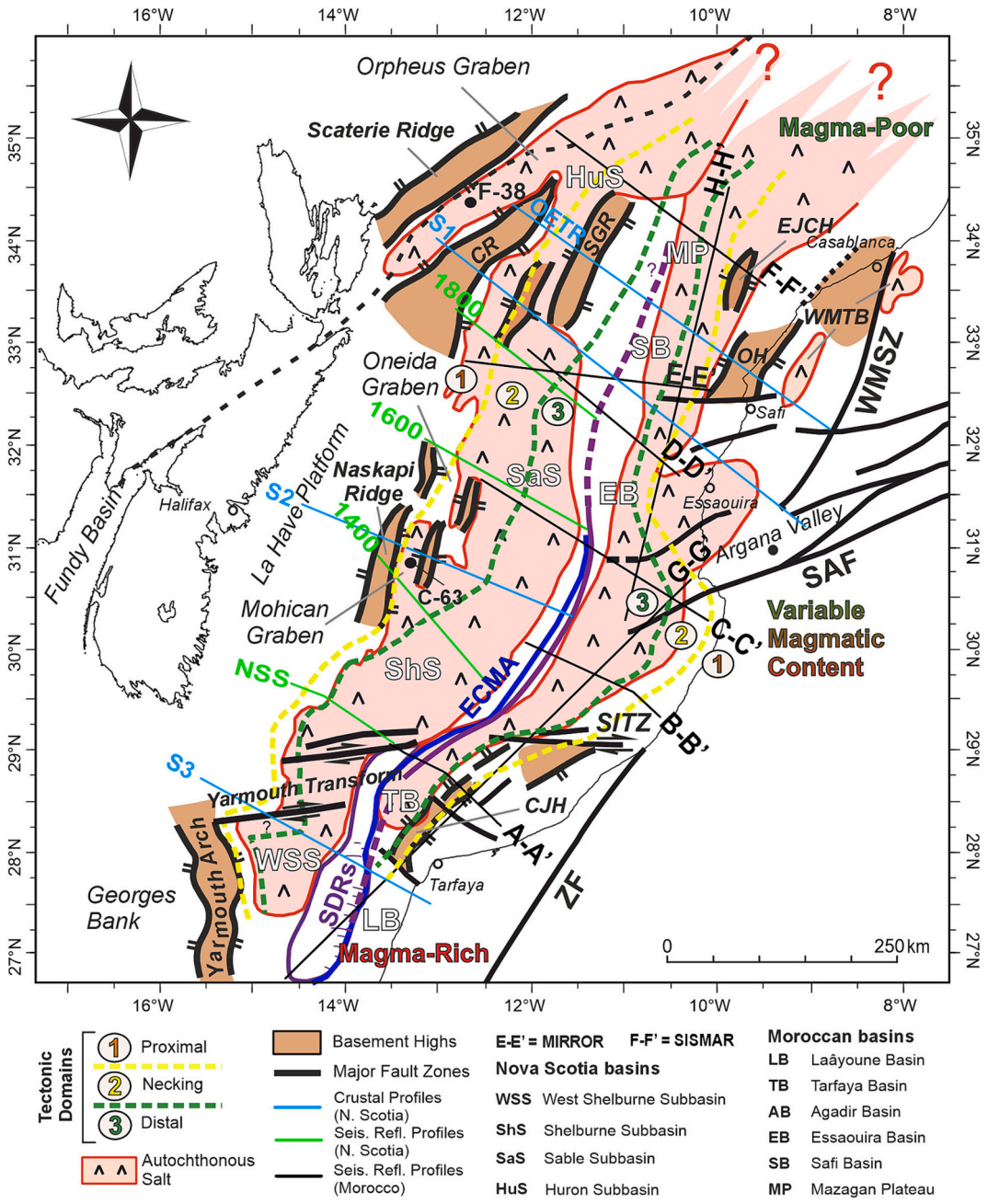

Fig. 22. Minimum closure paleo-reconstruction based on poles from Sahabi et al. (2004) and modified from the version presented by Louden et al. (2013). The location of Africa is maintained as a fixed and Nova Scotia is rotated. Basement highs, faults and salt distribution on the North American margin compiled from Deptuck et al. (2015), Deptuck and Kendell (2017) and, on the NW Africa conjugate, from Le Roy and Piqué (2001), Lyazidi et al. (2003) and Uranga et al. (2022). The tectonic domains interpretation on the Nova Scotia margin is based on the presented crustal and seismic reflection profiles (Fig. 8c). WMTB: Western Meseta Triassic basins; CCHFZ: Cobequid-Chedabucto Fault System; SGR: South Griffin Ridges; CR: Canso Ridge; EJCH: El Jadida Central Horst; OH: Oualida Horst; CJH: Cap Juby Horst; WMSZ: Western Meseta Shear Zone; ZF: Zemmour Fault; SITZ: Sidi Ifni Transfer Zone.

from these conjugate transfer zones to the Shelburne Subbasin (Nova Scotia, ShS in Fig. 22) and the Agadir Basin (Morocco) is characterized by a change of salt-tectonic structural styles (compare Figs. 23a and b) and the width of the primary salt basin (Figs. 21 and 22). This suggests that these transfer zones may have played an important role in segmenting the margin and partitioning crustal deformation and evaporite deposition during rifting (Nemčok et al., 2005).

The conjugate composite seismic lines NSS (Nova Scotia South) and A-A' (Fig. 23a) show an asymmetric crustal architecture, with a wider primary salt basin on the Nova Scotia margin than on the Moroccan side (for a more detailed characterization of the Tarfaya Basin, see Uranga et al., 2022). Care is needed in comparing the two margins since the Nova Scotian side is north of the Yarmouth Transform zone, but the Moroccan side is south of the SITZ (Fig. 22). In any case, the basement topography in the Scotian basin exhibits a gently tapered, stepped geometry controlled by a set of normal faults (see Fig. 2.6 in Deptuck et al., 2015 and Fig. 6a on Deptuck and Kendell, 2017), whereas on the Moroccan conjugate, a more abrupt deepening of the basement is caused by only two major normal faults (Figs. 12 and 23a). Moreover, on both transects, the base of the autochthonous salt in the distal domain is offset by the distalmost normal faults.

The pairing of the conjugate seismic transects 1400 (Shelburne

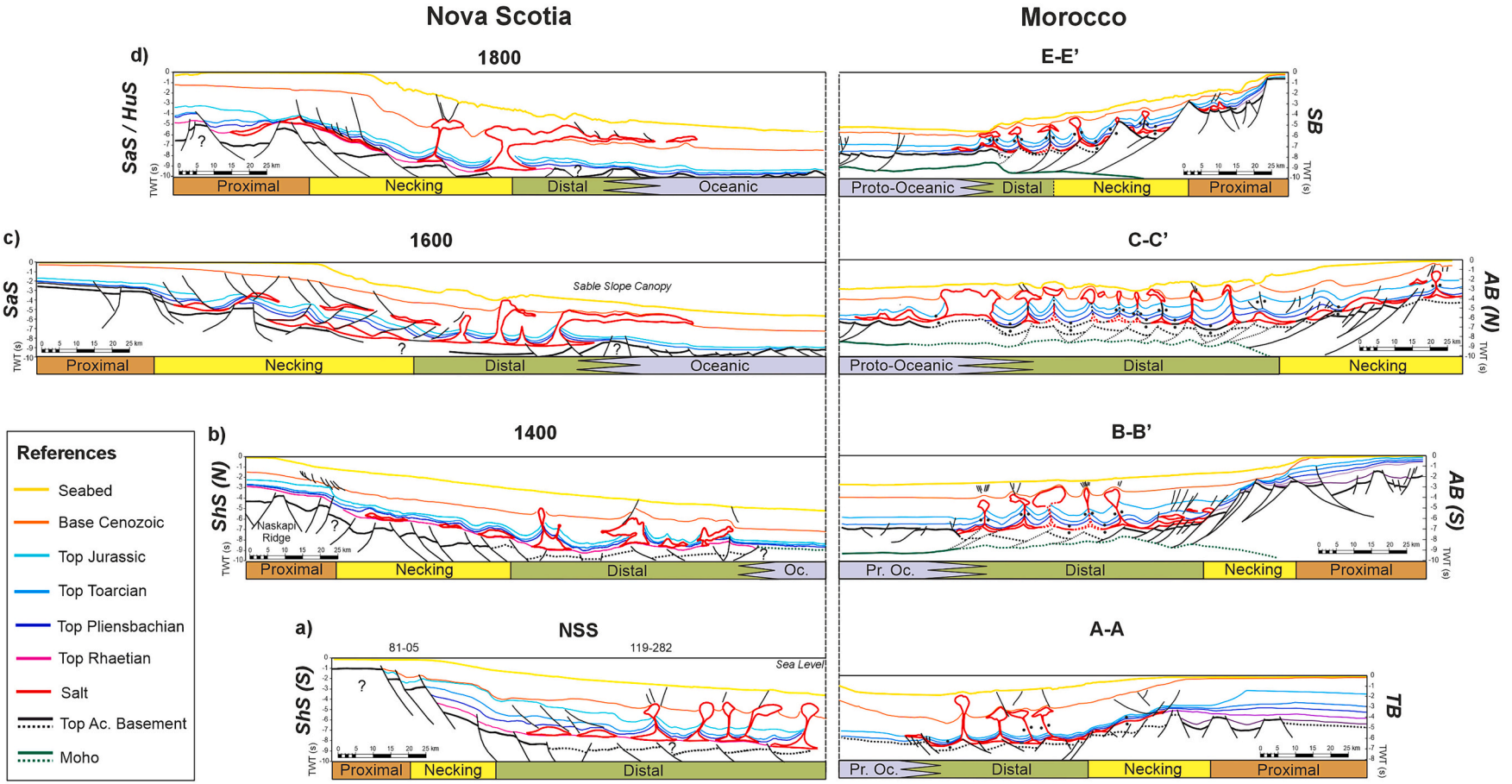

Fig. 23. Seismic interpretation of conjugate transects from the Nova Scotia (left) and Moroccan margins (for location see Fig. 22). Seismic lines 1800, 1600 and 1400 were reinterpreted from the Play Fairway Analysis Atlas (OETR, 2011) and the composite line NSS from the Canada Nova Scotia Offshore Petroleum Board. All the horizons except Top Pliensbachian, Top Rhaetian and Top Salt are based on previous interpretations. The criteria for establishing the Top Pliensbachian, and Top Rhaetian horizons, considered a proportional sediment accumulation rate between the Top Basement and the Top Toarcian. The tectonic domains definition on the Nova Scotia margin is based on the crustal profiles presented in Fig. 8c.

Subbasin, ShS in Fig. 22b) and B-B′ (Agadir South Basin) (Fig. 23b) shows that on the Nova Scotia margin, the Naskapi Ridge constitutes the proximal boundary of the primary salt basin in the Shelburne Subbasin. On the conjugate Moroccan margin, the Precambrian/Paleozoic basement high outcropping at Sidi Ifni constitutes the landward boundary of the primary salt basin (Fig. 21). As on seismic transects NSS/A-A' (Fig. 23a), the basement morphology is asymmetric, with a gentle deepening of the basement caused by both landward and basinward dipping faults on the Nova Scotia margin. Conversely, in the southern Agadir Basin (Morocco), an abrupt deepening of the basement at the necking domain is caused mainly by a single normal fault which localized most of the thinning (Fig. 23b). As a result, the autochthonous salt is confined to the distal domain on the Moroccan margin but is interpreted in both the distal and necking domains on the Nova Scotia margin.

Northward, the conjugate seismic transects 1600 (Sable Subbasin in Nova Scotia) and C-C′ (Northern Agadir Basin in Morocco) (Fig. 23c) show that the autochthonous salt is progressively deposited in more proximal rift domains. Correspondingly, the base salt is offset by normal faults in both necking domains and, although not clearly, possibly in the distal domains. One of the main differences between the two margins is that the salt structures interpreted on the Moroccan side are squeezed by contractional rejuvenation related to the Atlasian contraction (Fig. 23c) (Uranga et al., 2022).

Finally, Fig. 23d shows the pairing of the conjugate seismic transects 1800 and E-E', located in the northern Sable/Huron Subbasin (SaS/HuS; Nova Scotia) and in the Safi Basin (Morocco). Transect 1800, on the Scotian margin, confirms the continued progressive occurrence of autochthonous salt in successively more proximal tectonic domains. On this transect, salt is interpreted to be isolated in the proximal grabens, bounded by salt-free basement highs like the Canso or the South Griffin ridges (CR and SGR respectively in Fig. 22), similar to what has been interpreted on the conjugate Safi Basin on the Moroccan side (Figs. 16 and 23d).

In summary, the map of Fig. 22, combined with the pairing of conjugate transects presented in Fig. 23, illustrates a progressive northward trend of salt deposition in successively more proximal tectonic domains on both margins. In the south, salt is confined to the distal domains, but it extends from the distal to the proximal domains in the north (Figs. 21, 22 and 23). Moreover, whereas only the base salt is offset by rift-related faults in the south, the base and top salt, as well as supra-salt Jurassic strata, are offset in the north (Fig. 23).

5. Discussion

5.1. Timing of salt deposition

Evaporites can accumulate more rapidly than most other sedimentary rocks (Warren, 2006). For instance, the maximum accumulation rate of gypsum in shallow water of the Mediterranean Sea is 5 cm/yr, and halite can accumulate at 10 cm/yr (Schreiber and Hsü, 1980). Moreover, in mixed clastic/evaporitic environments, Warren (2006) reported that a succession of alternating halite and clay of >1 km thick was deposited in 10,000 years (10 cm/yr) in the Danakil Depression, located at the Afar Triple Junction of the East African Rift.

In the Moroccan Atlantic margin, several authors have proposed that rifting migrated from east to west and from south to north (Medina, 1995; Le Roy et al., 1997; Le Roy and Piqué, 2001). This migration might have caused an earlier (Carnian/Norian) deposition of salt in the eastern depocenters, like onshore Essaouira (Figs. 6 and 7). Moreover, the onset of the Atlas rifting predated the opening of the Central Atlantic (Hafid et al., 2006; Vergés et al., 2017), as indicated by the Late Permian (Aït Chayeb et al., 1998) or late Early Triassic (Medina, 1995) *syn*-rift succession outcropping in the Argana Valley (Western High Atlas, for location, see Fig. 4). According to the stratigraphic correlation presented by Hafid (2000) (Fig. 7), the oldest evaporites identified in the onshore Essaouira Basin may be Carnian in age (Dutuit, 1966; Jalil, 1996). Based on sedimentary facies analysis, Hafid (2000, 2006) considered that salt onshore Essaouira was deposited during a transitional stage between rifting and drifting, when fault activity in that area had almost ceased. Thus, this salt can be regarded as post-tectonic and late syn-rift. Although this might be the case for the upper evaporitic succession, some of the interpreted profiles show that the lower evaporitic interval is usually offset by normal faults, confined within grabens and has a patchy distribution (see Figs. 9 to 16 in Hafid, 2000), and hence can be considered as syn-tectonic and syn-rift.

On the conjugate North American margin, in the Georges Bank Basin (Fig. 6), researchers have described a thick succession of syn-rift Carnian to Norian salt (Fig. 6), correlative with the Osprey evaporites of the Grand Banks, offshore Newfoundland (Holser et al., 1988; Cousminer and Steinkraus, 1988). These isolated and older evaporitic depocenters are confined within proximal grabens and are distinct from the widespread, continuous salt province developed later in the Central Atlantic rift valley (Fig. 6). The offshore wells located in the Georges Bank Basin, the Orpheus, and the Mohican grabens (Fig. 22) sampled Upper Triassic to Lower Jurassic salt dominated by halite (Barss et al., 1979; Jansa et al., 1980; Weston et al., 2012). The Glosscap C-63 exploration well (C-63 in Fig. 22) located in the Mohican Graben encountered 441 m of Late Norian to Rhaetian halite interbedded with dolomite, siltstone, and shale (Weston et al., 2012). Interestingly, the evaporitic succession is capped by a 152 m thick interval of tholeiitic basalt geochemically related to the CAMP (Fig. 5a from Deptuck and Kendell, 2017) and similar to what is described onshore Essaouira (β3 in Fig. 7) and in the Western Meseta Triassic basins (Fig. 4) (Afenzar and Essamoud, 2017). Moreover, Deptuck and Kendell (2017) correlate these volcanic rocks with a strong reflection observed in the neighboring Oneida Graben (Fig. 22), where a lowermost Jurassic salt succession is interpreted overlying the basalt (Fig. 5b from Deptuck and Kendell, 2017), similar to what is described in the MAC 1 well in the onshore Essaouira Basin (Figs. 7 and 22). These observations suggest that the Mohican Graben in Nova Scotia and the onshore Essaouira Basin can be considered as analogous and indicate that salt deposition in these proximal depocenters may have started earlier than in the Central Atlantic rift valley.

On the Moroccan margin, a thick evaporitic succession was deposited along the embryonic Central Atlantic rift valley as rifting progressively propagated to the west during Rhaetian to Hettangian times. The palynomorphs of this age sampled in clay inclusions from the salt cored at the DSDP-546 well, located offshore El Jadida (Figs. 4 and 22), provide the only reliable biostratigraphic data available for the upper section of the salt offshore Morocco (Fenton, 1984), whereas the basal section is poorly constrained in age (see Fig. 6–4 in Hafid et al., 2008). Nevertheless, on seismic transect D-D′ (Fig. 15), the base of the autochthonous salt is interpreted to be interfingered with volcanic rocks. Assuming that this unit is part of the CAMP event (200–203 Ma) (Knight et al., 2004; see Fig. 4.3 in Marzoli et al., 2018), the age of the offshore salt in this segment of the Moroccan margin could be constrained between 203 and 199 Ma (the CAMP sets the lower age limit, and the top of the Hettangian sets the upper limit). In this scenario, the Atlantic evaporitic succession may have been deposited in 1 to 4 Myr. Moreover, the widespread, distal Atlantic salt would have largely been younger than the more proximal, fault-bounded salt basins (Mohican and onshore Essaouira), but with a time overlap around the CAMP event.

At basin scale, the deposition of thick evaporitic successions usually takes place rapidly in isolated tectonic depressions, often well below sea level (Konstantinou and Karner, 2022) and fed by inflow and marine groundwater seeps in arid paleoclimatic conditions (Warren, 2006). These circumstances were met during the initial breakup of Pangea when the Central Atlantic rift valley constituted a segmented but interconnected tectonic depression fed by marine seeps sourced from the Tethys Ocean (Jansa et al., 1980; Hafid, 2000; Tari and Jabour, 2013). Assuming that the distal salt in the Central Atlantic valley was accumulated in a time range of 1 to 4 Myr (Rhaetian to Hettangian) and considering a northward propagation of rifting, the question becomes

the validity of considering the autochthonous salt layer as a near-isochronous marker along the length of the margins. Accordingly, Withjack et al. (1998) and Olsen (1997) analyzed the diachronicity in the opening of the Central Atlantic between the Carolina Trough (US) and the Scotian Basin, allowing us to estimate the along-strike rift-propagation rates of the North American margin. For example, from the Taylorsville Basin (US) to the Fundy Basin (Canada), approximately 1200 km apart (see Fig. 5 in Withjack et al., 1998), the diachronicity for the end of rifting is broadly 20 Myr. However, if we take the Newark Basin as the southern reference, then the diachronicity for the end of rifting is 8 Myr over 850 km. Normalizing these estimations to a distance of 850 km, which is the approximate S—N length of our study area on the conjugate Moroccan margin, the S—N diachronicity for the end of rifting would be in the range of 8 to 14 Myr. These are reasonable estimations that are also supported by numerical modeling studies (Van Wijk and Blackman, 2005; Le Pourhiet et al., 2018). Therefore, we infer that the propagation of rifting is significantly slower (~8–14 Myr) than salt accumulation (~1–4 Myr) in the Central Atlantic and, consequently, the offshore autochthonous salt can be regarded as a near-isochronous stratigraphic marker horizon.

5.2. Mapping of tectonic domains

Delimiting tectonic domains in rifted margins usually presents significant challenges due to the inherent complexities and often gradational nature of these transitions. The ambiguity in defining precise boundaries arises from variations in geological and geophysical characteristics across these domains, often complicating the interpretation of margin evolution and tectonic history. In our study, we primarily relied on seismic reflection data to determine these boundaries, supplemented, when necessary, by free air gravity and magnetic anomaly data and the available wide angle reflection profiles to enhance our assessments. The primary criterion for establishing these boundaries was the interpretation of the top of the acoustic basement. However, in areas where salt structures obscured this interface, we used the base of the autochthonous salt layer as an alternative marker to infer the underlying structural architecture and therefore, setting a minimum value for the top basement depth. Given the primary goals of our study to elucidate the relationship between salt deposition and crustal architecture on a margin scale, the interpretations we present are informed by these criteria. However, the inherent uncertainties associated with the geophysical methods used and the data quality suggest that there could be minor adjustments to these boundary delineations, but in any case, they would affect our final conclusions. Following, we offer a synthesis of the observations that characterize the criteria for delimiting the main tectonic domains where the autochthonous salt was deposited.

The seismic interpretation of the presented dip-oriented profiles (Figs. 12 to 17) indicates that the proximal domain features a top basement located between 2 s and 4 s TWT, accompanied by the development of graben and half-graben structures. These structures are delineated by normal faults that exhibit both continentward and basinward vergence. Basinward, in the necking domain, the top basement depth increases progressively, transitioning from an average of 3 s to approximately 7 s TWT. This deepening is interpreted to be caused by seaward-verging crustal-scale normal faults. The distal domain is characterized by a gentler decrease on top basement depths that ranges, on average, from 7 to 8.5 s TWT, with maximum values at the Mazagan Plateau, where it reaches a depth of 10 s TWT. The interpretation of the top basement in this domain is less certain due to the presence of salt. However, at the same time, the identification of the base of the autochthonous salt layer provides a critical constraint, serving as a minimum depth marker for the top basement and thereby helping to define the crustal architecture of this domain more accurately. The seaward limit of the distal domain is commonly marked by a step-up in top basement topography, representing a positive paleorelief averaging 1 s TWT, and called the outer high. This feature usually coincides with the S1 magnetic anomaly (Roeser et al., 2002), constitutes the transition to the proto-oceanic domain, and the distal limit of the autochthonous salt basin.

5.3. A conceptual model for the rift-to-drift transition in the northern Central Atlantic

As pointed out by Vink (1982), continents do not rift apart instantaneously but propagate along strike with a V-shaped geometry toward "locked zones", in a manner like crack propagation (Courtillot, 1982; Morgan and Parmentier, 1985). This implies that deformation is not isochronous along strike, but rather, gets younger in the direction of propagation. More recently, numerical models have focused on assessing the factors controlling the dynamics of rifting propagation and its obliquity (Van Wijk and Blackman, 2005; Allken et al., 2012; Le Pourhiet et al., 2017, 2018). In brittle-ductile coupled lithospheric systems, rift linkage depends strongly on the mechanical strength of the coupling, the rifting offset, and the amount of strain weakening (Huismans and Beaumont, 2011; Allken et al., 2012; Le Pourhiet et al., 2018; Neuharth et al., 2021; Gouiza and Naliboff, 2021).

As in many well-known examples, such as the Red Sea, the South Atlantic, or the South China Sea (Bosworth, 2015; Stockli and Bosworth, 2019; Nürnberg and Müller, 1991; Mohriak and Leroy, 2013; Le Pourhiet et al., 2018), the lithospheric breakup in the Central Atlantic took place diachronously along the length of the margin, migrating from south to north (Medina, 1995; Withjack et al., 1998; Le Roy and Piqué, 2001). During propagation, salt rapidly accumulated, serving as a near-isochronous marker which acted as a tape recorder of the along-strike variations of the tectonic settings where it was deposited. In other words, the salt would have been deposited during a later stage of rifting in the south but, at the same time, at an earlier stage to the north, as proposed for the Red Sea by Rowan (2014). Based on this concept and the interpretations presented in this study, a 3D evolutionary model for the rift-drift transition of the Moroccan/Nova Scotia conjugate margin is presented (Fig. 24).

5.3.1. Carnian-Norian

The pre-Mesozoic inherited structural fabric and basement composition had a major influence on the tectonic evolution during rifting and opening of the Central Atlantic Ocean (Piqué et al., 1998; Le Roy and Piqué, 2001; Nemčok et al., 2005). The Atlantic coastal region of Morocco is characterized by thick EN*E*-WSW and NE-SW trending depocenters of early rift successions of Carnian to Norian age, locally including evaporites (Figs. 6 and 24a) (Le Roy and Piqué, 2001). These grabens and half-grabens resulted from the extensional reactivation of inherited Variscan structures (Piqué et al., 1998; Brahim et al., 2002). An example is the NE-SW-trending South Atlas Fault (SAF in Fig. 24a) which, during the *syn*-rift stage, controlled the accommodation space within isolated, salt-bearing depocenters located in the Western Atlas and the onshore Essaouira Basin (EB in Fig. 24a). Other related structures include the NE-SW-oriented Zemmour Fault in the south (ZF in Figs. 22 and 24a) or the N-S trending Western Meseta Shear Zone in the north (WMSZ in Figs. 22 and 24a), which also controlled the syn-rift sedimentation during the Triassic (Dillon, 1974; Piqué et al., 1980; Hinz et al., 1982a; Laville and Piqué, 1991; Le Roy and Piqué, 2001). Moreover, the related early depocenters (like the Tan- Tan/Tarfaya graben in Fig. 24a) were delimited by ENE-WSW oriented transfer zones, which were also inherited from the Variscan orogeny, like the Sidi Ifni Transfer Fault (SITZ in Figs. 22 and 24a). During the early stages of rifting, these transfer zones isolated clastic-dominated grabens from evaporite-rich depocenters and subsequently, they played a major role on the along-strike segmentation of the Central Atlantic margin.

On the conjugate Nova Scotia margin, thick Carnian to Norian successions were deposited in proximal NE-SW oriented grabens (like the Fundy Basin or the La Have Platform, see Figs. 6 and 22). In general, no Carnian to Norian evaporitic successions have been described in these

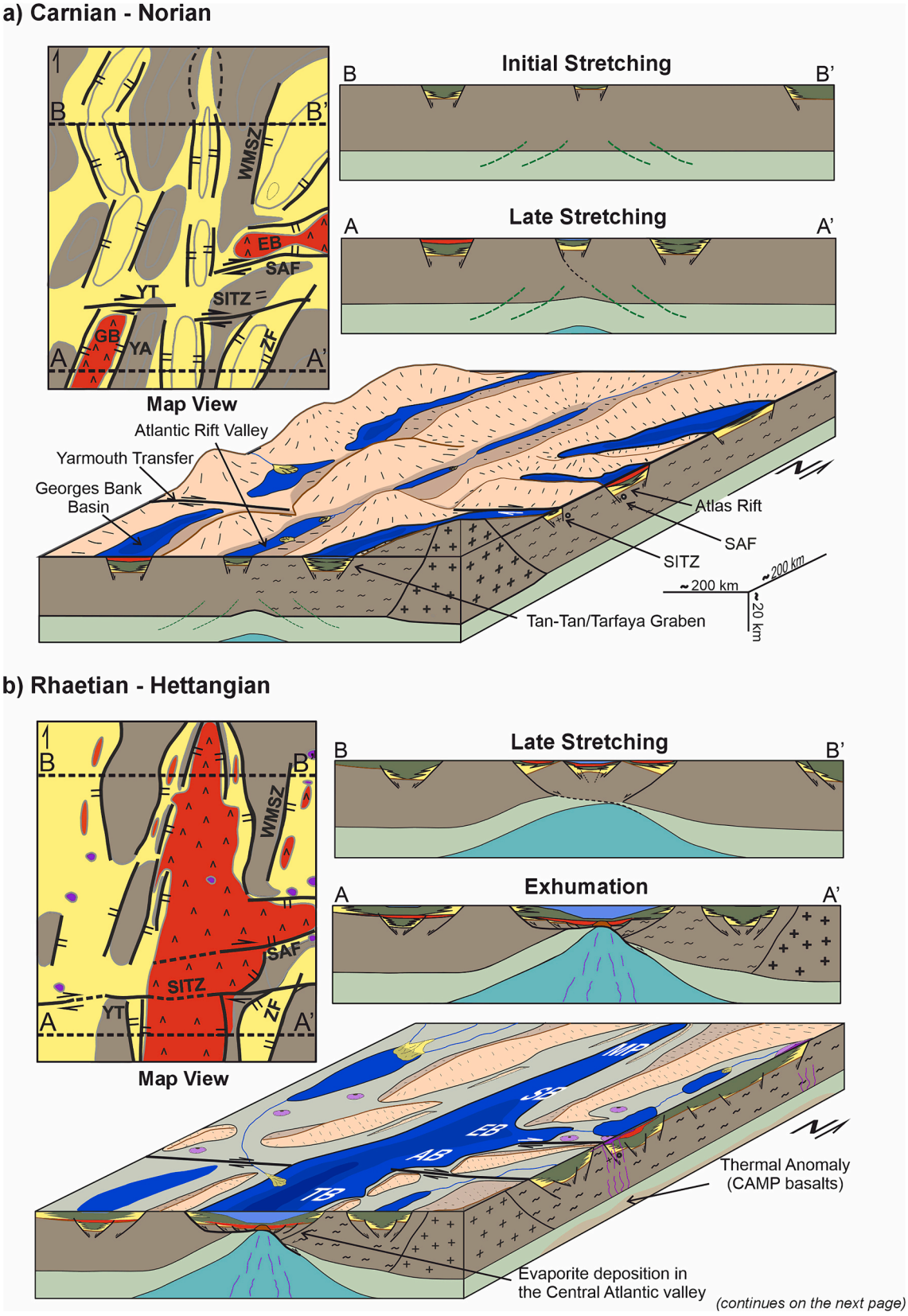

Fig. 24. Conceptual evolutionary model for the rift-drift transition on the conjugate Moroccan- Nova Scotia margin a) Carnian to Norian crustal stretching stage illustrating the northward progression of rifting and the suggested early salt deposition in the onshore Essaouira (EB) and Georges Bank (GB) basins. Major Variscan inherited structures: WMSZ: Western Meseta Shear Zone, SAF: South Atlas Fault, SITZ: Sidi-Ifni Transfer Zone, YA: Yarmouth Arch, ZF: Zemmour Fault; b) During the Rhaetian-Hettangian, salt was deposited during the exhumation stage in the Tarfaya Basin while, approximately at the same time it was being deposited during the stretching stage in the Mazagan Plateau c) During Sinemurian – Pliensbachian, initial drifting stage takes place in the south; CBF: Continental breakup front. See text for explanation.

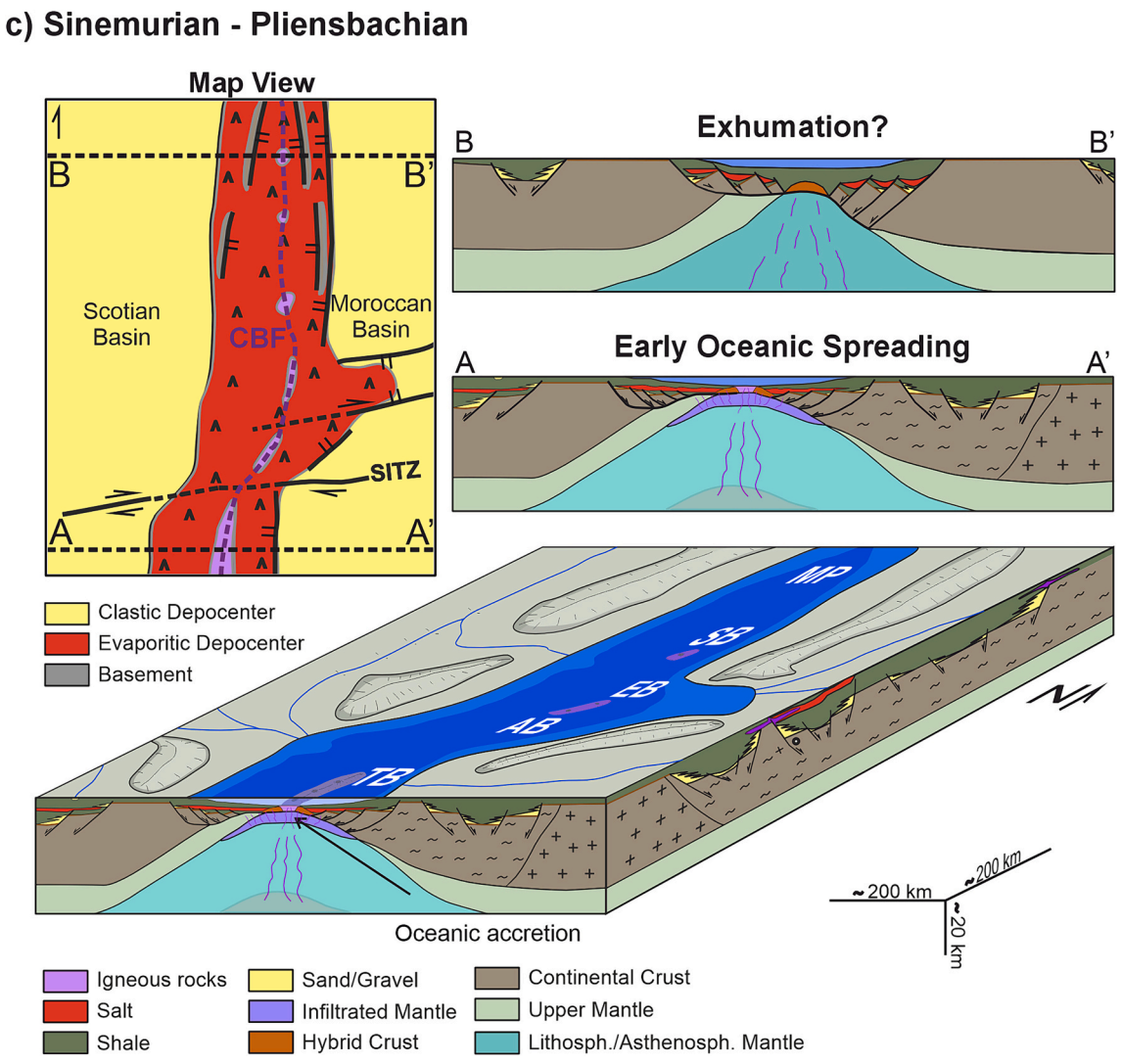

Fig. 24. (*continued*).

grabens except for the Georges Bank Basin (US) (GB in Fig. 24a) (Klitgord et al., 1988; Holser et al., 1988) and the northern Osprey evaporites penetrated in the Carson Subbasin, offshore Newfoundland (Jansa et al., 1980). As on the Moroccan margin, these evaporites are interpreted to have been deposited in intracontinental grabens sourced by marine waters from the western Tethys Ocean during the early phases of rifting (Jansa et al., 1980; Clement and Holser, 1988). Moreover, on the Nova Scotia margin, salt-bearing depocenters were also isolated from salt-free depocenters by basement highs like the Yarmouth Arch (see Fig. 22 and YA in Fig. 24a) and by transfer faults such as the Yarmouth Transfer (Fig. 24a).

5.3.2. Rhaetian-Hettangian: tectonic setting during salt deposition

The Rhaetian marks the localization of the extensional deformation on the N-S to NNE-SSW-oriented Central Atlantic rift axis (Fig. 24b) (Piqué and Laville, 1996; Le Roy and Piqué, 2001) where a thick evaporitic sequence composed mainly of halite was deposited (Gouiza, 2011; Tari and Jabour, 2013; Wenke, 2014). The structural and compositional inheritance of the prerift basement imposed along-strike rheological heterogeneities, which may have induced a diachronous rift propagation (Gouiza and Naliboff, 2021), with extensional deformation progressively migrating northward (Olsen, 1997; Withjack et al., 1998; Le Roy and Piqué, 2001; Medina, 1995). Consequently, the relatively rapid deposition of salt took place in different tectonic domains along the future rifted margin.

Along the southern segment of the Tarfaya Basin, the absence of salt coincides with the transition from a magma-rich (south) to a magma-poor (north) segment of the margin, as proposed by Dehler et al. (2004), Reston (2009) and Louden et al. (2013), based on the interpretation of SDRs on the conjugate West Shelburne Subbasin (Figs. 21 and 22). Moreover, this study reveals that in the southern Tarfaya Basin, deep reflections dipping to the southwest can be interpreted as SDRs (Fig. 19a). Notably, this marks the first time SDRs have been identified on the African side of the conjugate Nova Scotia / Moroccan margin. The identification of SDRs on the Moroccan margin is more difficult than on its North American conjugate due to the presence of Cenozoic volcanic rocks related to the growth of the Canary Islands that deteriorate the quality of the seismic data of the underlying reflectors. The absence of salt in the Moroccan conjugate section of the Tarfaya Basin can be attributed to several geological factors. The presence of an inherited oblique-striking pre-rift basement block to the southwest, the rapid emplacement of magmatic flows that competed with salt for limited accommodation space, and the narrowness of the depocenter are key contributors (see Figs. 4b, 5, and 6b in Uranga et al., 2022). These combined factors contributed to creating a topographic barrier that separated a salt-free southern depocenter from a salt-rich northern one. Similar configurations between salt-bearing and salt-free margins are observed in other well-documented regions, such as the Rio Grande-

Walvis Ridge, which divides the salt-free Austral from the salt-rich Central segments of the Southern Atlantic, and the transition between the Kwanza and Namibe basins in West Africa (Rowan, 2014; Stica et al., 2014; Pichel et al., 2023).Moreover, it is possible that the magmatic source that fed this rapid volcanic emplacement was favored by the presence of leaky transfer zones (Deptuck and Kendell, 2017) as it is the case, for example, in South Mozambique, Argentina and SW Africa (Koopmann et al., 2014; Biari et al., 2021; Roche et al., 2021). Conversely, on the conjugate Nova Scotia margin, the primary salt basin extends farther southward than on its Moroccan counterpart (West Shelburn Subbasin in Fig. 22). This extension can be attributed to the absence of pre-rift basement blocks segmenting the basin, and to the asymmetrical nature of the conjugate margin, which allows for a wider expansion of the primary salt depocenter on the Nova Scotia side (see section 4).

Northward, in the salt-bearing northern sector of the Tarfaya Basin, as well as in the southern Agadir Basin, the autochthonous salt is almost entirely confined to the distal domain, distally onlapping the outer high, with at most very small overrun onto oceanic crust (Figs. 12 and 13). The base of the autochthonous salt is offset by normal faults, but the top salt is not. This suggests, first, that salt was deposited when the extensional deformation was localized distally, and second, that the emplacement of oceanic crust began shortly after evaporite deposition. In other words, the salt was deposited during the hyperextension/exhumation stage and, therefore, the salt basin in this segment of the Moroccan margin classifies as *syn*-exhumation (sensu Rowan, 2014) (Fig. 24b). Moreover, structural restoration shows that the original salt layer exhibited a basinward-thickening, wedge-shaped geometry, indicating that the vertical accommodation space was maximum at the distal trough (Uranga et al., 2022). Interestingly, this narrow syn-exhumation salt basin contrasts, in terms of lateral extent, with the classical definition proposed by Rowan (2014), in which syn-exhumation salt extends from the proximal to the distal domains. We offer three possible explanations for this discrepancy. First, the Tarfaya salt basin is very close to the transition between a magma-rich and a magma-poor margin segment. The definition of syn-exhumation salt basins was proposed for magma-poor margins, where extensional deformation was the main mechanism during rifting. Conversely, in the Tarfaya Basin, magmatism was at least as important as extensional deformation, possibly resulting in a comparatively narrow distal domain where magmatic flows filled, in part, the available accommodation space. Second, the asymmetric basement architecture of the conjugate margin results in a narrower Moroccan side and a wider Nova Scotia salt basin (see above) (Figs. 23a and 24b). Third, the topographic relief of the basin in which evaporites accumulated may have been greater than the depth of the brine, such that more proximal areas were subaerially exposed and never had salt deposited.

The seismic interpretation of the base of the autochthonous salt in seismic transect A-A' (Fig. 12) is challenging. Even though the salt pedestals of the proximal buried structures were confidently interpreted, the base of the salt at the distalmost diapir may be interpreted at an even deeper level. To reduce the uncertainty, it is crucial to check the consistency of the interpretation by comparing it with neighboring transects. In this case, seismic transect B-B′ (Fig. 13) has a higher signal to noise ratio and a greater vertical extent which allows a more robust interpretation of the base of the salt at the distalmost diapir, adding a strong argument to justify the preferred interpretation of transect A-A' (Fig. 12).

From south to north in the Agadir Basin, the relationship between autochthonous salt and rift structures changes significantly. The Agadir Basin is limited by two major transfer zones: the SITZ to the south and the SAF to the north (Figs. 21, 22 and 24b). By comparison of seismic transects B-B′ (Fig. 13) and C-C′ (Fig. 14) it can be noted that there is a progressive and significant increase in the width of the distal and necking domains from south to north (Fig. 21). This northward increase in stretching can be related to the relative motions of the transfer faults bounding the Agadir Basin. Larger strike-slip offsets on the northern SAF than in the southern SITZ would need to be accommodated by an increase in dip-oriented extension on the northern necking and distal domains and adjusted laterally by minor strike-slip tear faults (Fig. 21). In contrast to the south (Fig. 13), the northern Agadir (Fig. 14) and the offshore Essaouira Basin (Fig. 20) contain salt in the necking domain. Moreover, as pointed out by Tari and collaborators in many works (e.g., Tari et al., 2003; Tari and Jabour, 2013, amongst others) and by Pichel et al. (2019), base-salt relief had a profound impact on salt tectonics in this part of the margin. These studies show a significant increase in original salt thickness and connectivity in the central segment of the offshore Essaouira Basin, adding complexity to its overall structural setting (for example see Fig. 7 in Pichel et al., 2019; Davison et al., 2010). This thicker salt accumulation observed at the central segment of the Essaouira Basin could be attributed to a basinwide increase in the vertical accommodation space generated by the reactivation of the inherited Variscan transtentional faults trending obliquely to the margin and related to the Atlas rift, such as the SAF (Figs. 21 and 24b). The interference between the Atlas and Atlantic rift systems likely resulted in a wider salt basin with an overall increase in lateral connectivity. Regardless of the cause, the distribution of salt and the offset of both base and top salt suggest that the northern Agadir and south to central offshore Essaouira basins can be classified as late *syn*-thinning to early syn-exhumation (sensu Rowan, 2014).

Northward, the Essaouira Basin is characterized by the presence of salt in more proximal tectonic domains (Fig. 21). This may have a combined cause. First, we have already cited the deposition of an early Carnian-Norian evaporite in the onshore Essaouira Basin (Hafid, 2000) with an Atlasian geochemical affinity (Holser et al., 1988). Assuming a progressive westward migration of extensional deformation during the Triassic, this older salt would have been deposited at an earlier stage of rifting (Fig. 24a). Second, an increased tectonic subsidence in this area promoted by the extensional reactivation of inherited N-S and E-W-oriented Variscan structures related to the intersecting Atlantic and Atlasic rift, respectively, might have facilitated the transgression of the late (Rhaetian to Hettangian) evaporitic sequences, forming an embayment (Fig. 24b), akin to the concept proposed by Tari et al. (2012) for the Lower Cretaceous deposits. Considering these unique characteristics, the onshore and near offshore Essaouira salt basin should be examined separately from the rest of the classical "Atlantic-type" Moroccan basins and treated as a particular case in the conceptual model presented in this study.

From the northern segment of the offshore Essaouira Basin, through the Safi Basin and on to the Mazagan Plateau (Figs. 15–17), the relationship between autochthonous salt and rifting is yet again different in several ways. First, igneous intrusions are interpreted to be interfingered with the salt in part of the area. Second, salt is broadly distributed from the proximal to the distal domains (Fig. 21). Third, both the top and the base of the autochthonous salt are offset by normal faults, in addition to much of the Jurassic (Fig. 18). Fourth, the salt is often laterally confined within half-grabens developed over rotated Paleozoic basement blocks (Hinz et al., 1984). Fifth, from the proximal to the distal domain, salt structures are interpreted at progressively deeper structural levels, indicating major syn- to post-salt differential tectonic subsidence related to rifting (Fig. 17). For these reasons, salt in the northernmost segment of the study area is classified as late syn-stretching to early syn-thinning (Rowan, 2014) (Fig. 24b). Moreover, the original autochthonous salt layer was progressively thinner to the north (Tari et al., 2003), compatible with a less mature rifting and with a consequent reduction in accommodation space during salt deposition to the north.

We interpret a similar pattern of autochthonous salt basin configuration on the conjugate Nova Scotia margin. As shown on Figs. 22 and 23, from south to north, the autochthonous salt layer is interpreted in progressively more proximal tectonic settings. In the south, salt in the Shelburne Subbasin is mainly confined to the distal domain, with only the base salt offset by normal faults in the distal trough (Fig. 23a). In the

north, the Sable and Huron subbasins display autochthonous salt that is widely distributed across the proximal, necking, and distal domains (Figs. 22 and 23), with both the base and top salt offset by normal faults (Fig. 23d). As on the Moroccan margin, the evidence suggests that salt in the Scotian Basin can be classified as syn-exhumation in the south and as syn-stretching in the north.

The comparison of salt structural styles on both margins supports the hypothesis that the autochthonous salt records the northward V-shaped propagation of rifting on both conjugates. One of the main differences between the margins, however, is their asymmetry in crustal architecture, especially in the southern segment. In Nova Scotia, the autochthonous salt was deposited on a wide area over a gently dipping, stepped pre-salt basement topography, whereas most of the autochthonous salt was deposited in a narrow, deeper, fault-bounded trough, on the conjugate segment of the Moroccan margin (Tarfaya and Agadir basins).

In the study area, salt deposition occurred simultaneously with one of the largest volcanic events recorded in Earth's history, responsible for the formation of the CAMP (200–203 Ma), a well-studied Large Igneous Province (Fiechtner et al., 1992; Knight et al., 2004; Marzoli et al., 2018). The origin of this volcanic event is related to asthenospheric upwelling and lithospheric extension (Verati et al., 2007). On the conjugate Moroccan/Scotian margin, CAMP tholeiitic basalts are interbedded with the autochthonous salt in the onshore Essaouira Basin and the Mohican Graben (Wade and MacLean, 1990; Pe-Piper et al., 1992; Hafid, 2000). In the Essaouira and Safi basins, massive submarine paleo volcanoes are interfingered with the autochthonous salt layer and acted as buttresses hampering the early gravitational gliding of salt (Fig. 15). These paleo volcanoes are interpreted in areas where a thinner autochthonous salt layer is observed (Tari and Jabour, 2013; Pichel et al., 2019) suggesting that volcanic rocks and salt competed for the available accommodation space. The interfingering of the autochthonous salt (Rhaetian-Hettangian) and this volcanic unit suggests that the latter could be ascribed to the CAMP event and, therefore, would predates the first proto oceanic crust dated as Sinemurian (Ady et al., 2022; Neumaier et al., 2019).

5.3.3. Sinemurian-Pliensbachian: early oceanic spreading

The characterization of the OCT is key for understanding the processes acting during the rift-to-drift transition. Based on four wide-angle refraction profiles (Fig. 8c) on the Nova Scotia margin, various authors proposed different interpretations for the composition and location of the OCT, although in many cases, velocity gradient data alone cannot univocally define it (Funck et al., 2004; Wu et al., 2006; Makris et al., 2010; Biari et al., 2017). From south to north, the SMART 3 profile is interpreted to image an underplated intrusive body matching the magma-rich segment of the margin (OETR, 2011); the OCT on the SMART 2 profile is suggested to be composed of serpentinized mantle beneath oceanic and continental crust (Wu et al., 2006); and the OCT on the SMART 1 and OETR is interpreted as partially serpentinized mantle with variable amounts of igneous intrusions (Funck et al., 2004; Makris et al., 2010) (Fig. 8c). On the conjugate Moroccan margin, Biari et al. (2015) specify that the MIRROR and SISMAR profiles image an OCT with a thick crust (7–8 km) seaward from the S1 anomaly, which they interpret as oceanic crust with pockets of serpentine during the early accretionary stages, and in this study, we classify as the proto-oceanic domain (Figs. 8c and 17). Interestingly, there is no symmetric counterpart of this segment on the SMART 1 and OETR conjugate profiles, which show a thin crust (4–5 km), interpreted as partially serpentinized mantle beneath oceanic crust, seaward from the ECMA anomaly (compare profiles on Fig. 8c). Three different hypotheses try to explain this thickness and compositional asymmetry. First, for the Moroccan margin, Holik et al. (1991) suggested that it may be related to magmatic underplating caused by the establishment of the Canary hotspot 60 Ma ago. Second, several authors Maillard et al. (2006) propose the existence of a lithospheric detachment fault with associated volcanic material originating from the asthenospheric mantle defining an African upper plate and a North American lower plate setting (Tari and Molnar, 2005; Maillard et al., 2006; Sibuet et al., 2012). Third, Biari et al. (2017) proposed that the asymmetry is the result of an early slow spreading center (Cannat et al., 2006; Smith, 2013; Sauter et al., 2013) creating seafloor by faulting the existing lithosphere on the Nova Scotia margin, and magmatic oceanic crust including pockets of serpentinite on the Moroccan margin (see Fig. 14 in Biari et al., 2017).

The seismic transects presented in this study show a thick proto-oceanic domain with a rugose top-basement topography on the Moroccan margin (Figs. 13, 14, and 15). Moreover, the top-basement reflections show layered, highly reflective units usually displaying internal unconformities that are interpreted as volcaniclastic material infilling half-grabens. Underlying these reflections, more transparent and chaotic seismic facies are interpreted as an intensely intruded oceanic crust. From the proto-oceanic to the oceanic domain, these seismic facies assemblages transition over short distance to a basement with a smoother topography and characterized by a seismically transparent, homogeneous, and thinner crust interpreted as normal oceanic crust. The contact between both domains is abrupt and frequently marked by the presence of normal faults (Figs. 14, 15, and 16). Moreover, from the analysis of the conjugate transects presented in Fig. 23, it can be observed that the salt basin configuration displays an asymmetrical configuration caused by a gently stepped pre-salt topography on the Nova Scotia margin (Deptuck and Kendell, 2017, 2020) and a more abrupt deepening of the basement on the Moroccan side. Overall, the evidence presented in this study supports the hypotheses of an early development of an asymmetric spreading center in this segment of the Central Atlantic, with a lithospheric detachment (Figs. 24b and c) defining an upper (NW Africa) and lower (North America) plate configuration, although the effect of hotspot-related magmatic underplating cannot be entirely ruled out and may contribute secondarily to the observed thickening of the crust in the proto-oceanic domain.

The seaward limit of the autochthonous salt basin on the Nova Scotia/Morocco conjugate margins matches the geometry of the ECMA and the S1 magnetic anomalies, respectively (Fig. 22) (Barrett and Keen, 1976; Roeser, 1982; Roeser et al., 2002; Sahabi et al., 2004; Contrucci et al., 2004; Klingelhoefer et al., 2009; Davis et al., 2018; amongst others). Moreover, in the present study, this distal limit on the Moroccan margin coincides with the presence of an outer high, usually characterized by a high seismic reflectivity, suggesting that it might be composed of igneous rocks. As pointed out by Dehler and Welford (2012), to the north, the ECMA (and the S1, see Roeser et al., 2002) gradually displays a lower amplitude suggesting a decreasing number of igneous additions.

The classical magma-rich vs. magma-poor rifted margin classification has been challenged in recent studies (Bronner et al., 2011; Gillard et al., 2017; Peace et al., 2018; Tugend et al., 2018; Harkin et al., 2019; Sapin et al., 2021; Koulakov et al., 2022; Liu et al., 2022; Pérez-Gussinyé et al., 2023). It has become widely accepted that the OCT in magma-poor margins can vary in width and contain different amounts of magmatic material hosted in continental and/or exhumed mantle rocks forming a hybrid crust, like in the Newfoundland/Iberia conjugate margins, the Gulf of Guinea, or the SE Indian margin (Bronner et al., 2011; Gillard et al., 2017; Tugend et al., 2018). In the study area, the along-strike transition from a magma-rich (south) to a magma-poor (north) segment (Louden et al., 2013) is gradual and matches a northward decrease in the S1 magnetic anomaly values, suggesting a progressive and segmented drop in the volume of magmatic additions at the OCT (Fig. 22) (Koulakov et al., 2022). In the study area, this zone with "variable magmatic content" (Fig. 22) is delimited by two major transfer zones, the Yarmouth / Sidi Ifni transfer zone to the south and the South Atlas transfer zone to the north, which broadly matches the "transition zone" proposed by Dehler and Welford (2012) for the Nova Scotia margin, although they considered that a sharper transition between segments exists and emphasized the importance of the northern boundary (see Fig. 5d in Dehler and Wellford, 2012). Our study suggests

that the existence of these major transfer zones set a first-order control on the along-strike segmentation between magma-rich and magma-poor rifted margins (Fig. 21) and could have acted as preferential conduits for magmatic emplacement (Roche et al., 2021), especially in the Tarfaya, Agadir and Essaouira basins (Sidi Ifni and the South Atlas transfer zones).

Just as the timing of rifting got younger from south to north, we infer that the timing of emplacement of proto-oceanic crust also progressed in the same direction (Fig. 24c). Early spreading began first, and shortly after salt deposition ceased, in the Tarfaya and southern Agadir salt basins. This timing is indicated by the distal onlap of the salt onto the outer high (probably representing breakup of the salt layer) and by the lack of extensional faulting of the top salt or its overburden, indicating that postsalt extension was accommodated by newly formed crust. In contrast, coeval extension in the north (Safi Basin and Mazagan Plateau) was still being recorded by faulting of the salt layer and its overburden. The northern areas were still in the late thinning or early exhumation stage while spreading was happening to the south (Fig. 24c), and only later did spreading commence in the north.

5.4. Post-salt tectonics

The post-salt tectonics involving the salt and its overburden also varied from south to north, controlled primarily by the spatial and thickness distribution of the autochthonous salt determined by its relationship to the rift geometries. In the south, where the salt is interpreted as *syn*-exhumation, we observe very little evidence for gravity-driven movement, in contrast to the model of Rowan (2014). This is likely due to the narrow, trough-like geometry of the salt basin and the consequent lack of adequate pressure or elevation head. Instead, there is a series of isolated diapirs triggered and driven primarily by progradational loading, with more landward and basinward diapirs having counterregional and vertical feeders, respectively (see Uranga et al., 2022). The amount of diapiric salt increases toward the north, compatible with a marked increase in salt thickness, connectivity, and gravitational translation in the central segment of the offshore Essaouira Basin (Tari et al., 2003; Davison et al., 2010; Pichel et al., 2019). Although faults offset the salt more than in the south, the salt was thick enough to allow gravitational salt tectonics in this syn-thinning salt basin, similar to what is seen in the northern Red Sea (Rowan, 2014). Moving northward, although gravitational salt-tectonic processes were still active (Tari and Jabour, 2013; Pichel et al., 2019), they were progressively hindered due to the increasing base- and top-salt offset. In the Safi Basin and Mazagan Plateau, the combination of fault-bounded salt depocenters and ongoing post-salt extension resulted in a dominant style of variably decoupled thick-skinned extension, as is typical of syn-stretching salt basins (Rowan, 2014).

6. Conclusions

The tectonic evolution of the Moroccan Atlantic margin reflects a complex interplay between rift propagation, structural inheritance, salt deposition and magmatic emplacement. Through the interpretation of newly acquired and legacy seismic data, this study presents a new integrated 3D conceptual model for the rift-to-drift transition of this segment of the Central Atlantic.

Assuming a rapid and widespread deposition of salt relative to rift propagation, the autochthonous salt can be regarded as a near-isochronous marker. From the analysis of the base salt topography, it can be argued that salt was deposited in different tectonic settings along the margin as a result of a V-shaped propagating rift system, which evolved from an initial stage of westward localization of the extensional deformation into a northward-propagating system. Salt accumulation started during Carnian-Norian times in the eastern depocenters (Essaouira and Western Meseta Triassic basins). This could be linked to the progressive westward (basinward) localization of extensional deformation and by the interaction between the Atlas and Atlantic rifts, leading to increased subsidence in this region. To the west, in the Central Atlantic rift valley, salt probably has a younger Rhaetian-Hettangian age, as indicated by drill core data. The seismic interpretations presented in this study suggest that salt was deposited during the exhumation stage in the southern segment of the study area (Tarfaya and southern Agadir basins), whereas at approximately the same time, it was being deposited during the late syn-stretching to early syn-thinning stage in the north (Safi Basin and Mazagan Plateau).

The diachronicity in rift propagation was strongly influenced by inherited Variscan structures, including inverted faults and shear zones, that played a crucial role in the along-strike segmentation of the margin, and which separated depocenters with different extension rates. Moreover, one of these, the Sidi Ifni Transfer Zone, located at the boundary between rheologically distinct pre-rift units, also marks the transition between a magma-rich/salt-poor (south) and a magma-poor/salt-rich (north) segment of the margin, suggesting there is a direct link between compositional/structural inheritance and magmatic supply during rifting and breakup.

Finally, the comparison between the conjugate Moroccan and Nova Scotia margins reveals similarities and differences. Salt on both margins was deposited in the same time span, recording the rift localization, from the proximal to the distal domain. Moreover, interpretation of the autochthonous salt on the Nova Scotia margin suggests that salt was deposited during the exhumation stage in the south and during the stretching stage in the north, as in the Moroccan side. However, both margins also show some differences in their crustal architecture. First, the deepening of the basement is asymmetric on both margins, with a gently tapered, stepped basement geometry controlled by several normal faults on the Nova Scotia margin, and a more abrupt deepening of the basement on the Moroccan margin, caused mainly by two crustal-scale normal faults. Second, this study confirms earlier works that revealed asymmetries in the crustal thickness and composition of the ocean continent transition, suggesting that magmatic processes had a greater influence on the Moroccan margin, while mantle exhumation played a more significant role on the Nova Scotia margin. In this regard, this study supports the hypothesis of an early development of an asymmetric spreading center, with a final detachment system during crustal separation defining an upper (NW Africa) and lower (North America) plate configuration.

Declaration of competing interest

The authors declare that they have no known competing financial interests or personal relationships that could have appeared to influence the work reported in this paper.

Data availability

The authors do not have permission to share data.

Acknowledgements

The authors would like to thank Geoex MCG and particularly Mike Powney for granting access to previously unpublished seismic data. Moreover, we also acknlowledge Dr. Frauke Klingelhoefer from Ifremer (France) and Dr. Michael Schnabel from the BGR (Germany) and ONHYM for granting access to public seismic datasets from the Moroccan margin. The authors would like to thank Dr. Michal Nemčok and Dr. Mohamed Gouiza for their insightful reviews which greatly improved the quality of the article. We acknowledge the support of the research project Structure and Deformation of Salt-bearing Rifted Margins (SABREM), PID2020-117598GB-I00, funded by MCIN/ AEI /10.13039/501100011033. Dr. Rodolfo Uranga was supported by doctoral and post-doctoral grants from the Universitat de Barcelona. Schlumberger is acknowledged for providing Petrel software, Eliis for providing

Paleoscan software and Petroleum Experts for providing Move software. Dr. Mark Rowan was partially supported by the Salt-Sediment Interaction Research Consortium at The University of Texas at El Paso, run by Kate Giles and currently funded by Chevron, Hess, PGS, and Woodside.

Appendix A. Supplementary data

Supplementary data to this article can be found online at https://doi.org/10.1016/j.earscirev.2024.104818.

References

Ady, B.A., Whittaker, R.C., Powney, M., Lawrence, S.R., 2022. A New Deformable Plate Model for the Morocco-North America Conjugate Margin and Its Implication for the Opening of the Central Atlantic. Abstract from the 7th Conjugate Margins Conference.

Afenzar, A., Essamoud, R., 2017. Early Mesozoic Detrital and Evaporitic Syn-Rift Series of Mohammedia-Benslimane-ElGara-Berrechid Basin (Meseta, Morocco): Sedimentary and Palaeoenvironmental Evolution and Comparison with Neighboring Basins. Int. J. Adv. Earth Sci. Eng. 6 (1), 596–621.

Aït Chayeb, E., Youbi, N., El-Boukhari, A., Bouabdelli, M., Amrhar, M., 1998. Le volcanisme permien et mésozoïque inférieur du bassin d'Argana (Haut-Atlas occidental, Maroc): un magmatisme intraplaque associé à l'ouverture de l'Atlantique central. J. Afr. Earth Sci. 26 (4), 499–519.

Allen, J., Beaumont, C., Deptuck, M.E., 2020. Feedback between synrift lithospheric extension, sedimentation and salt tectonics on wide, weak continental margins. Pet. Geosci. 26 (1), 16–35.

Allken, V., Huismans, R.S., Thieulot, C., 2012. Factors controlling the mode of rift interaction in brittle-ductile coupled systems: a 3D numerical study. Geochem. Geophys. Geosyst. 13 (5).

Alves, T.M., Gawthorpe, R.L., Hunt, D.W., Monteiro, J.H., 2002. Jurassic tectono-sedimentary evolution of the Northern Lusitanian Basin (offshore Portugal). Mar. Pet. Geol. 19 (6), 727–754.

Alves, T.M., Moita, C., Sandnes, F., Cunha, T., Monteiro, J.H., Pinheiro, L.M., 2006. Mesozoic–Cenozoic evolution of North Atlantic continental-slope basins: The Peniche basin, western Iberian margin. AAPG Bull. 90 (1), 31–60.

Araujo, M.N., Pérez-Gussinyé, M., Muldashev, I., 2023. Oceanward rift migration during formation of Santos–Benguela ultra-wide rifted margins. In Nemčok, M., Doran, H., Doré, A. G., Ledvényiová, L. and Rybár, S. (eds.). Tectonic Development, thermal history and Hydrocarbon Habitat Models of Transform margins: their differences from Rifted Margins. Geol. Soc. Lond. Spec. Publ. 524, 65–91.

Barrett, D.L., Keen, C.E., 1976. Mesozoic magnetic lineations, the magnetic quiet zone, and seafloor spreading in the Northwest Atlantic. J. Geophys. Res. 81 (26), 4875–4884.

Barss, M.S., Bujak, J.P., Williams, G.L., 1979. Palynological Zonation and Correlation of Sixty-Seven Wells, Eastern Canada, vol. 78. Geological Survey of Canada.

Baudon, C., Redfern, J., Van Den Driessche, J., 2012. Permo-Triassic structural evolution of the Argana Valley, impact of the Atlantic rifting in the High Atlas, Morocco. J. Afr. Earth Sci. 65, 91–104.

Benabdellouahed, M., Klingelhoefer, F., Gutscher, M.A., Rabineau, M., Biari, Y., Hafid, M., et al., 2017. Recent uplift of the Atlantic Atlas (offshore West Morocco): Tectonic arch and submarine terraces. Tectonophysics 706, 46–58.

Bertotti, G., Gouiza, M., 2012. Post-rift vertical movements and horizontal deformations in the eastern margin of the Central Atlantic: Middle Jurassic to early cretaceous evolution of Morocco. Int. J. Earth Sci. 101, 2151–2165.

Bertrand, J.M., Jardim de Sá, E.F., 1990. Where are the Eburnian–Transamazonian collisional belts? Can. J. Earth Sci. 27 (10), 1382–1393.

Biari, Y., Klingelhoefer, F., Sahabi, M., Aslanian, D., Schnurle, P., Berglar, K., Reichert, C., 2015. Deep crustal structure of the NW African margin from combined wide-angle and reflection seismic data (MIRROR seismic survey). Tectonophysics 656, 154–174. https://doi.org/10.1016/j.tecto.2015.06.019.

Biari, Y., Klingelhoefer, F., Sahabi, M., Funck, T., Benabdellouahed, M., Schnabel, M., et al., 2017. Opening of the Central Atlantic Ocean: implications for geometric rifting and asymmetric initial seafloor spreading after continental breakup. Tectonics 36 (6), 1129–1150.

Biari, Y., Klingelhoefer, F., Franke, D., Funck, T., Loncke, L., Sibuet, J.C., Basile, C., Austin, J., Rigoti, C.A., Sahabi, M., Benabdellouahed, M., Roest, W.R., 2021. Structure and evolution of the Atlantic passive margins: a review of existing rifting models from wide-angle seismic data and kinematic reconstruction. Mar. Pet. Geol. 126, 104898.

Bishop, A.N., 2020. Greater North Atlantic Liassic Petroleum System Synthesis. OERA Technical Report OG-2020-01.

Black, R., Latouche, L., Liégeois, J.P., Caby, R., Bertrand, J.M., 1994. Pan-African displaced terranes in the Tuareg shield (Central Sahara). Geology 22 (7), 641–644.

Bosworth, W., 2015. Geological evolution of the Red Sea: historical background, review, and synthesis. Red Sea 45–78.

Brahim, L.A., Chotin, P., Hinaj, S., Abdelouafi, A., El Adraoui, A., Nakcha, C., et al., 2002. Paleostress evolution in the Moroccan African margin from Triassic to present. Tectonophysics 357 (1–4), 187–205.

Bronner, A., Sauter, D., Manatschal, G., Péron-Pinvidic, G., Munschy, M., 2011. Magmatic breakup as an explanation for magnetic anomalies at magma-poor rifted margins. Nat. Geosci. 4 (8), 549–553.

Brown, R.H., 1980. Triassic rocks of Argana Valley, southern Morocco, and their regional structural implications. AAPG Bull. 64 (7), 988–1003.

Brun, J.P., Beslier, M.O., 1996. Mantle exhumation at passive margins. Earth Planet. Sci. Lett. 142 (1–2), 161–173.

Cannat, M., Sauter, D., Mendel, V., Ruellan, E., Okino, K., Escartin, J., et al., 2006. Modes of seafloor generation at a melt-poor ultraslow-spreading ridge. Geology 34 (7), 605–608.

Carracedo, J.C., Day, S., Guillou, H., Badiola, E.R., Cañas, J.A., Torrado, F.P., 1998. Hotspot volcanism close to a passive continental margin: the Canary Islands. Geol. Mag. 135 (5), 591–604.

Chao, P., Manatschal, G., Zhang, C., Chenin, P., Ren, J., Pang, X., Zheng, J., 2023. The transition from continental to lithospheric breakup recorded in proto-oceanic crust: Insights from the NW South China Sea. Bulletin 135 (3–4), 886–902.

Chenin, P., Manatschal, G., Ghienne, J.F., Chao, P., 2022. The syn-rift tectono-stratigraphic record of rifted margins (Part II): a new model to break through the proximal/distal interpretation frontier. Basin Res. 34 (2), 489–532.

Choubert, G., 1952. Histoire géologique du domaine de l'Anti-Atlas. Notes Mem. Serv. Geol. Maroc 100–196.

Choubert, G., 1963. Histoire géologique de l'Anti-Atlas de l'Archéen à l'aurore des temps primaires. Notes Mem. Serv. Geol. Maroc 62, 352p.

Clement, G.P., Holser, W.T., 1988. Geochemistry of Moroccan evaporites in the setting of the North Atlantic Rift. J. Afr. Earth Sci. 7 (2), 375–383.

Contrucci, I., Klingelhöfer, F., Perrot, J., Bartolomé, R., Gutscher, M.A., Sahabi, M., Rehault, J.P., 2004. The crustal structure of the NW Moroccan continental margin from wide-angle and reflection seismic data. Geophys. J. Int. 159 (1), 117–128.

Courtillot, V., 1982. Propagating rifts and continental breakup. Tectonics 1 (3), 239–250.

Cousminer, H.L., Steinkraus, W.E., 1988. Biostratigraphy of the COST G-2 well (Georges Bank): a record of Late Triassic synrift evaporite deposition; Liassic doming; and Mid-Jurassic to Miocene postrift marine sedimentation. In: Developments in Geotectonics, (22),. Elsevier, pp. 167–184.

Davis, J.K., Bécel, A., Buck, W.R., 2018. Estimating emplacement rates for seaward-dipping reflectors associated with the US East Coast magnetic Anomaly. Geophys. J. Int. 215 (3), 1594–1603.

Davison, I., 2005. Central Atlantic margin basins of North West Africa: geology and hydrocarbon potential (Morocco to Guinea). J. Afr. Earth Sci. 43 (1–3), 254–274.

Davison, I., Anderson, L.M., Bilbo, M., 2010. Salt Tectonics and Sub-salt Exploration Plays in the Essaouira Basin, Morocco. Rediscovering the Atlantic: New Ideas for an Old Sea. II Central and North Atlantic Conjugate Margins Conference, Lisbon 2010, p. 76.

Decalf, C.C., Heyn, T., 2023. Salt geometry in the Central Basin of the Nova Scotia passive margin, offshore Canada based on new seismic data. Mar. Pet. Geol. 149, 106065.

Dehler, S.A., Welford, J.K., 2012. Variations in rifting style and structure of the Scotian margin, Atlantic Canada, from 3D gravity inversion. Geol. Soc. Lond. Spec. Publ. 369 (1), 289–300.

Dehler, S.A., Keen, C.E., Funck, T., Jackson, H.R., Louden, K.E., 2004. The limit of volcanic rifting: a structural model across the volcanic to non-volcanic transition off Nova Scotia. In: AGU Spring Meeting Abstracts (Vol. 2004, pp. T31D-04).

Deptuck, M.E., Kendell, K.L., 2017. A review of Mesozoic-Cenozoic salt tectonics along the Scotian margin, eastern Canada. In: Soto, J.I., Flinch, J., Tari, G. (Eds.), Permo-Triassic Salt Provinces of Europe, North Africa and the Atlantic Margins, pp. 287–312.

Deptuck, M.E., Kendell, K.L., 2020. Atlas of 3D seismic surfaces and thickness maps, central and southwestern Scotian Slope. In: CNSOPB Geoscience Open File Report 2020-002MF–2020-006MF, p. 51.

Deptuck, M.E., Brown, D.E., Altheim, B., 2015. Call for bids NS15–1—exploration history, geologic setting, and exploration potential: Western and Central regions. CNSOPB geoscience open file report, 49 p, 2015-001MF. Available at: www.cnsopb.ns.ca/geoscience/geoscience-publications.

Diebold, J.B., Stoffa, P.L., 1988. A large aperture seismic experiment in the Baltimore Canyon Trough. In: Sheridan, R.E., Grow, J.A. (Eds.), The Atlantic Continental Margin. Geological Society of America.

Dillon, W.P., 1974. Structure and development of the southern Moroccan continental shelf. Mar. Geol. 16 (3), 121–143.

Dutuit, J.M., 1966. Apport des découvertes de vertebrés a la stratigraphie du Trias continental du Couloir d'Argana du Haut Atlas occidental (Maroc). Notes Mém. Serv. Géol. Maroc 26, 29–31.

Dyment, J., Lesur, V., Hamoudi, M., Choi, Y., Thebault, E., Catalan, M., the WDMAM Task Force, the WDMAM Evaluators, and the WDMAM Data Providers, 2015. World Digital Magnetic Anomaly Map Version 2.0, Map. available at. http://www.wdmam.org.

Ebinger, C.J., Casey, M., 2001. Continental breakup in magmatic provinces: an Ethiopian example. Geology 29 (6), 527–530.

El Khatib, J., 1995. Étude structurale et stratigraphique d'un segment de la marge continentale atlantique sud-marocaine: le bassin de Tarfaya-Laâyoune. Doctoral dissertation. Nice.

Ennih, N., Liégeois, J.P., 2008. The boundaries of the West African craton, with special reference to the basement of the Moroccan metacratonic Anti-Atlas belt. Geol. Soc. Lond. Spec. Publ. 297 (1), 1–17.

Epin, M.E., Manatschal, G., Sapin, F., Rowan, M.G., 2021. The tectono-magmatic and subsidence evolution during lithospheric breakup in a salt-rich rifted margin: insights from a 3D seismic survey from southern Gabon. Mar. Pet. Geol. 128, 105005.

Fenton, J.P.G., 1984. Palynological investigation of the Triassic-Middle Jurassic sequences at Deep Sea Drilling Project Leg 79, Sites 545, 546, and Hole 547B, off

Central Morocco. In: Hinz, K., Winterer, E.L., et al. (Eds.), Initial Reports of the Deep Sea Drilling Project, Washington (U.S.A.), vol. 79, pp. 715–718.
Ferrer, O., Roca, E., Benjumea, B., Muñoz, J.A., Ellouz, N., Marconi Team, 2008. The deep seismic reflection MARCONI-3 profile: Role of extensional Mesozoic structure during the Pyrenean contractional deformation at the eastern part of the Bay of Biscay. Mar. Pet. Geol. 25 (8), 714–730.
Ferrer, O., Jackson, M.P.A., Roca, E., Rubinat, M., 2012. Evolution of salt structures during extension and inversion of the Offshore Parentis Basin (Eastern Bay of Biscay). Geol. Soc. Lond. Spec. Publ. 363 (1), 361–380.
Fiechtner, L., Friedrichsen, H., Hammerschmidt, K., 1992. Geochemistry and geochronology of early Mesozoic tholeiites from Central Morocco. Geol. Rundsch. 81 (1), 45–62.
Frizon de Lamotte, D., Crespo-Blanc, A., Saint-Bézar, B., Comas, M., Fernandez, M., Zeyen, H., Ayarza, H., et al., 2004. TRASNSMED-transect I (Betics, Alboran Sea, Rif, Moroccan Meseta, High Atlas, Jbel Saghro, Tindouf basin). In: Cavazza, W., Roure, F. M., Spakman, W., Stampfli, G.M., Ziegler, P.A. (Eds.), The TRANSMED Atlas – The Mediterranean Region from Crust to Mantle. Springer, Berlin. ISBN 3-540-22181-6.
Frizon de Lamotte, D.F., Leturmy, P., Missenard, Y., Khomsi, S., Ruiz, G., Saddiqi, O., Michard, A., 2009. Mesozoic and Cenozoic vertical movements in the Atlas system (Algeria, Morocco, Tunisia): an overview. Tectonophysics 475 (1), 9–28.
Fullea, J., Camacho, A.G., Negredo, A.M., Fernández, J., 2015. The Canary Islands hot spot: New insights from 3D coupled geophysical–petrological modelling of the lithosphere and uppermost mantle. Earth Planet. Sci. Lett. 409, 71–88.
Funck, T., Jackson, H.R., Louden, K.E., Dehler, S.A., Wu, Y., 2004. Crustal structure of the northern Nova Scotia rifted continental margin (eastern Canada). J. Geophys. Res. Solid Earth 109 (B9).
Geoffroy, L., 2005. Volcanic passive margins. Compt. Rendus Geosci. 337 (16), 1395–1408.
Geoffroy, L., Burov, E.B., Werner, P., 2015. Volcanic passive margins: another way to break up continents. Sci. Rep. 5 (1), 14828.
Gillard, M., Sauter, D., Tugend, J., Tomasi, S., Epin, M.E., Manatschal, G., 2017. Birth of an oceanic spreading center at a magma-poor rift system. Sci. Rep. 7 (1), 1–6.
Goldflam, P., Hinz, K., Weigel, W., Wissmann, G., Blundell, D.J., 1980. Some features of the northwest African margin and magnetic quiet zone. Phil. Trans. R. Soc. Lond. A Math. Phys. Eng. Sci. 294 (1409), 87–96.
Gouiza, M., 2011. Mesozoic Source-to-Sink Systems in NW Africa: Geology of Vertical Movements during the Birth and Growth of the Moroccan Rifted Margin. PhD Dissertation. Vrije Universiteit Amsterdam.
Gouiza, M., Naliboff, J., 2021. Rheological inheritance controls the formation of segmented rifted margins in cratonic lithosphere. Nat. Commun. 12 (1), 1–9.
Gouiza, M., Bertotti, G., Hafid, M., Cloetingh, S.A.P.L., 2010. Kinematic and thermal evolution of the Moroccan rifted continental margin: Doukkala-High Atlas transect. Tectonics 29 (5).
Guiraud, R., Bosworth, W., 1997. Senonian basin inversion and rejuvenation of rifting in Africa and Arabia: synthesis and implications to plate-scale tectonics. Tectonophysics 282 (1–4), 39–82.
Haddou, J., Tari, G., 2007. Subsalt exploration potential of the Moroccan salt basin. Lead. Edge 26 (11), 1454–1460.
Hafid, M., 2000. Triassic–early Liassic extensional systems and their Tertiary inversion, Essaouira Basin (Morocco). Mar. Pet. Geol. 17 (3), 409–429. https://doi.org/10.1016/S0264-8172(98)00081-6.
Hafid, M., Salem, A.A., Bally, A.W., 2000. The western termination of the Jebilet–high Atlas system (offshore Essaouira Basin, Morocco). Mar. Pet. Geol. 17 (3), 431–443. https://doi.org/10.1016/S0264-8172(98)00082-8.
Hafid, M., Zizi, M., Bally, A.W., Salem, A.A., 2006. Structural styles of the western onshore and offshore termination of the High Atlas, Morocco. Compt. Rendus Geosci. 338 (1–2), 50–64.
Hafid, M., Tari, G., Bouhadioui, D., El Moussaid, I., Echarfaoui, H., Aït Salem, A., Nahim, M., Dakki, M., 2008. Atlantic Basins. In: Michard, A., Saddiqi, O., Chalouan, A., Lamotte, D.F. (Eds.), Continental Evolution: The Geology of Morocco, Lecture Notes in Earth Sciences, vol. 116. Springer, Berlin, Heidelberg. https://doi.org/10.1007/978-3-540-77076-3_6.
Harkin, C., Kusznir, N., Tugend, J., Manatschal, G., McDermott, K., 2019. Evaluating magmatic additions at a magma-poor rifted margin: an East Indian case study. Geophys. J. Int. 217 (1), 25–40.
Heezen, B.C., Tharp, M., 1965. Tectonic fabric of the Atlantic and Indian Oceans and continental drift. Phil. Trans. R. Soc. A Math. Phys. Eng. Sci. 258 (1088), 90–106.
Heyman, M.A.W., 1989. Tectonic and depositional history of the moroccan continental margin: chapter 21: European-African margins. In: Tankard, A.J., Balkwill, H.R. (Eds.), Extensional Tectonics and Stratigraphy of the North Atlantic Margins. https://doi.org/10.1306/M46497C21. AAPG Memoir 46.
Hinz, K., Dostmann, H., Fritsch, J., 1982a. The continental margin of Morocco: Seismic sequences, structural elements and geological development. In: von Rad, U., Hinz, K., Sarnthein, M., Seibold, E. (Eds.), Geology of the Northwest African Continental Margin. Springer Verlag, Berlin, pp. 34–60.
Hinz, K., et al., 1982b. Preliminary results from DSDP Leg 79 Seaward of the Mazagan Plateau off Central Morocco. In: von Rad, U., Hinz, K., Sarnthein, M., Seibold, E. (Eds.), Geology of the Northwest African Continental Margin. Springer, Berlin, Heidelberg.
Hinz, K., Winterer, E.L., Baumgartner, P.O., Bradshaw, M.J., Channell, J.E.T., Jaffrezo, M., et al., 1984. Site 544. Initial Rep. Deep Sea Drill. Proj. 79, 25–80. https://doi.org/10.2973/dsdp.proc.79.102.1984.
Holik, J.S., Rabinowitz, P.D., Austin Jr., J.A., 1991. Effects of Canary hotspot volcanism on structure of oceanic crust off Morocco. J. Geophys. Res. Solid Earth 96 (B7), 12039–12067.
Hölker, A.B., Manatschal, G., Holliger, K., Bernoulli, D., 2003. Tectonic nature and seismic response of top-basement detachment faults in magma-poor rifted margins. Tectonics 22 (4).
Holser, W.T., Clement, G.P., Jansa, L.F., Wade, J.A., 1988. Evaporite deposits of the North Atlantic rift. In: Manspeizer, W. (Ed.), Triassic-Jurassic Rifting: Continental Breakup and the Origin of the Atlantic Ocean and Passive Margins. Elsevier, pp. 525–556. Chapter 22.
Hudec, M.R., Norton, I.O., Jackson, M.P., Peel, F.J., 2013. Jurassic evolution of the Gulf of Mexico salt basin. AAPG Bull. 97 (10), 1683–1710.
Huismans, R.S., Beaumont, C., 2002. Asymmetric lithospheric extension: the role of frictional plastic strain softening inferred from numerical experiments. Geology 30 (3), 211–214.
Huismans, R.S., Beaumont, C., 2003. Symmetric and asymmetric lithospheric extension: Relative effects of frictional-plastic and viscous strain softening. J. Geophys. Res. Solid Earth 108 (B10).
Huismans, R., Beaumont, C., 2011. Depth-dependent extension, two-stage breakup and cratonic underplating at rifted margins. Nature 473 (7345), 74–78.
Jackson, M.P., Hudec, M.R., 2017. Salt Tectonics: Principles and Practice. Cambridge University Press.
Jaffal, M., Klingelhoefer, F., Matias, L., Teixeira, F., Amrhar, M., 2009. Crustal structure of the NW Moroccan margin from deep seismic data (SISMAR Cruise). Compt. Rendus Geosci. 341 (6), 495–503.
Jalil, N., 1996. Les vertébrés permiens et triassiques de la formation d'Argana (Haut Atlas occidental: list faunique préliminaire et implications stratigraphiques). In: Medina, F. (Ed.), Le Permien et le Trias du Maroc: État des connaissances. Presses universitaires du Maghreb, Marrakech, pp. 227–250.
Jammes, S., Manatschal, G., Lavier, L., 2010. Interaction between prerift salt and detachment faulting in hyperextended rift systems: the example of the Parentis and Mauléon basins (Bay of Biscay and western Pyrenees). AAPG Bull. 94 (7), 957–975.
Jansa, L.F., 1981. Mesozoic carbonate platforms and banks of the eastern north American margin. Mar. Geol. 44 (1–2), 97–117.
Jansa, L.F., Bujak, J.P., Williams, G.L., 1980. Upper Triassic salt deposits of the western North Atlantic. Can. J. Earth Sci. 17 (5), 547–559.
Jones, I.F., Davison, I., 2014. Seismic imaging in and around salt bodies. Interpretation 2 (4), SL1–SL20.
Keen, C.E., Potter, P., 1995. The transition from a volcanic to nonvolcanic rifted margin off eastern Canada. Tectonics 14, 359–371.
Keen, C.E., MacLean, B.C., Kay, W.A., 1991. A deep seismic reflection profile across the Nova Scotia continental margin, offshore eastern Canada. Can. J. Earth Sci. 28 (7), 1112–1120.
Klingelhoefer, F., Labails, C., Cosquer, E., Rouzo, S., Geli, L., Aslanian, D., Olivet, J.-L., Sahabi, M., Nouzé, H., Unternehr, P., 2009. Crustal structure of the SW-Moroccan margin from wide-angle and reflection seismic data (the DAKHLA experiment) part a: Wide-angle seismic models. Tectonophysics 468 (1–4), 63–82. https://doi.org/10.1016/j.tecto.2008.07.022.
Klingelhoefer, F., Biari, Y., Sahabi, M., Aslanian, D., Schnabel, M., Matias, L., Benabdellouahed, M., Funck, T., Gutscher, M., Reichert, C., Austin, J.A., 2016. Crustal structure variations along the NW-African continental margin: a comparison of new and existing models from wide-angle and reflection seismic data. Tectonophysics 674, 227–252. https://doi.org/10.1016/j.tecto.2016.02.024.
Klitgord, K.D., Schouten, H., 1986. Plate kinematics of the Central Atlantic. In: Vogt, Peter R., Tucholke, Brian E. (Eds.), The Western North Atlantic Region. The Geological Society of America.
Klitgord, K.D., Hutchinson, D.R., Schouten, H., 1988. US Atlantic continental margin; structural and tectonic framework. In: Sheridan, R.E., Grow, J.A. (Eds.), The Atlantic Continental Margin. The Geological Society of America.
Knight, K.B., Nomade, S., Renne, P.R., Marzoli, A., Bertrand, H., Youbi, N., 2004. The Central Atlantic Magmatic Province at the Triassic–Jurassic boundary: paleomagnetic and 40Ar/39Ar evidence from Morocco for brief, episodic volcanism. Earth Planet. Sci. Lett. 228 (1–2), 143–160.
Konstantinou, A., Karner, G., 2022. Salt deposition in ultra-deep brine settings by dynamic inflow and evaporation. In: Second International Meeting for Applied Geoscience and Energy. Society of Exploration Geophysicists and American Association of Petroleum Geologists, pp. 431–435.
Koopmann, H., Franke, D., Schreckenberger, B., Schulz, H., Hartwig, A., Stollhofen, H., di Primio, R., 2014. Segmentation and volcano-tectonic characteristics along the SW African continental margin, South Atlantic, as derived from multichannel seismic and potential field data. Mar. Pet. Geol. 50, 22–39.
Koulakov, I., Schlindwein, V., Liu, M., Gerya, T., Jakovlev, A., Ivanov, A., 2022. Low-degree mantle melting controls the deep seismicity and explosive volcanism of the Gakkel Ridge. Nat. Commun. 13 (1), 3122.
Kuiper, Y.D., Michard, A., Ruellan, E., Holm-Denoma, C.S., Crowley, J.L., 2021. New petrographic and U–Pb geochronology data from the Mazagan Escarpment, offshore Morocco: Support for an African origin. J. Afr. Earth Sci. 181, 104249.
Labails, C., 2007. La marge sud-marocaine et les premieres phases d'ouverture de l'Ocean Atlantique Central. Ph.D Thesis. Universite de Bretagne Occidentale, Brest, France.
Labails, C., Olivet, J.L., Dakhla Study Group, 2009. Crustal structure of the SW Moroccan margin from wide-angle and reflection seismic data (the Dakhla experiment). Part B—The tectonic heritage. Tectonophysics 468 (1–4), 83–97.
Labails, C., Olivet, J.L., Aslanian, D., Roest, W.R., 2010. An alternative early opening scenario for the Central Atlantic Ocean. Earth Planet. Sci. Lett. 297 (3–4), 355–368.
Lau, K.W.H., Nedimović, M.R., Louden, K.E., 2018. Continent-ocean transition across the northeastern Nova Scotian margin from a dense wide-angle seismic profile. J. Geophys. Res. Solid Earth 123 (5), 4331–4359.

Lavier, L.L., Manatschal, G., 2006. A mechanism to thin the continental lithosphere at magma-poor margins. Nature 440 (7082), 324–328.
Laville, E., Piqué, A., 1991. La Distension crustale atlantique et atlasique au Maroc au debut du Mesozoique; le rejeu des structures hercyniennes. Bull. Soc. Geol. France 162, 1161–1171.
Le Pourhiet, L., May, D.A., Huille, L., Watremez, L., Leroy, S., 2017. A genetic link between transform and hyper-extended margins. Earth Planet. Sci. Lett. 465, 184–192.
Le Pichon, X., 1968. Sea-floor spreading and continental drift. J. Geophys. Res. 73 (12), 3661–3697.
Le Pourhiet, L., Chamot-Rooke, N., Delescluse, M., May, D.A., Watremez, L., Pubellier, M., 2018. Continental break-up of the South China Sea stalled by far-field compression. Nat. Geosci. 11 (8), 605–609.
Le Roy, P., Piqué, A., 2001. Triassic–Liassic Western Moroccan synrift basins in relation to the Central Atlantic opening. Mar. Geol. 172 (3–4), 359–381. https://doi.org/10.1016/S0025-3227(00)00130-4.
Le Roy, P., Piqué, A., Le Gall, B., Ait Brahim, L., Morabet, A.M., Demnati, A., 1997. Les bassins cotiers triasico-liasiques du Maroc occidental et la diachronie du rifting intra-continental de l'Atlantique central. Bull. Soc. Géol. France 168 (5), 637–648.
Leleu, S., Hartley, A.J., van Oosterhout, C., Kennan, L., Ruckwied, K., Gerdes, K., 2016. Structural, stratigraphic and sedimentological characterisation of a wide rift system: The Triassic rift system of the Central Atlantic Domain. Earth-Sci. Rev. 158, 89–124.
Leprêtre, R., Missenard, Y., Barbarand, J., Gautheron, C., Saddiqi, O., Pinna-Jamme, R., 2015. Postrift history of the eastern central Atlantic passive margin: Insights from the Saharan region of South Morocco. J. Geophys. Res.: Solid Earth 120 (6), 4645–4666.
Liu, C., Shan, X., Yi, J., Shi, Y., Ventura, G., 2022. Volcanism at the end of continental rifting: the cretaceous syn-rift to post-rift transition in the Songliao Basin (NE China). Gondwana Res. 111, 174–188.
Louden, K., Wu, Y., Tari, G., 2013. Systematic variations in basement morphology and rifting geometry along the Nova Scotia and Morocco conjugate margins. Geol. Soc. Lond. Spec. Publ. 369 (1), 267–287. https://doi.org/10.1144/SP369.9.
Lyazidi, A., El Wartiti, M., Fadli, D., 2003. Évolution géodynamique du bassin triasique de Berrechid-ElGara-BenSlimane: Dynamique sédimentaire et géométrie des dépôts (Méseta Nord occidentale, Maroc) Geodynamic evolution of the Berrechid-ElGara-BenSlimane Triassic basin (Northwestern Meseta, Morocco): Depositional dynamics and geometry of sedimentary bodies. Pangea Infos 39, 23–36.
Maillard, A., Malod, J., Thiébot, E., Klingelhoefer, F., Réhault, J.P., 2006. Imaging a lithospheric detachment at the continent–ocean crustal transition off Morocco. Earth Planet. Sci. Lett. 241 (3–4), 686–698.
Makris, J., Nunn, K., Roberts, D., Luheshi, M., 2010. A crust and basin study of the Nova Scotia margin and its ocean transition based on densely spaced ocean bottom seismic observations. In: Central and North Atlantic Conjugate Margins Conference Lisbon, 2010, re-Discovering the Atlantic. New Winds for an Old Sea, Volume 4. Método Directo, Lisbon, pp. 162–166.
Manatschal, G., Müntener, O., Lavier, L.L., Minshull, T.A., Péron-Pinvidic, G., 2007. Observations from the Alpine Tethys and Iberia–Newfoundland margins pertinent to the interpretation of continental breakup. Geol. Soc. Lond. Spec. Publ. 282 (1), 291–324.
Marzoli, A., Callegaro, S., Dal Corso, J., Davies, J.H., Chiaradia, M., Youbi, N., Bertrand, H., et al., 2018. The Central Atlantic magmatic province (CAMP): a review. In: Tanner, L.H. (Ed.), The Late Triassic World, pp. 91–125.
McKenzie, D., 1978. Some remarks on the development of sedimentary basins. Earth Planet. Sci. Lett. 40 (1), 25–32.
Medina, F., 1995. Syn-and post-rift evolution of the El Jadida–Agadir basin (Morocco): constraints for the rifting models of the central Atlantic. Can. J. Earth Sci. 32 (9), 1273–1291.
Michard, A., Frizon de Lamotte, D., Saddiqi, O., Chalouan, A., 2008a. An outline of the geology of Morocco. In: Michard, A., Saddiqi, O., Chalouan, A., Frizon de Lamotte, D. (Eds.), Continental Evolution: The Geology of Morocco. Springer, Berlin, Heidelberg, pp. 1–31.
Michard, A., 1976. Chapitre 6: L'Evolution Structural du Maroc. In: Michard (ed.) Eléments de géologie marocaine. Notes Mem. Serv. Geol. (Maroc). 252 (1), 307-343.
Michard, A., Hoepffner, C., Soulaimani, A., Baidder, L., 2008. In: Michard, A., Saddiqi, O., Chalouan, A., Lamotte, D.F. (Eds.), Continental Evolution: The Geology of Morocco. Lecture Notes in Earth Sciences, 116. Springer, Berlin, Heidelberg, pp. 65–132.
Mohn, G., Manatschal, G., Beltrando, M., Masini, E., Kusznir, N., 2012. Necking of continental crust in magma-poor rifted margins: evidence from the fossil Alpine Tethys margins. Tectonics 31 (1).
Mohriak, W.U., Leroy, S., 2013. Architecture of rifted continental margins and break-up evolution: insights from the South Atlantic, North Atlantic and Red Sea–Gulf of Aden conjugate margins. Geol. Soc. Lond. Spec. Publ. 369 (1), 497–535.
Moragas, M., Baqués, V., Martín-Martín, J.D., Sharp, I., Lapponi, F., Hunt, D., Zeller, M., Vergés, J., Messager, G., Gindre-Chanu, L., Swart, R., Machado, V., 2023. Paleoenvironmental and diagenetic evolution of the Aptian Pre-Salt succession in Namibe Basin (Onshore Angola). Mar. Pet. Geol. 150, 106153.
Morgan, J.P, Parmentier, E.M., 1985. Causes and rate-limiting mechanisms of ridge propagation: A fracture mechanics model. J. Geophys. Res. Solid Earth 90 (B10), 8603–8612.
Nemčok, M., Frost, B., 2023. Along-strike magma-poor/magma-rich spreading transitions. In Nemčok, M., Doran, H., Doré, A. G., Ledvényiová, L. and Rybár, S. (eds.) Tectonic Development, thermal history and Hydrocarbon Habitat Models of Transform margins: their differences from Rifted margins. Geol. Soc. Lond. Spec. Publ. 524, 147–164.
Nemčok, M., Rybár, S., 2016. Rift–drift transition in a magma-rich system: the Gop Rift–Laxmi Basin case study, West India. Geol. Soc. Lond. Spec. Publ. 445 (1), 95–117.
Nemčok, M., Stuart, C., Segall, M., Allen, R.B., Christensen, C., Hermeston, S.A., Davison, I., 2005. Structural development of southern Morocco: Interaction of tectonics and deposition. In: Post, P.J., Rosen, N.C., Olson, D.L., Palmes, S.L., Lyons, K.T., Newton, G.B. (Eds.), Petroleum Systems of Divergent Continental Margin Basins, vol. 25. SEPM Society for Sedimentary Geology.
Nemčok, M., Welker, C., Sinha, S., Choudhuri, M., Sharma, S., Venkatraman, S., Sinha, N., 2018. Proximal and distal margin examples from the eastern continental passive margin of India. Atlas Struct. Geol. Interpret. Seism. Images 241–252.
Nemčok, M., Pospísil, L., Melnik, A., Henk, A., Doré, A.G., Rybár, S., Sinha, S., Choudhuri, M., Sharma, S., Stuart, C., Welker, C., Sinha, N., Nuttall, P., Venkatraman, S., 2023. Crust first–mantle second and mantle first–crust second; lithospheric break-up scenarios along the Indian margins. In: Nemčok, M., Doran, H., Doré, A.G., Ledvényiová, L., Rybár, S. (Eds.), Tectonic Development, Thermal History and Hydrocarbon Habitat Models of Transform Margins: their Differences from Rifted Margins, 524. Geological Society, London, pp. 147–164. Special Publications.
Neuharth, D., Brune, S., Glerum, A., Heine, C., Welford, J.K., 2021. Formation of continental microplates through rift linkage: Numerical modeling and its application to the Flemish Cap and Sao Paulo Plateau. Geochem. Geophys. Geosyst. 22 (4), e2020GC009615.
Neumaier, M., Back, S., Littke, R., Kukla, P.A., Schnabel, M., Reichert, C., 2016. Late Cretaceous to Cenozoic geodynamic evolution of the Atlantic margin offshore Essaouira (Morocco). Basin Res. 28 (5), 712–730.
Neumaier, M., Littke, R., Back, S., Kukla, P., Schnabel, M., Reichert, C., 2019. Hydrocarbon charge assessment of frontier basins–a case study of the oceanic crust of the Moroccan Atlantic margin. Pet. Geosci. 25 (2), 151–168.
Nirrengarten, M., Manatschal, G., Yuan, X.P., Kusznir, N.J., Maillot, B., 2016. Application of the critical Coulomb wedge theory to hyper-extended, magma-poor rifted margins. Earth Planet. Sci. Lett. 442, 121–132.
Nürnberg, D., Müller, R.D., 1991. The tectonic evolution of the South Atlantic from late Jurassic to present. Tectonophysics 191 (1–2), 27–53.
OETR (Offshore Energy Technical Research Association), 2011. Play fairway analysis atlas—offshore Nova Scotia. Nova Scotia department of energy report, NSDOE records storage file no. 88-11-0004-01 (349 pp.). http://energy.novascotia.ca/oil-and-gas/offshore/play-fairway-analysis.
Olsen, P.E., 1997. Stratigraphic record of the early Mesozoic breakup of Pangea in the Laurasia-Gondwana rift system. Annu. Rev. Earth Planet. Sci. 25 (1), 337–401.
Osmundsen, P.T., Redfield, T.F., 2011. Crustal taper and topography at passive continental margins. Terra Nova 23 (6), 349–361.
Pavlis, N.K., Holmes, S.A., Kenyon, S.C., Factor, J.K., 2012. The development and evaluation of the Earth Gravitational Model 2008 (EGM2008). J. Geophys. Res. Solid Earth 117 (B4).
Peace, A.L., Welford, J.K., Geng, M., Sandeman, H., Gaetz, B.D., Ryan, S.S., 2018. Rift-related magmatism on magma-poor margins: Structural and potential-field analyses of the Mesozoic Notre Dame Bay intrusions, Newfoundland, Canada and their link to North Atlantic opening. Tectonophysics 745, 24–45.
Pe-Piper, G., Jansa, L.F., Lambert, R.S.J., 1992. Early Mesozoic magmatism on the eastern Canadian margin: Petrogenetic and tectonic significance. In: Puffer, P.J., Ragland, P. (Eds.), Mesozoic Magmatism of Eastern North America, vol. 268. Geological Society of America, Boulder, CO, pp. 13–36.
Pérez-Gussinyé, M., Reston, T.J., Morgan, J.P., 2001. Serpentinization and magmatism during extension at non-volcanic margins: the effect of initial lithospheric structure. Geol. Soc. Lond. Spec. Publ. 187 (1), 551–576.
Pérez-Gussinyé, M., Ranero, C.R., Reston, T.J., Sawyer, D., 2003. Mechanisms of extension at nonvolcanic margins: evidence from the Galicia interior basin, west of Iberia. J. Geophys. Res. Solid Earth 108 (B5).
Pérez-Gussinyé, M., Collier, J.S., Armitage, J.J., Hopper, J.R., Sun, Z., Ranero, C.R., 2023. Towards a process-based understanding of rifted continental margins. Nat. Rev. Earth Environ. 4 (3), 166–184.
Péron-Pinvidic, G., Manatschal, G., 2009. The final rifting evolution at deep magma-poor passive margins from Iberia-Newfoundland: a new point of view. Int. J. Earth Sci. 98 (7), 1581–1597.
Péron-Pinvidic, G., Manatschal, G., Osmundsen, P.T., 2013. Structural comparison of archetypal Atlantic rifted margins: a review of observations and concepts. Mar. Pet. Geol. 43, 21–47.
Pichel, L.M., Huuse, M., Redfern, J., Finch, E., 2019. The influence of base-salt relief, rift topography and regional events on salt tectonics offshore Morocco. Mar. Pet. Geol. 103, 87–113.
Pichel, L.M., Ferrer, O., Jackson, C.A.L., Roca, E., 2022. Physical modelling of the interplay between salt-detached gravity gliding and spreading across complex rift topography, Santos Basin, offshore Brazil. Basin Res. 34 (6), 2042–2063.
Pichel, L.M., Legeay, E., Ringenbach, J.C., Callot, J.P., 2023. The West African salt-bearing rifted margin—Regional structural variability and salt tectonics between Gabon and Namibe. Basin Res. 35 (6), 2217–2248.
Piqué, A., Laville, E., 1996. The Central Atlantic rifting: Reactivation of Palaeozoic structures? J. Geodyn. 21 (3), 235–255.
Piqué, A., Michard, A., 1989. Moroccan Hercynides, a synopsis. The Paleozoic sedimentary and tectonic evolution at the northern margin of West Africa. Am. J. Sci. 289, 286–330.
Piqué, A., Jeannette, D., Michard, A., 1980. The Western Meseta Shear Zone, a major and permanent feature of the Hercynian belt in Morocco. J. Struct. Geol. 2 (1–2), 55–61.
Piqué, A., Aït Brahim, L., Ait Ouali, R., Amrhar, M., Charroud, M., Gourmelen, C., Laville, E., Rekhiss, F., Tricart, P., 1998. Evolution structurale des domaines

atlasiques du Maghreb au Méso-Cénozoïque; le rôle des structures héritées dans la déformation du domaine atlasique de l'Afrique du Nord. Bull. Soc. Géol. France 169 (6), 797–810.
Quirk, D.G., Hertle, M., Jeppesen, J.W., Raven, M., Mohriak, W.U., Kann, D.J., et al., 2013. Rifting, subsidence and continental break-up above a mantle plume in the central South Atlantic. Geol. Soc. Lond. Spec. Publ. 369 (1), 185–214.
Rasmussen, E.S., Lomholt, S., Andersen, C., Vejbæk, O.V., 1998. Aspects of the structural evolution of the Lusitanian Basin in Portugal and the shelf and slope area offshore Portugal. Tectonophysics 300 (1–4), 199–225.
Reston, T.J., 2009. The structure, evolution and symmetry of the magma-poor rifted margins of the North and Central Atlantic: a synthesis. Tectonophysics 468 (1–4), 6–27.
Roca, E., Muñoz, J.A., Ferrer, O., Ellouz, N., 2011. The role of the Bay of Biscay Mesozoic extensional structure in the configuration of the Pyrenean orogen: Constraints from the MARCONI deep seismic reflection survey. Tectonics 30 (2).
Roche, V., Leroy, S., Guillocheau, F., Revillon, S., Ruffet, G., Watremez, L., Acremont, E., Nonn, C., Vetel, W., Despinois, F., 2021. The Limpopo Magma-Rich Transform margin, South Mozambique–2: Implications for the Gondwana Breakup. Tectonics 40 (12), e2021TC006914.
Roeser, H.A., 1982. Magnetic anomalies in the magnetic quiet zone off Morocco. In: Geology of the northwest African continental margin (pp. 61-68). Springer, Berlin, Heidelberg. In: von Rad, U., Hinz, K., Sarnthein, M., Seibold, E. (Eds.), Geology of the Northwest African Continental Margin. Springer, Berlin, Heidelberg.
Roeser, H.A., Steiner, C., Schreckenberger, B., Block, M., 2002. Structural development of the Jurassic magnetic Quiet Zone off Morocco and identification of Middle Jurassic magnetic lineations. J. Geophys. Res. Solid Earth 107 (B10), EPM–1.
Rowan, M.G., 2014. Passive-margin salt basins: Hyperextension, evaporite deposition, and salt tectonics. Basin Res. 26 (1), 154–182.
Rowan, M.G., 2020. The South Atlantic and Gulf of Mexico salt basins: crustal thinning, subsidence and accommodation for salt and presalt strata. In: McClay, K.R., and Hammerstein, J.A. (eds.), Passive margins: Tectonics, Sedimentation and Magmatism. Geol. Soc. Lond. Spec. Publ. 476, 333–363.
Rowan, M.G., 2022. The ocean-continent transition of late synrift salt basins: Extension and evaporite deposition in the southern Gulf of Mexico and global analogs. In: Koeberl, Christian, Claeys, Philippe, Montanari, Alessandro (Eds.), From the Guajira Desert to the Apennines, and from Mediterranean Microplates to the Mexican Killer Asteroid: Honoring the Career of Walter Alvarez.
Rowan, M.G., Giles, K.A., 2021. Passive versus active salt diapirism. AAPG Bull. 105 (1), 53–63.
Rowan, M.G., Sumner, H.S., Huston, H., Venkatraman, S., Dunbar, D., 2012. Constraining Interpretations of the Crustal Architecture of the Northern Gulf of Mexico.
Sahabi, M., Aslanian, D., Olivet, J.L., 2004. Un nouveau point de départ pour l'histoire de l'Atlantique central. Compt. Rendus Geosci. 336 (12), 1041–1052. https://doi.org/10.1016/j.crte.2004.03.017.
Sapin, F., Ringenbach, J.C., Clerc, C., 2021. Rifted margins classification and forcing parameters. Sci. Rep. 11 (1), 1–17.
Sauter, D., Cannat, M., Rouméjon, S., Andreani, M., Birot, D., Bronner, A., et al., 2013. Continuous exhumation of mantle-derived rocks at the Southwest Indian Ridge for 11 million years. Nat. Geosci. 6 (4), 314–320.
Savva, D., Chrest, T., Saint-Ange, F., MacDonald, A., Luheshi, M., Cuilhe, L., 2016. Structural Impact of the Yarmouth Arch in the Central Atlantic Opening and on the SW Nova Scotian Margin Architecture (SW Nova Scotia) (Abstract presented during the AAPG Annual Convention and Exhibition).
Schettino, A., Turco, E., 2009. Breakup of Pangaea and plate kinematics of the Central Atlantic and Atlas regions. Geophys. J. Int. 178 (2), 1078–1097.
Schreiber, B.C., Hsü, K.J., 1980. Evaporites. In: Hobson, G.D (Ed.), Developments in Petroleum Geology. Applied Science Ltd, London, pp. 87–138.
Sehrt, M., 2014. Variscan to Neogene long-term landscape evolution at the Moroccan passive continental margin (Tarfaya Basin and western Anti-Atlas) (Doctoral dissertation).
Shimeld, J., 2004. A comparison of salt tectonic subprovinces beneath the Scotian Slope and Laurentian Fan. In: Post, P.J., Olsen, D.L., Lyons, K.T., Palmes, S.L., Harrison, P. F., Rosen, N.C. (Eds.), Salt-Sediment Interactions and Hydrocarbon Prospectivity: Concepts, Applications, and Case Studies for the 21st Century, Houston: 24th Annual Gulf Coast Section SEPM Foundation Bob F. Perkins Research Conference, pp. 291–306.
Sibuet, J.C., Rouzo, S., Srivastava, S., 2012. Plate tectonic reconstructions and paleogeographic maps of the central and North Atlantic oceans. Can. J. Earth Sci. 49 (12), 1395–1415.
Simancas, J.F., Tahiri, A., Azor, A., Lodeiro, F.G., Poyatos, D.J.M., El Hadi, H., 2005. The tectonic frame of the Variscan–Alleghanian orogen in Southern Europe and Northern Africa. Tectonophysics 398 (3–4), 181–198.
Smith, D., 2013. Mantle spread across the sea floor. Nat. Geosci. 6 (4), 247–248.
Stanton, N., Manatschal, G., Autin, J., Sauter, D., Maia, M., Viana, A., 2016. Geophysical fingerprints of hyper-extended, exhumed and embryonic oceanic domains: the example from the Iberia–Newfoundland rifted margins. Mar. Geophys. Res. 37 (3), 185–205.
Stica, J.M., Zalán, P.V., Ferrari, A.L., 2014. The evolution of rifting on the volcanic margin of the Pelotas basin and the contextualization of the Paraná–Etendeka LIP in the separation of Gondwana in the South Atlantic. Mar. Pet. Geol. 50, 1–21.
Stockli, D.F., Bosworth, W., 2019. Timing of extensional faulting along the magma-poor central and northern Red Sea rift margin—Transition from regional extension to necking along a hyperextended rifted margin. In: Rasul, N.M., Stewart, I.C. (Eds.), Geological Setting, Palaeoenvironment and Archaeology of the Red Sea. Springer, pp. 81–111.
Strozyk, F., Back, S., Kukla, P.A., 2017. Comparison of the rift and post-rift architecture of conjugated salt and salt-free basins offshore Brazil and Angola/Namibia, South Atlantic. Tectonophysics 716, 204–224.
Tari, G., Jabour, H., 2013. Salt tectonics along the Atlantic margin of Morocco. Geol. Soc. Lond. Spec. Publ. 369 (1), 337–353.
Tari, G., Molnar, J., 2005. Correlation of syn-rift structures between Morocco and Nova Scotia, Canada. In: Transactions GCSSEPM Foundation, 25th Ann. Res. Conf. SEPM, pp. 132–150.
Tari, G., Molnar, J., Ashton, P., Hedley, R., 2000. Salt tectonics in the Atlantic margin of Morocco. Lead. Edge 19 (10), 1074–1078.
Tari, G., Molnar, J., Ashton, P., 2003. Examples of salt tectonics from West Africa: a comparative approach. Geol. Soc. Lond. Spec. Publ. 207 (1), 85–104.
Tari, G., Brown, D., Jabour, H., Hafid, M., Loudenk, K., Zizi, M., 2012. The conjugate margins of Morocco and Nova Scotia. In: Roberts, D.G., Bally, A.W. (Eds.), Regional Geology and Tectonics: Phanerozoic Passive Margins, Cratonic Basins and Global Tectonic Maps, 1, pp. 285–323.
Tari, G., Novotny, B., Jabour, H., Hafid, M., 2017. Salt tectonics along the Atlantic margin of NW Africa (Morocco and Mauritania). In: Soto, J.I., Flinch, J., Tari, G. (Eds.), Permo-Triassic Salt Provinces of Europe, North Africa and the Atlantic Margins. Elsevier, pp. 331–351.
Tetreault, J.L., Buiter, S.J.H., 2018. The influence of extension rate and crustal rheology on the evolution of passive margins from rifting to break-up. Tectonophysics 746, 155–172.
Tixeront, M., 1973. Lithostratigraphie et minéralisations cuprifères et uranifères stratiformes, syngénétiques et familières des formations détritiques permo-triasiques du couloir d'Argana, Haut Atlas occidental (Maroc). Notes Mém. Serv. Géol. Maroc 33 (249), 147–177.
Tugend, J., Manatschal, G., Kusznir, N.J., Masini, E., 2015. Characterizing and identifying structural domains at rifted continental margins: application to the Bay of Biscay margins and its Western Pyrenean fossil remnants. Geol. Soc. Lond. Spec. Publ. 413 (1), 171–203.
Tugend, J., Gillard, M., Manatschal, G., Nirrengarten, M., Harkin, C., Epin, M.E., Sauter, D., Autin, J., Kusznir, N., Mcdermott, K., 2018. Reappraisal of the magma-rich versus magma-poor rifted margin archetypes. Geol. Soc. Lond. Spec. Publ. 476 (1), 23–47.
Uranga, R.M., Ferrer, O., Zamora, G., Muñoz, J.A., Rowan, M.G., 2022. Salt tectonics of the offshore Tarfaya Basin, Moroccan Atlantic margin. Mar. Pet. Geol. 105521.
Van Wijk, J.W., Blackman, D.K., 2005. Dynamics of continental rift propagation: the end-member modes. Earth Planet. Sci. Lett. 229 (3–4), 247–258.
Verati, C., Rapaille, C., Féraud, G., Marzoli, A., Bertrand, H., Youbi, N., 2007. 40Ar/39Ar ages and duration of the Central Atlantic Magmatic Province volcanism in Morocco and Portugal and its relation to the Triassic–Jurassic boundary. Palaeogeogr. Palaeoclimatol. Palaeoecol. 244 (1–4), 308–325.
Vergés, J., Moragas, M., Martín-Martín, J.D., Saura, E., Casciello, E., Razin, P., et al., 2017. Salt tectonics in the Atlas mountains of Morocco. In: Soto, J.I., Flinch, J., Tari, G. (Eds.), Permo-Triassic Salt Provinces of Europe, North Africa and the Atlantic Margins. Elsevier, pp. 563–579.
Villeneuve, M., Cornée, J.J., 1994. Structure, evolution and palaeogeography of the West African craton and bordering belts during the Neoproterozoic. Precambrian Res. 69 (1–4), 307–326.
Vine, F.J., Matthews, D.H., 1963. Magnetic anomalies over oceanic ridges. Nature Publishing.
Vink, G.E., 1982. Continental rifting and the implications for plate tectonic reconstructions. J. Geophys. Res. Solid Earth 87 (B13), 10677–10688.
Wade, J.A., MacLean, B.C., 1990. The geology of the Southeastern margin of Canada. In: Keen, M.J., Williams, G.L. (Eds.), Geology of the Continental Margin of Eastern Canada. Geological Survey of Canada, Canada, pp. 190–238.
Warren, J.K., 2006. Evaporites: Sediments, Resources and Hydrocarbons. Springer Science & Business Media.
Weigel, W., Wissmann, G., Goldflam, P., 1982. Deep Seismic Structure (Mauritania and Central Morocco). In: von Rad, U., Hinz, K., Sarnthein, M., Seibold, E. (Eds.), Geology of the Northwest African Continental Margin. Springer, Berlin Heidelberg, pp. 132–159.
Wenke, A., 2014. Sequence Stratigraphy and Basin Analysis of the Tarfaya-Laâyoune Basins Morocco, on-and Offshore Morocco. Doctoral dissertation, Heidelberg. https://doi.org/10.11588/heidok.00017905.
Wernicke, B., 1985. Uniform-sense normal simple shear of the continental lithosphere. Can. J. Earth Sci. 22 (1), 108–125.
Weston, J.F., MacRae, R.A., Ascoli, P., Cooper, M.K.E., Fensome, R.A., Shaw, D., Williams, G.L., 2012. A revised biostratigraphic and well-log sequence-stratigraphic framework for the Scotian margin, offshore eastern Canada. Can. J. Earth Sci. 49 (12), 1417–1462.
Whitmarsh, R.B., Manatschal, G., Minshull, T.A., 2001. Evolution of magma-poor continental margins from rifting to seafloor spreading. Nature 413 (6852), 150–154.
Withjack, M.O., Schlische, R.W., Olsen, P.E., Zhang, Q., 1998. Diachronous rifting, drifting, and inversion on the passive margin of central eastern North America: an analog for other passive margins. AAPG Bull. 82 (5), 817–835.
Wu, Y., Louden, K.E., Funck, T., Jackson, H.R., Dehler, S.A., 2006. Crustal structure of the Central Nova Scotia margin off Eastern Canada. Geophys. J. Int. 166 (2), 878–906.
Zhang, C., Sun, Z., Manatschal, G., Pang, X., Li, S., Sauter, D., et al., 2021. Ocean-continent transition architecture and breakup mechanism at the mid-northern South China Sea. Earth Sci. Rev. 217, 103620.
Zühlke, R., Bouaouda, M.S., Ouajhain, B., Bechstädt, T., Leinfelder, R., 2004. Quantitative Meso-/Cenozoic Development of the Eastern Central Atlantic Cont.